A7 Makaroro River dam site – Phase 1C: Field characterisation of possible secondary fault displacement

R. M. Langridge P. Villamor N. J. Litchfield
M. Page W. Ries I. A. Ansell
D. McNamara F. Martin Gonzalez

GNS Science Consultancy Report 2013/68
July 2013

WI 13/05
HBRC Plan No. 4527

DISCLAIMER

BIBLIOGRAPHIC REFERENCE

Langridge, R. M.; Villamor, P.; Litchfield. N. J.; Page, M.; Ries, W.; Ansell, I. A.; McNamara, D.; Martin Gonzalez, F. 2013. A7 Makaroro River dam site – Phase 1C: Field characterisation of possible secondary fault displacement, *GNS Science Consultancy Report* 2013/68. 81 p.

CONTENTS

FIGURES

TABLES

APPENDICES

APPENDIX FIGURES

APPENDIX TABLES

EXECUTIVE SUMMARY

GNS Science has undertaken a field study to investigate the possibility of active secondary faulting in the vicinity of the proposed A7 dam site on the Makaroro River, central Hawke's Bay. The A7 site is located c. 750 m east of the primary active Mohaka Fault which has a short earthquake recurrence interval (average c. 1125 yr) and poses a credible shaking hazard to the dam site. Prior studies for the A7 dam site commissioned to GNS Science addressed the tectonic setting and characteristics of nearby active faults, as well as a literature review of the potential for secondary faulting at the dam site as a consequence of primary faulting along the Mohaka Fault.

This current study focusses on site specific fieldwork undertaken to further evaluate the possibility of recent (late Quaternary) secondary faulting at, or near the proposed A7 dam site, and to define secondary faulting parameters such as possible displacement size, sense of movement, and recurrence. Based on our brief and previous investigations, we selected likely candidate sites for excavation to bedrock on the true left side of the valley on Smedley Station. The three trench sites were located to: 1) investigate the bedrock within the A7 dam footprint; 2) to intercept a NNE-striking mapped fault/shear zone; and 3) test whether evident linear hillslope geomorphology was related to recent faulting near the dam site.

To assess recent displacement on bedrock exposed in the trenches we have: 1) mapped the bedrock structure (bedding and defects) in detail to identify faults/shear zones that could have potentially moved with fault displacements; 2) assessed whether bedrock faults had displaced the late Quaternary cover deposits or the strath surface (bedrock/cover contact); and, 3) assessed if fault rocks have characteristics of recent movement (i.e., non-cohesive materials such as fault breccias and gouge or clays.

The surface fault rupture history of an active fault, the Gwavas Fault, located 5 km to the north of the A7 dam site and its relevance to the potential for faulting at the dam site have also been investigated through paleoseismic trenching.

Smedley South trench

The Smedley South trench was excavated within the footprint of the proposed dam site into an alluvial terrace and hillslope adjacent to the Makaroro River gorge. The c. 6 m deep floor of this trench exposed a c. 40 m length of greywacke bedrock overlain by alluvial gravel and tephric deposits. The bedrock/alluvial strath is overlain by coarse alluvial gravels, fining upward into medium gravels and fine-grained orange-brown tephric material and a surface soil. At one end of the trench, a younger back-edge channel was filled with fine-grained material, including discrete tephra, and overlain by hillslope deposits. Geologic ages come from a radiocarbon date and tephra correlations that indicate that the gravels overlying the bedrock/alluvial strath are at least 10,000 years old. **We found no evidence of recent displacement (faulting) of the bedrock/alluvial strath surface and no evidence of displacement of the cover deposits in this trench.**

Several faults, some with soft clay infills, were mapped from the bedrock up to the bedrock/alluvial strath contact. Soft clay infill observed in some bedrock faults is interpreted as not being the product of recent faulting, but rather the result of weathering (i.e., the soft clay material is not fault gouge, but old cataclasite/mylonite weathered to soft clay). **Collectively, these observations suggest that there has not been any fault displacement along the length of this trench in at least the last 10,000 years.**

Smedley Middle trench

The Smedley Middle trench was excavated c. 200 m NNE of the Smedley South trench and also through an alluvial terrace to bedrock. The floor of this trench exposed a c. 13 m length of greywacke bedrock, which was overlain by a similar sequence of alluvial gravel, tephra and soil as observed in the Smedley South trench. We also **found no evidence of recent displacement (faulting) of the bedrock/alluvial strath surface, nor evidence for faulting within the gravel cover deposits** overlying the strath in the Smedley Middle trench.

Smedley North trench

This trench was excavated c. 450 m to the NNE of the Smedley Middle trench and exposed a c. 40 m length of greywacke bedrock at its floor. The purpose of this trench was to test whether NNE-oriented hillslope ridges aligned parallel to Donovan Gully and the regional tectonic grain were related to active faulting. The detailed analysis of the bedrock structure exposed in the Smedley North trench, together with the lack of evidence for recent faulting within the cover deposits overlying the bedrock, suggests that the strike of the bedrock strata is probably the reason for the prominent hillslope grain rather than being controlled by recent faulting. Infill in bedrock faults exposed in Smedley North trench was not related to recent faulting. Some faults were filled with Holocene tephric materials that had infiltrated from the top into the upper part of shear zones/faults. In addition, detailed analysis of a prominent 020/80° E trending shear zone in bedrock that displayed soft materials close to the bedrock strath showed that fault infill was old weathered cataclasite. **All field observations in the Smedley North trench suggest that there was no recent fault displacement there**.

Bedrock attitudes in the three Smedley trenches were dominated by north-northeast strikes with bed dips to the southeast (average c. 017/59° SE), i.e. consistent with the regional tectonic fabric. Faults exposed in the bedrock had rather more random strikes and dips. However, there appeared to be two preferential tendencies for fault attitudes: (i) a tendency toward NNE-striking faults, particularly when there was a concentration of argillite beds within the greywacke. This is because weaker argillite beds are often utilised to take up strain (faulting) within a volume of rock; and (ii) a tendency toward ESE-striking faults, which were roughly perpendicular to the other main set of faults.

Gwavas Fault investigations

GNS Science were also asked to investigate the relevance, role, and activity of a fault trace we call the 'Gwavas Fault', located c. 6 km north of the A7 dam site in the Gwavas Forest. A fourth trench was excavated across a c. 2 m high fault scarp, recognised as an active fault trace on a LiDAR DEM map, at Pinchgut Creek. The trench exposed a zone of normal faulting where coarse alluvial gravels are faulted against a section of orange-brown tephric deposits on the downthrown side of the fault zone. Based on radiocarbon dates and tephra analyses and by comparison to the Smedley trenches, the orange-brown tephra-rich section spans the Holocene. We recognise up to 7 faulting events that have occurred since the abandonment of the alluvial gravel surface on which the tephra-rich sequence rests, and which we assume to have an age of c. 10,000-14,000 yr. These data yield a preliminary recurrence interval of surface rupture displacement along the Gwavas Fault of 2000-2800 yr, and an average single-event vertical displacement of 0.33-0.5 m for the Gwavas Fault. Individual faulting events could range between c. 30-100 cm. A roadcut nearby to the trench site shows the Gwavas Fault in bedrock. At this location the greywacke is highly sheared and fractured around the core of the fault, with an attitude (034/76° E) that is consistent with the strike and dip of the fault from the map and trench (i.e. c. 017/75° SE).

We find no reason to connect the active deformation observed along the Gwavas Fault with inactive faults - shown on the Hawke's Bay QMap geologic map - that may extend southwards close to the A7 dam site. Re-mapping of the Gwavas Fault shows that it terminates to the south in the area of Leatherwood Road and that there are no clear indications of Holocene faulting along this trend to the south towards the proposed dam site. We conclude that approximately located inactive faults mapped at 1:250,000 scale shown crossing Smedley Station and in the vicinity of the A7 dam site should not be considered as representing well located, focussed surface fault rupture displacement hazards, i.e. primary active faults. Our observations from the exposed bedrock are that discrete faults and shear zones can exist commonly throughout the rockmass.

In summary, this study has found **no evidence for active secondary faulting within the greywacke rockmass exposed in investigation trenches near the proposed A7 dam site**. This covers a time period of at least 10,000 yr as indicated by the geologic deposits overlying the bedrock. However, the trench exposures are limited in extent, and we cannot therefore confidently state that there is no secondary faulting in places that we have not exposed, such as along the true right side of the river.

Literature review in a previous study indicated that the displacement on secondary faults could be c. 0.1-0.5 m (at 1 standard deviation uncertainty) up to 2 km or more from the primary fault rupture (Langridge et al., 2011). Although we did not find any secondary displacement within the Smedley trenches to be able to confirm the numbers from literature for the A7 site specifically, the displacements observed on the Gwavas Fault (0.33-0.5 m) are consistent with these values. The observed displacements at Gwavas along with the relative proximity of the Gwavas Fault to the Mohaka Fault (c. 200 m) compared to the distance between the potential secondary faulting at the A7 site and the Mohaka Fault (c. 750 m), coupled with the lack of evidence for displacement in the landscape (terraces, hill country) in the vicinity of the dam site and the absence of secondary fault displacements at the candidate trench sites, together provide a reasonable basis to state that **the size of potential secondary displacement at the dam site, would be within this range including uncertainties, derived from literature review**.

Based on an analysis of fault orientations in the bedrock and their relationship to the current tectonic stress or kinematic regime, the style of future potential displacements within the dam foundation is likely to comprise the following: (i) faults with vertical or sub-vertical dips will yield right-lateral fault movements on NNE-striking faults and left-lateral movement on ESE-striking faults, and (ii) dipping faults (<75°) will yield oblique (dextral-reverse) fault movement on NNE-striking faults and oblique (sinistral-normal) movement on ESE-striking faults.

The recurrence time of secondary faulting within the dam foundation cannot easily be assessed from this study, because we did not observe any late Quaternary displacements within the bedrock in the Smedley trenches. From the limited exposures we have excavated the results show that there has been no secondary faulting in these trenches during the last 10,000 years.

We recommend that further geologic mapping of the dam footprint, with sufficient analysis of potential late Quaternary displacement, during construction is essential to provide additional confirmation of the findings presented herein and to allow for any other areas of shearing and fault fabric to be assessed. The dams defensive design measures and principles can then be adjusted accordingly.

1.0 INTRODUCTION

The Hawke's Bay Regional Investment Company Ltd. (HBRIC; the Client) has requested that the Institute of Geological and Nuclear Sciences Ltd (trading as GNS Science) undertake field studies to provide information on the potential for recent secondary fault displacements within and near the footprint of the proposed A7 dam site on the Makaroro River. The focus of this work has been toward excavating to bedrock at targeted sites where mapped faults and shear zones are shown to intercept the dam foundation.

1.1 EXISTING STUDIES

GNS Science, along with Tonkin & Taylor Ltd., has been involved in the Feasibility Studies for the Ruataniwha Water Storage Scheme, particularly with respect to the location and feasibility of the main A7 dam structure (see (Tonkin and Taylor, 2012a, 2012b). Existing studies undertaken by GNS include:

- a regional analysis of active faulting and shaking spectra (GNS Report CR 2010/121; Langridge et al., 2010);
- an initial site evaluation of the A7 dam site (GNS Report CR 2011/117; Langridge and Villamor, 2011); and,
- an update for a revised location of the A7 dam including an analysis of the possibility of secondary faulting near the dam site (GNS Report CR 2011/300; Langridge et al., 2011).

Separate from the Ruataniwha Water Storage Scheme, geologic mapping of the Hawke's Bay region by the GNS Regional mapping team has been completed (Lee et al., 2011). This new map provides important insights and issues with respect to the location of the A7 dam site.

This current study implements the recommendations for further work in GNS Report CR 2011/300 (Langridge et al., 2011).

1.2 CURRENT STUDY

This study has focussed on whether there is potential for, or evidence of, recent secondary fault displacement through the footprint of the proposed A7 dam site. Secondary displacement is defined as a minor displacement (typically <1 m) that occurs on a secondary or subsidiary fault at the same time as earthquake rupture of a main fault trace. The proximity of the site to known primary active faults, i.e. long mappable faults that generate large earthquakes and surface displacements, implies the possibility that smaller secondary deformations on nearby structures and/or bedding within the bedrock could occur during co-seismic movements and which would need to be accommodated by defensive design measures within the dam. Hereafter, in this report we refer to both primary and secondary faulting in terms of recent (active) fault movements. A broader discussion of the relationship between primary and secondary faults is laid out in Langridge et al. (2011; Section 2) and illustrated in their Figure 2.1.

The proposed A7 dam site is located within the Wakarara Range, which is a structural block of uplifted Mesozoic greywacke, bounded by the Mohaka and Wakarara faults (Figure 1.1 and Figure 1.2). These faults, together with the Mangataura Fault at the southern end of the

block, have been considered in terms of understanding potential primary fault displacement effects and strong ground motions as outlined in previous GNS Science reports (see Langridge and Villamor, 2011; Langridge et al., 2010, 2011). These reports concluded that the fault most likely to produce primary co-seismic displacements in the vicinity of the dam site is the Mohaka Fault, within 1 km of the A7 dam site (Figure 1.1).

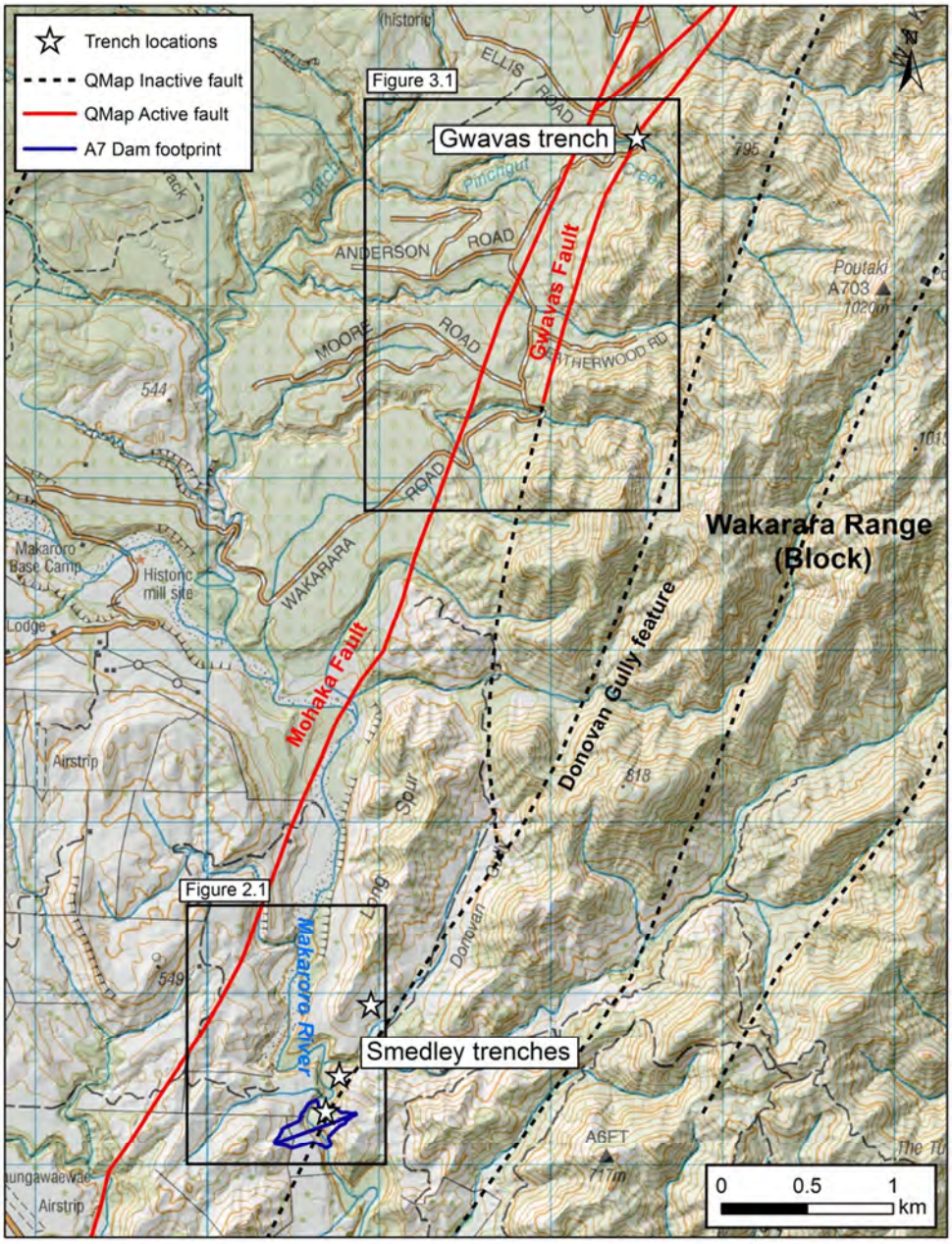

Figure 1.1 Location map of the study area. Three trenches were excavated on Smedley Station adjacent to the Makaroro River gorge (star symbols denote the locations of trenches). One further trench was excavated across the Gwavas Fault in the PanPac Gwavas Forest. Fault linework comes from QMap Hawke's Bay (Lee et al., 2011).

The previous GNS reports have specifically highlighted that there is potential for secondary fault displacement within the dam foundation, related to primary rupture of the Mohaka Fault (or possibly the Wakarara or Mangataura faults) by considering the: 1) proximity of the Mohaka Fault; 2) possible internal deformation within the Wakarara Block as a consequence of movement on either the Mohaka Fault or the Wakarara Fault; 3) proximity of mapped faults in the recently published QMap Hawke's Bay sheet (Lee et al., 2011); and 4) through a

global analysis of secondary displacements related to primary fault movement (Petersen et al., 2011; Langridge et al., 2011).

Map scale and the details on the map are important issues for site-specific studies undertaken for the project. The geologic map of Hawke's Bay (Lee et al., 2011) is published at a scale of 1:250,000. At this scale Lee et al. present several NNE-striking "approximately located, inactive faults" that appear as dashed faults on this map. One of these inactive faults passes through the Makaroro River gorge in the vicinity of the A7 dam site, and then along a side valley called Donovan Gully. For the purposes of this report we name this fault the Donovan Gully feature. Therefore, two points to consider when interpreting the Lee et al. (2011) geologic map are: (i) do these inactive faults show any activity in the vicinity of the dam site, or (ii) are they capable of displacement/movement? Langridge and Villamor (2011) noted several inactive faults from the Lee et al. map in a structural cross-section, highlighting that such features are sub-parallel to the Mohaka Fault and in one case close to the proposed dam site (Figure 1.1).

Site investigations by Tonkin and Taylor (Tonkin and Taylor, 2012a, 2012b) identified many small shear and clay zones, including a NNE-striking zone of shearing and deformation from outcrop and drillhole analysis near the Makaroro gorge (see Figure 1.2). Tonkin and Taylor refer to this zone as "shear zone SZ1" and as a "through-going zone of deformation" characterised by an increase of mudstone (argillite) beds within the greywacke. This zone is sub-parallel to the NE-trending Donovan Gully feature.

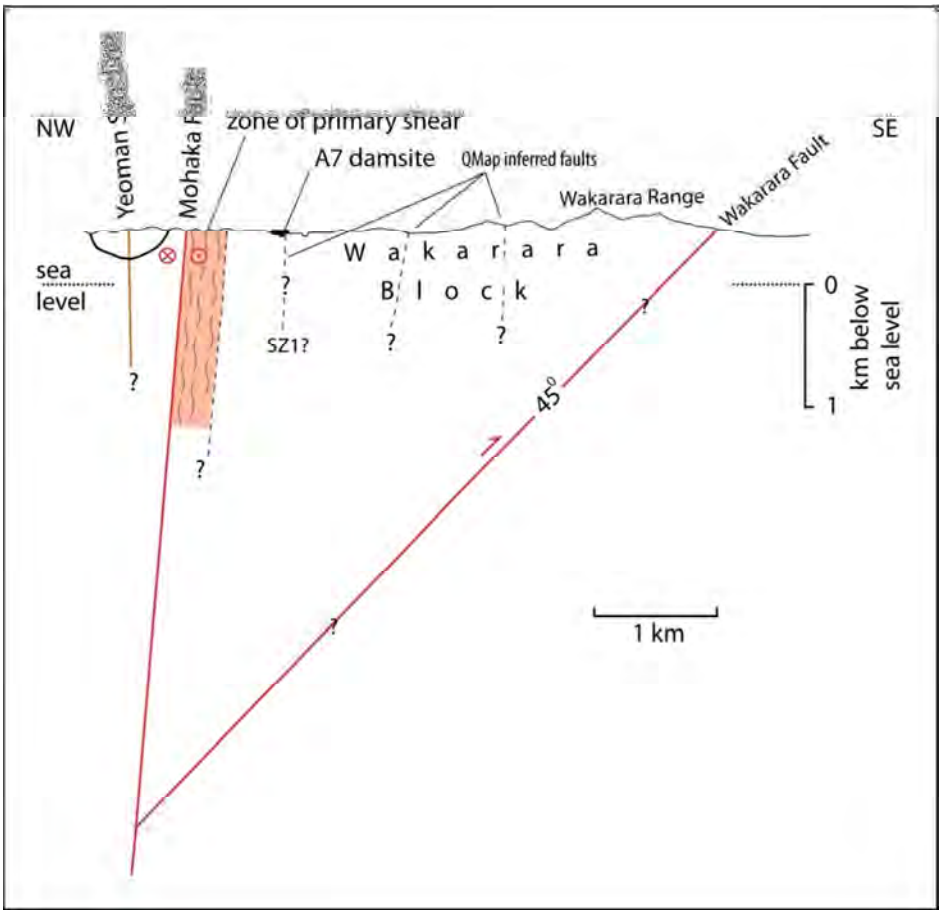

Figure 1.2 Simplified structural cross-section running NW-SE through the proposed A7 dam site on the Makaroro River (adapted from Langridge et al., 2011). Approximately mapped, inactive QMap faults come from Lee et al. (2011) and are potential zones of secondary deformation. The labelled fault SZ1 has been an important focus of this study. In this diagram we assign a dip of 45° to the reverse-slip Wakarara Fault.

Tonkin and Taylor also recognised the assignment of fault activity to traces within the Gwavas Forest (shown on Lee et al., 2011) and as splaying from the Mohaka Fault c. 5 km north of the dam site (Figure 1.1). One of these splays is shown as the northern continuation of one of the inactive faults within the Wakarara Block. An inference was drawn that activity on this fault could be transferred to the Donovan Gully feature/shear zone SZ1 that continues south into the Makaroro gorge in the area of the A7 dam site.

Therefore, the important questions for the proposed A7 dam site to be addressed from this current study are:

1. could secondary fault displacement occur on secondary/subsidiary faults/defects within the bedrock of the dam foundation area as a consequence of, for example, movements on the nearby major active faults?;
2. if so, what is the possible size, style and recurrence of the secondary fault displacements?; and
3. what is the relevance of the inactive Donovan Gully feature and/or shear zone SZ1 in the context of the bedrock underlying the dam site and indeed, what is the potential for fault displacement (large or small) anywhere within the dam foundation of the proposed A7 dam site?
4. are there active splays of the Mohaka Fault in the Gwavas Forest?; and
5. if so, what is the relationship of these active splays with respect to the approximate, inactive faults within the Wakarara Block and, more importantly, in the vicinity of the proposed A7 dam site?

1.3 PROJECT SCOPE AND BRIEF

The technical content of the project brief stated:

In Phase 1C of the feasibility study for the Ruataniwha project, our objectives have been to:

> (i) *"excavate 'paleoseismic' trenches that define whether there is "recent" (i.e., latest Pleistocene or Holocene) displacement across the fault (shear) zone SZ1 in proximity to the footprint of dam site A7, and if so, to quantify the amount and effects of active faulting. The focus of this study is a mapped fault (shear) zone SZ1 that strikes NNE-ward and which potentially traverses close to or within the footprint of the dam on the true left side of the Makaroro River gorge. Shear zone SZ1 has been interpreted as the southern continuation of an 'inactive' bedrock fault mapped on the QMap Hawke's Bay geologic sheet (Lee et al., 2011). It is important to test whether there has been any recent displacement across SZ1 and what its size is"*

and (ii), to excavate:

> *"a third trench to understand the activity on a known active fault trace"* located c. 6 km to the northeast of the A7 dam site.

To achieve these results, we planned to undertake the following tasks:

a. Confirm suitable excavation sites to expose SZ1 on the true left side of the Makaroro in the vicinity of the left abutment using recent Tonkin & Taylor and GNS Science reports (Langridge and Villamor, 2011; Langridge et al., 2010, 2011), field maps and data.
b. Excavate a large (80+ m long x 6 m deep) trench across the inset post-Q2 (Holocene?) alluvial terrace and hillslope edge adjacent to the true left side of the Makaroro River.

Log the trench using paleoseismic techniques to determine the presence and scale of deformation related to the SZ1 shear zone or overlying materials.

c. Excavate a second large (50+ m long x 4 m deep) trench across a linear ridge on the true left side of the Makaroro River, up a side valley known as Donovan Gully. Log the trench using paleoseismic techniques to determine the presence and scale of deformation related to the SZ1 shear zone or overlying materials, if present.
d. Excavate a third short (20 m long x 2 m deep) trench across a known active fault trace located sub-parallel to the Mohaka Fault c. 6 km north of the dam site in the Gwavas Forest. Log the trench using paleoseismic techniques to determine the scale and timing of deformation related to the active trace and overlying materials.
e. Sample organic material for radiocarbon dating and/or fine-grained sediments for tephra analysis and Optically Stimulated Luminescence (OSL) dating of geological deposits. These dates will be used to characterise periods of fault deformation (or lack of deformation).
f. Briefly report on the findings of Tasks 1a-1e. Prepare a preliminary Letter Report that summrises the field observations by February 14, 2013. Prepare a Final Report to precede Resource Consent for the A7 dam site.

In practice, it was not possible to excavate and log such a long and deep trench as planned in (b) above, due to the available space on the terraces and the depth to bedrock under them at Smedley Station. Instead, two shorter trenches were excavated to bedrock in the vicinity of the site in (b).

1.4 REPORT LAYOUT

In Chapter 1 of this report we outline: the brief and scope of the project; the proposed A7 dam site; the regional tectonic and earthquake setting; active faulting in the central Hawke's Bay area; and the potential for secondary faulting near the dam site. We also describe the reasoning and motivation for this current phase of work with respect to the previous GNS Science and Tonkin and Taylor investigations.

In Chapter 2 we present the results of field studies including three trenches excavated within, or very near to, the proposed footprint of the A7 dam site. A large part of Chapter 2 is devoted to presenting geologic results that address the issues of secondary faulting near the dam site.

In Chapter 3 we present the results of additional mapping of faults using high resolution lidar data, a trench excavation and examination of bedrock adjacent to an active fault within the PanPac Gwavas Forest, to address the issues of earthquake rupture activity and the role of splays of the Mohaka Fault, with regards to the potential for such splays to continue in the vicinity of the dam site.

In Chapter 4 we summarise the results of this work and consider the (possibility of the) occurrence and scale of secondary fault deformation (if present) within or adjacent to the footprint of the proposed A7 dam.

In Chapter 5 we provide recommendations for the further investigation of potential displacement hazards within the dam foundation during the construction phase.

1.5 BACKGROUND

1.5.1 The A7 Makaroro River dam site

The A7 Makaroro River dam is an integral part of a wider Ruataniwha Water Storage Scheme that aims to collect water from the Makaroro River and headwaters and to distribute it into five areas for storage and irrigation (Figure 1.3). The A7 dam is the most significant structure required for the proposed irrigation development. As such, seismic hazard and fault deformation at the proposed dam site is of importance especially in relation to the characterisation and mitigation of those hazards.

The proposed A7 dam site is in Central Hawke's Bay District, 60 km southwest of Napier, near the locale of Wakarara at NZMS 260 U22/907539 (Figure 1.1). The dam site is located within a gorge section of the Makaroro River, a tributary of the Waipawa-Tukituki river system that drains to Hawke Bay. Geologically, the site occurs within the "Wakarara Block", a narrow (5 km wide) greywacke range to the east of the Ruahine Ranges. The dam site is located in close proximity to a number of active faults including the Mohaka, Ruahine, Wakarara/Rangefront and the Mangataura faults (Figure 1.1 and Figure 1.3). Some of the geology and earthquake shaking hazards that could affect the district and areas near to this dam site were outlined in earlier GNS reports (Langridge and Villamor, 2011; Langridge et al. 2010, 2011).

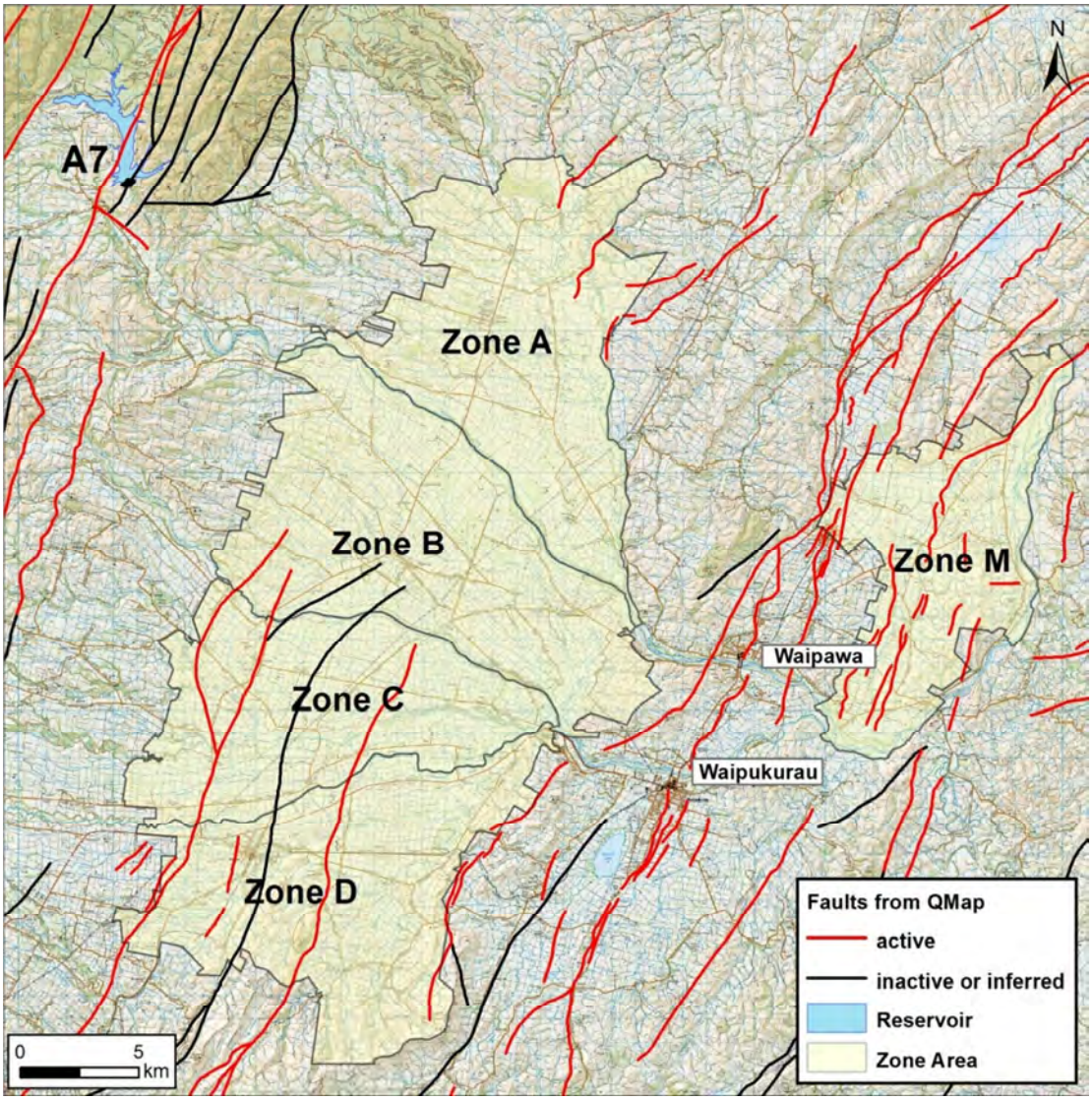

Figure 1.3 Regional physiography and plan of the Ruataniwha Water Storage Project. The proposed A7 Makaroro River dam site and reservoir are shown at top left. Water storage zones are labelled A-D and M. Active (red), inactive and inferred (black) faults are shown from QMap geologic map coverage (Lee et al., 2011).

The Scheme proposes a c. 80 m high dam to be constructed. The left abutment of the dam will be sited in greywacke bedrock against a hillslope above the river. The right abutment of the dam will be sited in a greywacke hillslope and the central portion of the dam traverses the gorge and a wide alluvial terrace. On the true left side of the Makaroro River near the A7 dam site - and where GNS Science undertook much of its work during this phase - the land is managed by Smedley Station.

The proposed A7 Makaroro dam site is located to the east of the Ruahine Ranges and west of the Dannevirke and Ruataniwha Depressions (Figure 1.4). The depressions are areas of subdued topography and typically young surficial (Quaternary) geology with somewhat lesser tectonic activity compared to the Ruahine ranges to the northwest and the coastal ranges to the southeast of them.

In addition to reports by GNS Science (Langridge and Villamor, 2011; Langridge et al. 2010, 2011), preliminary studies by Tonkin and Taylor at the A7 site are summarised in Tonkin & Taylor (2012a, 2012b). Their work included aerial photo analysis and interpretation, bedrock and shear mapping along the Makaroro River, shallow geophysical studies, drilling and the excavation of a trench adjacent to the proposed right abutment of the dam. The A7 reservoir

related to this dam will extend c. 5.8 km upstream and will flood farm land and overlap the trace of the active Mohaka Fault. Bedrock geology changes to the northwest of the Mohaka Fault, where Tertiary marine rocks predominate (Figure 1.4; Lee et al., 2011).

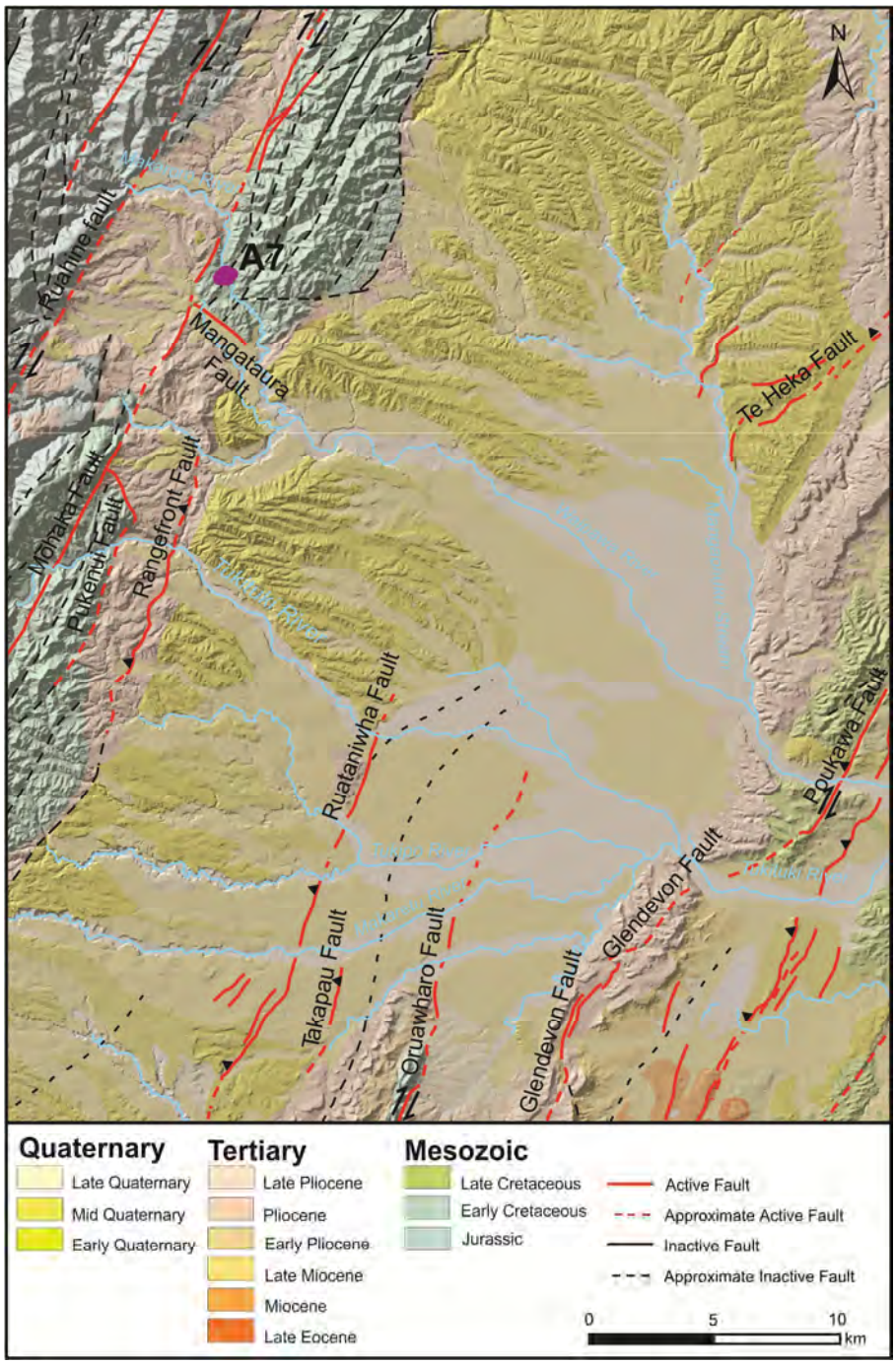

Figure 1.4 Quarter-million (QMap) scale geological map of the Hawke's Bay area prior to this study (Lee et al. 2011). Known active faults are shown as red solid lines and inferred active traces are shown as red dashed lines. Approximate faults are shown as black dashed lines. Up-thrown side of reverse faults is shown with triangles; black arrows indicate sense of strike-slip movement; and tick/ball symbols indicate down-thrown side of normal faults. Proposed A7 dam site is located within the Wakarara Block within greywacke bedrock (light blue). Yellow patterns indicate Quaternary sediments.

1.5.2 Regional tectonic and earthquake setting

New Zealand straddles the boundary between the Australian and Pacific plates, where relative plate motion (which varies from 30 to 50 mm/year) is obliquely convergent across the plate boundary (Figure 1.5). That relative plate motion is expressed in New Zealand by movement on many active faults (Figure 1.3 and Figure 1.4), a high rate of "small-to-moderate" earthquakes (M<7), the occurrence of many "large" earthquakes (M 7-7.9), and one "great" earthquake (M>8) in historical time (Figure 1.6). The most recent moderate to large earthquakes in New Zealand's historical record are the 2010 M_w 7.1 Darfield and 2011 M_w 6.2 Christchurch earthquakes, which caused strong ground motions, liquefaction, surface rupture, rockfalls and vertical deformation (Gledhill et al., 2010; Kaiser et al., 2012).

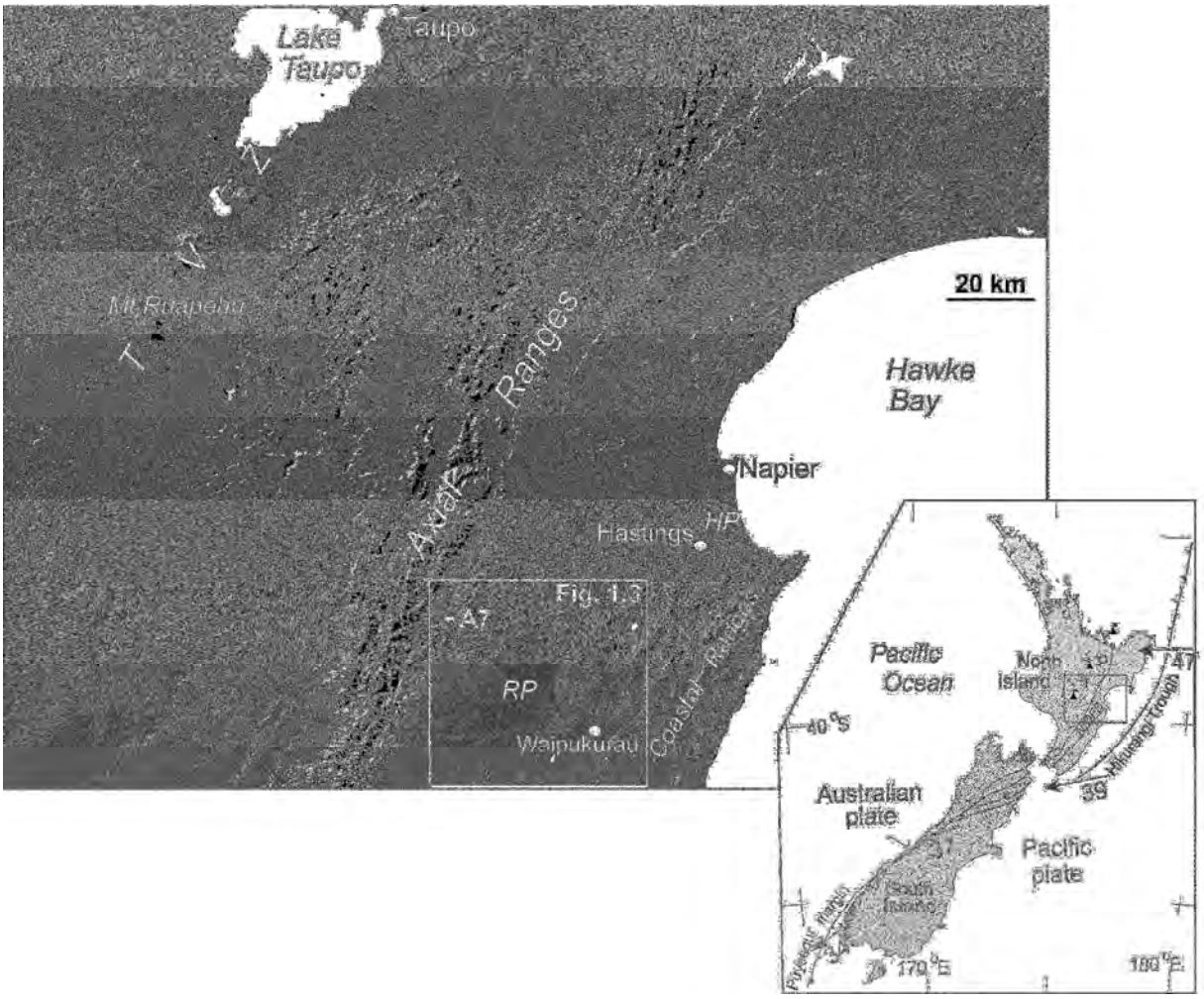

Figure 1.5 Plate tectonic setting of eastern and central North Island showing the major physiographic zones (e.g. Coastal Ranges, tectonic basins of Ruataniwha (RP) and Heretaunga (HP) Plains, Axial Ranges and Taupo Volcanic Zone (TVZ). The wider study area in central Hawke's Bay is outlined by a white box. Inset: Simplified plate tectonic setting of New Zealand with convergence rates in mm/yr. Taupo (T) and Okataina (O) Volcanic Centres are marked by open triangles. NIDFB refers to the North Island Dextral Fault Belt of Beanland (1995).

The tectonics of North Island is dominated by the Hikurangi subduction margin. This margin is characterised by a northwest-dipping subduction zone and by a 450 km long zone of right-lateral to oblique-slip faulting, called the North Island Dextral Fault Belt (NIDFB; Beanland 1995). A significant proportion of the relative plate motion across the North Island is accommodated by slip and large earthquakes on the faults of the NIDFB (Beanland et al., 1998). The proposed Ruataniwha Water Storage Project lies within the NIDFB, between the eastern edge of the North Island Axial Ranges and the western edge of the Ruataniwha

Basin, within one of the more tectonically active parts of this boundary zone (Figure 1.4 and Figure 1.5). In addition to upper plate faults, the eastern North Island, including Hawke's Bay is underlain by the Hikurangi subduction zone. In this region, the subducting Pacific plate also provides a potential source of large to great (i.e. M 7-8^{+}) earthquakes (e.g. Stirling et al., 2012; Wallace et al., 2012).

The Hawke's Bay region and eastern North Island has a well-documented record of historical earthquakes that have been both damaging and destructive. This history is described in more detail in previous GNS Science reports (e.g. Langridge et al., 2011). Moderate to large shallow historical earthquakes in the region are shown on Figure 1.6.

Figure 1.6 Epicentral locations of large earthquakes in New Zealand from 1848-2010 (http://www.geonet.org.nz/).

1.5.3 Active faulting in Central Hawke's Bay

The large earthquakes in the region have been and will be associated with the major active faults. In addition to being underlain by the subducting Pacific plate, the study area is traversed by a number of significant active faults, including the Mohaka Fault, Ruahine Fault, Ruataniwha Fault, and Waipukurau Fault Zone (Figure 1.4), which can generate earthquakes of estimated magnitudes in the range of about M_w 6.8 to 7.6, and with average recurrence intervals ranging from <1000 years to in excess of 10,000 years (Berryman and Beanland, 1991; Stirling et al., 2012). Such earthquakes on these faults would generate large (i.e. metre-scale) single-event surface rupture displacements. Active upper plate faults in the Hawke's Bay region have a variety of structural styles, ranging from strike-slip, e.g. Mohaka

Fault, to reverse or reverse-oblique slip, e.g. Ruataniwha Fault, Poukawa Fault Zone (Kelsey et al., 1998; Klos 2009).

2.0 BEDROCK TRENCHES AT SMEDLEY STATION

In this chapter we present the results from the excavation of trenches and pits on the true left side of the Makaroro River within and near the footprint of the proposed A7 dam site. A major goal of this work was to expose the greywacke bedrock in order to map the bedding (including strikes/dips) and defects (faults, fractures, shear zones) within the rock and to show their relationship to much younger units overlying the bedrock.

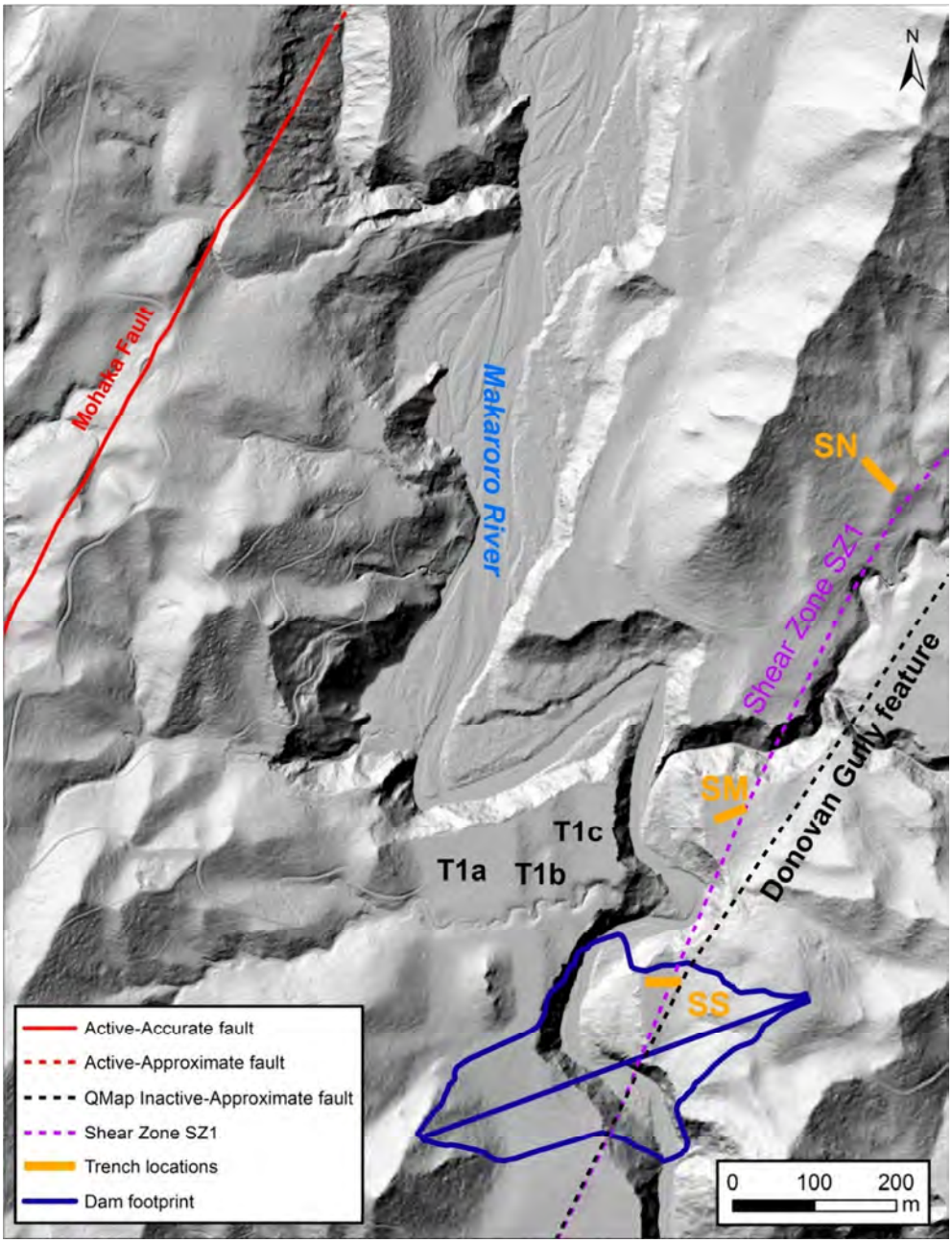

Figure 2.1 Lidar-derived hillshade model of the Makaroro River gorge area. The footprint of the A7 dam site is shown in dark blue. The NNE-trending structural fabric in the area is highlighted by the active Mohaka Fault (red) and the approximate location of the "Donovan Gully feature" (black dashes) and possible shear zone SZ1 (purple dashes). Trenches excavated on Smedley Station shown as yellow bars; e.g. SS = Smedley South trench.

One of the most important parts of the project relates to the site selection for the location of trenches. Our focus lay with investigating likely candidate targets that provided an opportunity to investigate/excavate: the bedrock within the A7 dam foundation area; the nature of the

Donovan Gully feature/shear zone SZ1; and intercept geomorphically-oriented linear features that may indicate recent fault movements. Our investigations were undertaken on the true left side of the river on Smedley Station in order to target the Donovan Gully feature/shear zone SZ1. These trenches were named Smedley South, Smedley Middle and Smedley North trenches and were located either on a prominent intermediate level terrace of the Makaroro River (Terrace T1c) and at a hillslope site where both excavation and 4-wheel drive access was possible (Figure 1.1 and Figure 2.2). For these reasons, these sites were considered our best candidate sites for characterising the potential for secondary deformation.

Following excavation, the bedrock trench floors and cover deposits were cleaned, gridded and logged in detail at a scale of c. 1:20 to closely analyse the bedrock. In each of the three trenches we exposed cover deposits of probable late Quaternary age overlying the greywacke bedrock. The cover deposits were composed primarily of gravels and finer deposits and were useful in assessing whether bedrock defects observed in the trenches had experienced any recent tectonic movements/displacements.

2.1 SMEDLEY SOUTH TRENCH

The Smedley South trench was excavated within the proposed foundation area of the dam adjacent to an exploratory trench excavated by Tonkin and Taylor in October 2011 (Figure 2.1). Prior to excavation of the trench, we excavated an exploratory pit at the site to determine the depth to greywacke bedrock and to assess the stability of cover deposits (mainly gravels) in terms of the safety of excavating a deep trench. Based on the instability of the thick gravels in vertical section, it was deemed practical to grade the sides of the Smedley South trench to a moderate angle (c. 40°; Figure 2.3).

The trench was excavated at an orientation of 086° (roughly E-W) across an alluvial terrace (T1c) where we might expect to intercept the Donovan Gully feature and/or “shear zone SZ1” described by Tonkin & Taylor (Figure 2.1). They show in their preliminary trench that SZ1 is a broad, mappable, SE-dipping zone of deformation that cuts across T1c and the hillslope.

The Smedley South trench was ~40 m long and up to 6 m deep. The base of the trench was excavated 20-50 cm into the top of the bedrock so that the eroded top of the bedrock could be observed in cross-section and that a relatively flat floor could be created in hard bedrock that could be gridded and logged in the same way that trench walls are usually logged (Figure 2.4).

The upper contact of the bedrock is formed by an erosion surface, which is in turn overlain by alluvial gravel and fine-grained cover deposits. Such an alluvial erosion surface is called a strath and is formed by lateral cutting as the river is carving out its floodplain. This strath is also important to the outcomes of this study as it provides a marker plane with which to investigate whether deformation on defects in the bedrock has affected the strath or the overlying cover deposits.

2.1.1 Stratigraphy at the Smedley South site

2.1.1.1 Terrace, cover-bed and pit stratigraphy

The Smedley South trench was excavated across the width of a gently sloping (5° E) abandoned alluvial surface (T1c), and at its eastern end into the edge of an eroded hillslope (Figure 2.1). The stratigraphy of the alluvial terrace at the site was most easily observed and logged from the vertical sides of an exploratory pit, adjacent to the Smedley South trench. The pit was excavated to a depth of c. 5 m where greywacke bedrock was encountered (Figure 2.5).

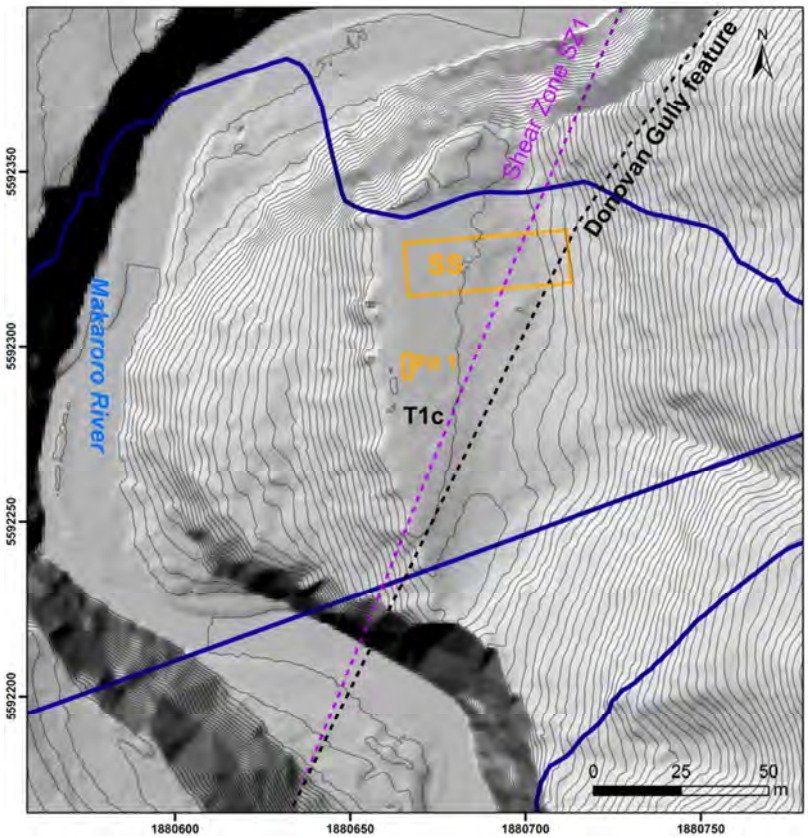

Figure 2.2 Location map of the Smedley South site within the proposed foundation area of the A7 dam (dark blue line). The trench was excavated on Terrace T1c with the aim of intercepting shear zone SZ1 (in purple).

Figure 2.3 Excavation of the Smedley South trench was achieved using a 30 tonne excavator, to a depth of up to 6 metres. The logged face (at right) was graded to an angle of c. 40 degrees for safety.

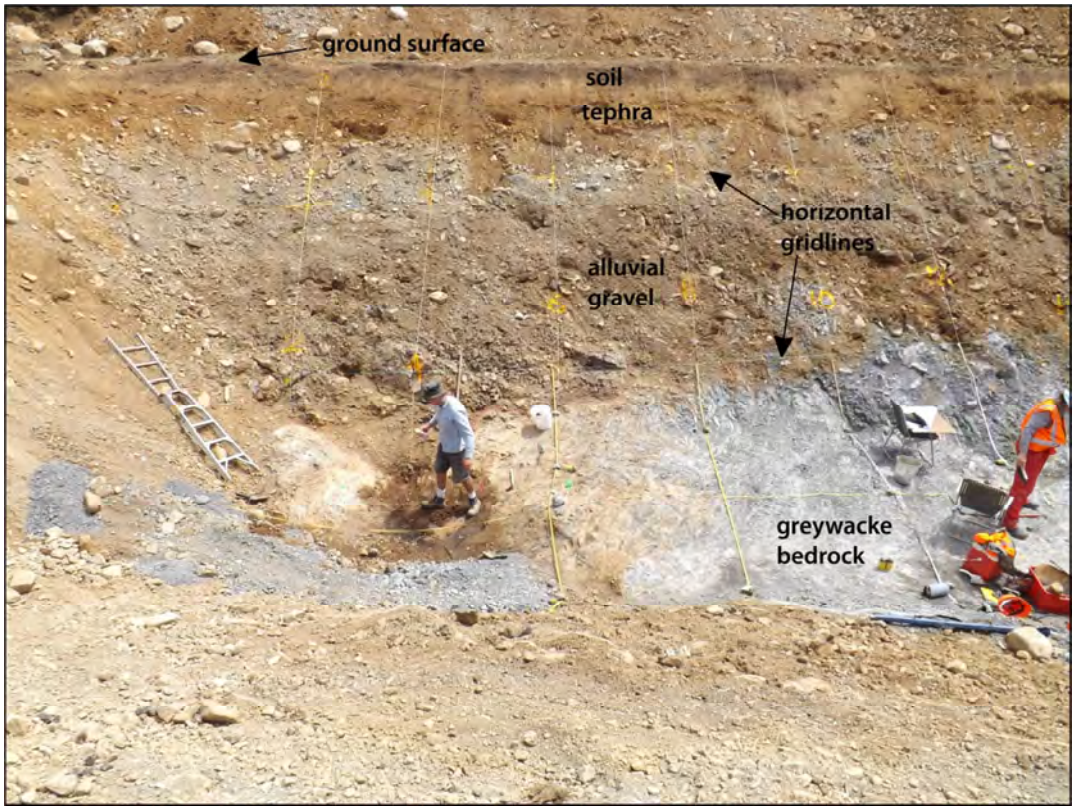

Figure 2.4 Layout of Smedley South trench. The grey material at the floor is greywacke bedrock, while the brown materials above it are gravel and tephra cover deposits. The 40° graded face was gridded with horizontal strings placed 2 m apart vertically and horizontally. The floor was also gridded for logging.

The stratigraphy exposed in the exploratory pit (Figure 2.5) corresponds with that observed in the centre and west end of the trench (Figure 2.4 and Figure 2.8). Greywacke bedrock is overlain by c. 3.3 m of very coarse gravel (equivalent to unit 11 in the trench). This coarser gravel is overlain by c. 1 m of finer (pebble) gravels (equivalent to unit 10) which is in turn overlain by c. 0.5-0.7 m of orange-brown fine sandy silts (e.g., units 2 and 2D). These brown fine-grained deposits are interpreted as mixed Holocene tephra (volcanic ash) or tephric silt, into which a soil has developed (e.g., unit 1). Such a sequence represents a classic alluvial cycle of river aggradation (coarse gravel) followed by alluvial degradation (fine gravel), fluvial abandonment and landscape stability (mantling of tephra).

At the east end of the trench the upper section of deposits is expanded where a broad channel cut has eroded into, and then deposited fine sediments on, the gravel terrace surface (and oxidised orange gravels) at the back edge of the terrace (Figure 2.7 to Figure 2.10). In this area, the upper section comprises a basal, fine channel gravel deposit (unit 12), and two distinct channel-filling sand and silt beds (units 4 and 4B). These channel deposits are overlain by a pair of relatively flat-lying and distinctive beds; a yellow tephra (unit 3B) and a grey silt (unit 3A). These beds appear to fill the uppermost part of the broad channel, as a ponded fill (Figure 2.8). Both the yellow tephra and grey silt form discontinuous beds that have been disrupted (boudinaged and/or liquefied), either by loading or from strong shaking.

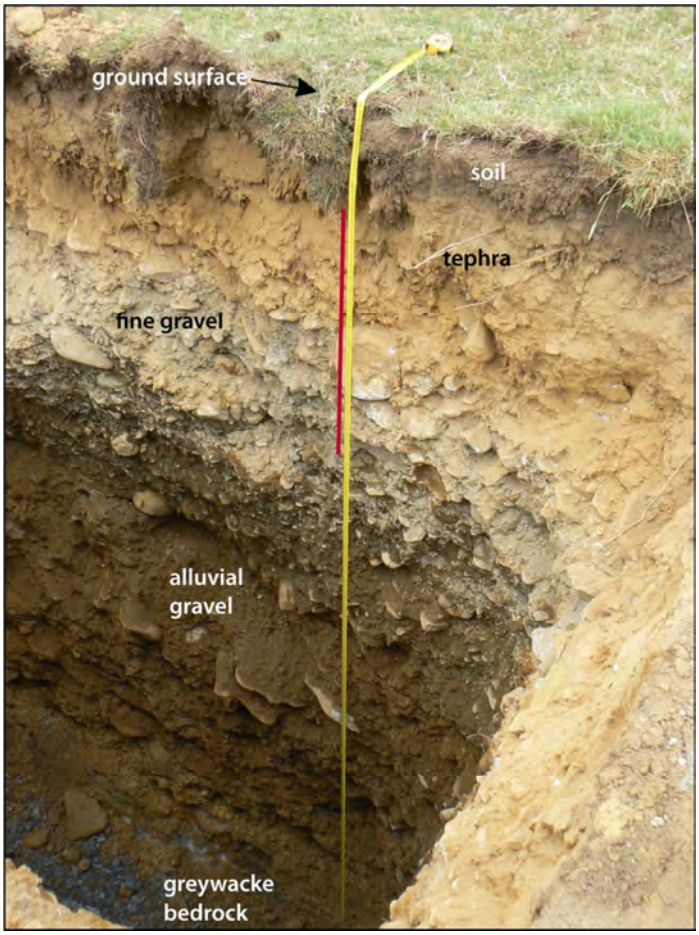

Figure 2.5 Exploratory pit excavated to bedrock at the Smedley South site. The red line marks one metre of depth extending toward the floor of the pit.

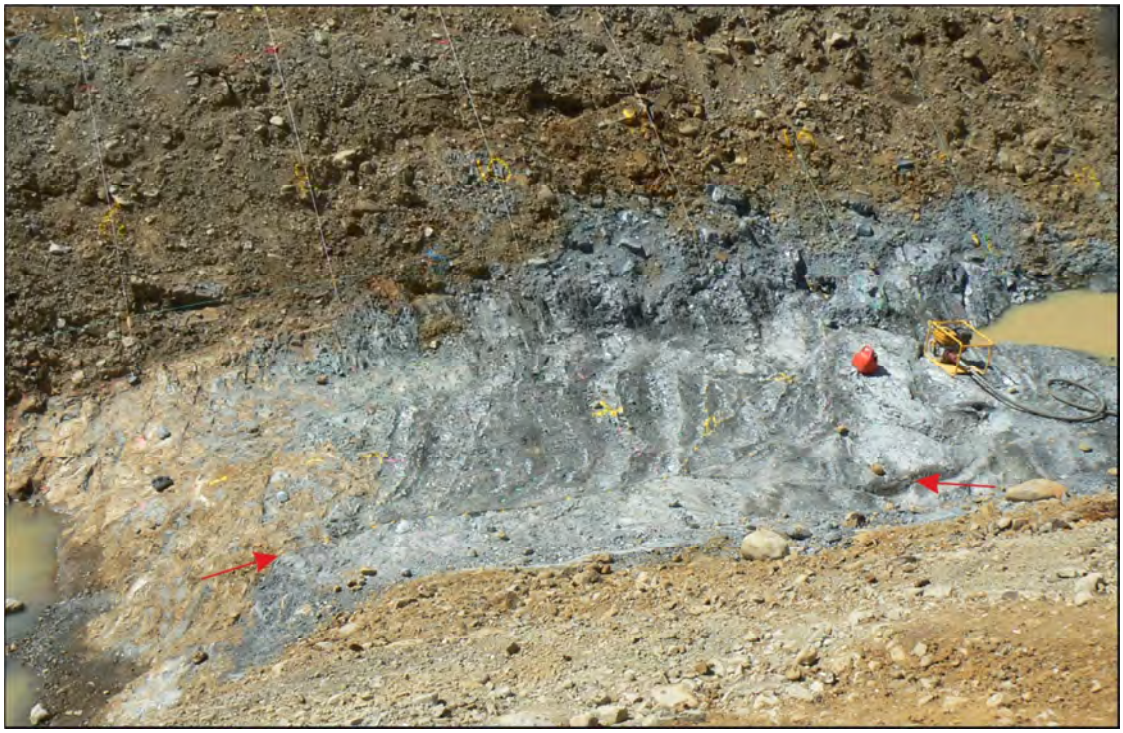

Figure 2.6 View of the variability within the greywacke bedrock in the floor of the Smedley South trench between metres-6 to -16. Light grey bands demark sandstone beds, while dark grey bands demark argillite beds. Red arrows mark a long fault that truncates the argillite-rich package of beds.

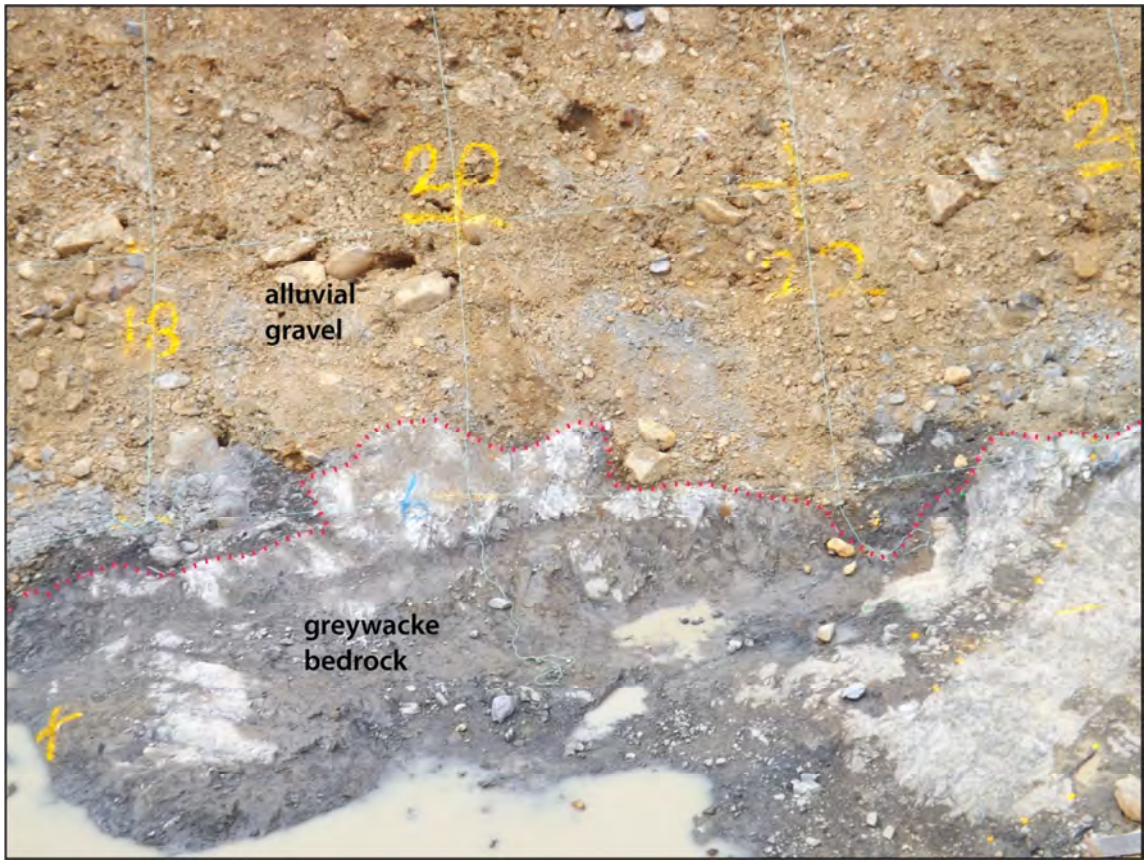

Figure 2.7 View of the floor and base of the batter in the Smedley South trench. The pink dotted line above the floor represents the erosional strath that separates the bedrock from the overlying orange-coloured (oxidised) gravel deposits.

In addition, there are several hillslope-derived units that have been deposited on top of the channel-fill units within the trench (Figure 2.8 to Figure 2.10). These include a wedge-shaped medium brown silty clay that dries with a prismatic soil texture (unit 1D). We infer that this unit was formerly a soil which slumped across the ponded section and in doing so, deformed the top of the ponded section (Figure 2.10). The brown colluvial soil is overlain by angular colluvial gravel (unit 1C) and capped by a thin young hillslope soil.

2.1.1.2 Geologic dating of cover beds

A critical component of this study is to characterise the age of the alluvial strath terrace and the cover deposits in this trench, because if there is fault deformation - or equally if there is no deformation – then we can attempt to characterise the amount of time since the last deformation. Because not all geologic deposits can be dated we developed a geomorphic and stratigraphic model while in the field that was consistent with our understanding of the landscape and recent geologic processes.

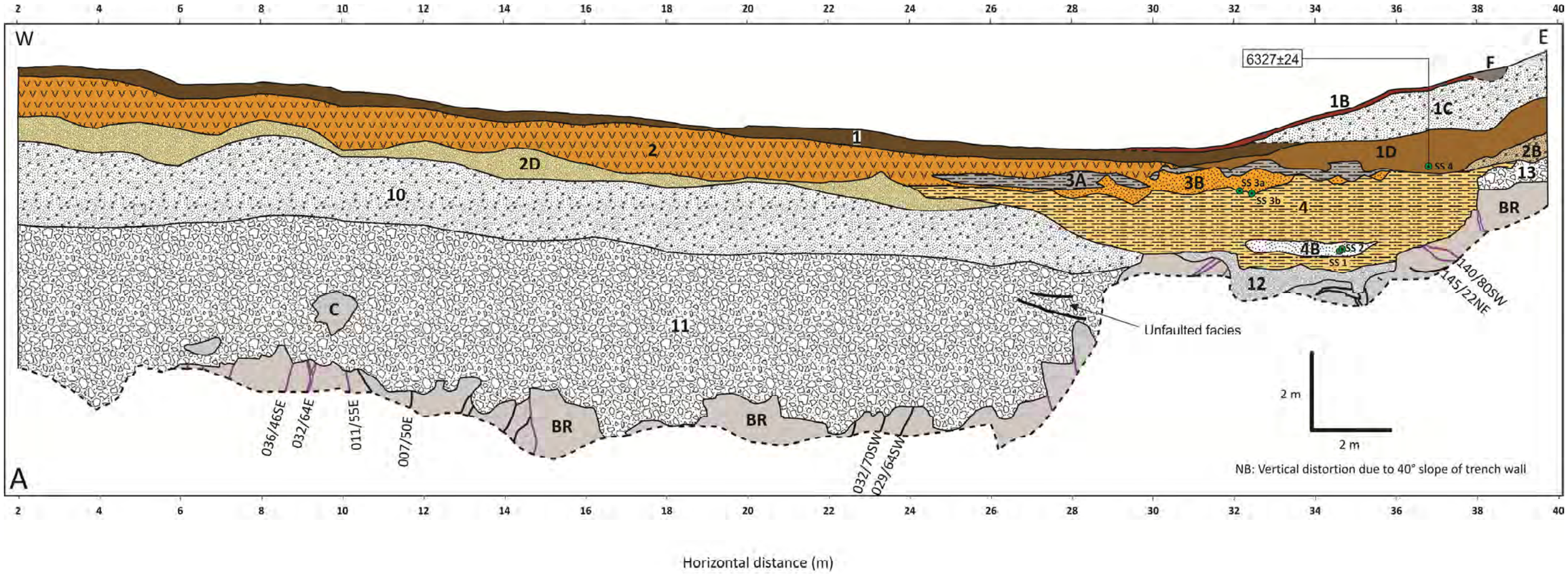

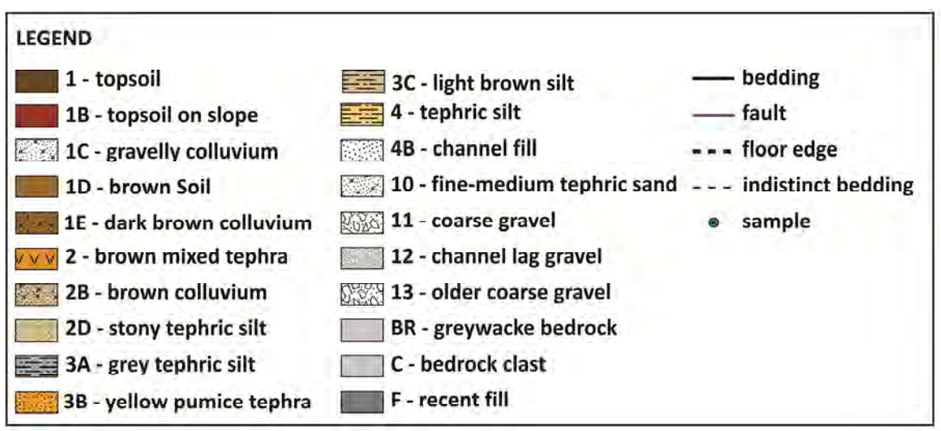

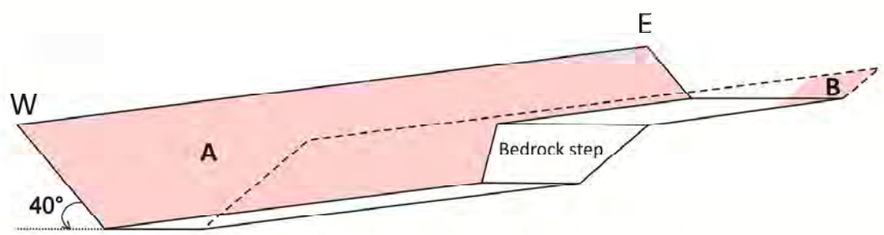

Schematic diagram of trench - not to scale

TEPHRA CORRELATIONS				
Sample Name	Unit	Sample Type	Correlation	Age C-14 yr BP
SS-2	4B	Tephric sand	No correlation	-
SS-3	3B	Yellow tephra	Karapiti Tephra	10,030±90
-	3A	Grey silt/stratigraphic correlation	Poronui Tephra	9,840±60

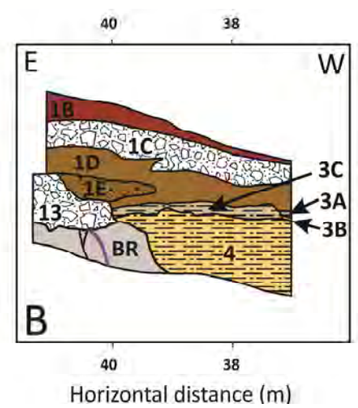

Figure 2.8 Smedley South trench walls. **A).** Geologic log of the North Wall of the trench. **B).** Geologic log of part of the South Wall at the eastern end of the trench. Log legend, 3-D geometry and geologic age constraints are also shown. Detailed unit descriptions are presented for each unit in Appendix 1.1.

This page is intentionally left blank.

The sequence of cover deposits and the presence of the bedrock strath exposed in the trench and pit are consistent with climate-driven alluvial stratigraphy that has developed during latest Pleistocene to Holocene times in the eastern North Island (Litchfield and Berryman, 2005). That is, aggradation during the last glacial period (thick gravels), typically followed by the deposition of degradation gravels in the post-glacial period (finer gravels). After the terrace is abandoned by further downcutting (by the Makaroro River) the terrace sequence is capped by overbank and channel-filling deposits (especially in the channel) and airfall tephra (volcanic ash). Therefore, we infer that the thick, coarse gravel sequence is related to aggradation that formed valley–wide alluvial terraces from c. 30,000-18,000 years before present (yr BP). This is often referred to as the Ohakean aggradation (Milne, 1973; Litchfield and Berryman, 2005). Finer gravels overlying this sequence may be related to subsequent post-Ohakean alluvial degradation.

In keeping with these conventions we refer to this flight of terraces as terrace T1, with the highest, broadest terrace being T1a. In terms of valley terrace heights, the Smedley South site correlates well with the lowest of this flight of three terraces that are all separated by c. 5 m of elevation (Figure 2.1). This may indicate that as the river incised from its highest level that it produced at least two degradational terraces, the lower of which we have named T1c.

In this model the thicker, coarser unit 11 gravels that were deposited across the bedrock strath belong to the Ohakean phase of aggradation (correlating to T1a) and the thinner, medium gravels that comprise unit 10 are a degradational suite of gravels (related to T1c) and would have been deposited following the cutting of an erosional contact on top of the older unit 11 gravels. This could indicate that the unit 10 gravels were deposited after the Last Glacial Maximum (LGM) and could be of age 14,000-10,000 yr BP.

Further, we anticipate that the tephra are likely to be of latest Pleistocene to Holocene age. This is because they cap the aggradation/degradation gravel sequence, but also because they have strong colours (orange-brown) and are associated with soil development, both of which imply weathering in a warmer (post glacial) climate. The main source area for Holocene tephra in the eastern North Island is from the Taupo Volcanic Zone, which comprises both large andesite volcanoes such as Mt. Ruapehu and large rhyolite calderas, such as Lake Taupo and the Okataina Volcanic Centre (Figure 1.5).

To date the sediments and test/validate the stratigraphic model we sampled organic material for radiocarbon dating; tephra, reworked tephra and sediment for tephra analysis, and a sediment sample for Optically Stimulated Luminescence (OSL) dating. A single bulk radiocarbon sample was collected from within the brown colluvial soil unit (unit 1D) that overlies the ponded section near the east end of the trench (Figure 2.8 and Figure 2.10). Sample SS-4 was submitted for radiocarbon dating at the Rafter Radiocarbon Laboratory and yielded an age of 6327 ± 24 ^{14}C yr BP. This date is calendar-calibrated to an age of 7028-7270 cal yr BP (Table 3.1). This bulk sample provides an average age of the organic material within a large sample of soil. Nonetheless, as this soil has slumped across the pond and forms part of the toe of the hillslope, it provides a minimum age for the cessation of ponding and for the construction of the current hillslope exposed in the east end of the trench.

Volcanic glass was separated from samples SS-3 (unit 3B) and SS-2 (unit 4B) for geochemical analysis at the Victoria University Tephra Analysis Unit. Sample SS-3 came from the yellow tephra near the top of the ponded section. Analysis of the volcanic glass within sample SS-3 indicates that this tephra is from the Taupo Volcanic Centre (TVC; Appendix 2).

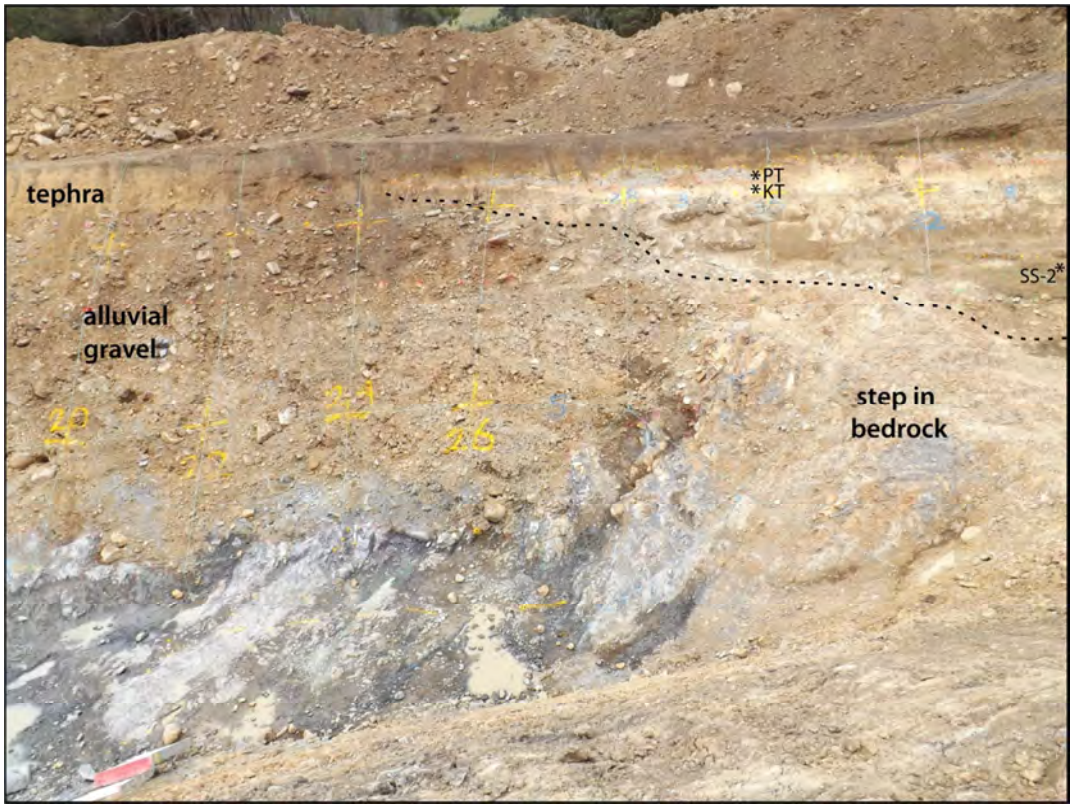

Figure 2.9 Photo of ponded channel fill stratigraphy at the east end of the Smedley South trench overlying alluvial gravels and bedrock (base of channel marked by a dashed line). Samples that provide age control to the cover beds are marked by stars (e.g. SS-2); PT and KT have been correlated to the Poronui and Karapiti tephras.

Figure 2.10 Photo showing the expanded section of cover deposits at the east end of the Smedley South trench. Samples for geologic dating were taken from the brown soil (SS-4), the yellow tephra (KT = Karapiti Tephra) and the channel sand (SS-2 at lower centre).

Based on glass chemistry this deposit is best correlated with the Karapiti, Taupo, Mapara or Motutere tephras. When compared to standard glass analyses and when major elements are plotted against each other (e.g. CaO vs. FeO) and K_2O vs. FeO), the Karapiti Tephra is the strongest candidate for a correlative with sample SS-3. If we also consider the stratigraphic position of the tephra and the radiocarbon age overlying this, then the most likely result is that this yellow tephra is the Karapiti Tephra from the TVC (10,030 ± 30 cal yr BP; Lowe et al., 2012)[1].

Sample SS-2 from within unit 4B, is a medium-grained tephric alluvial sand near the base of the channel fill near the east end of the trench. With this sample we hoped to be able to provide a minimum age on the gravel aggradation package, because unit 4B overlies the thicker gravel package (units 10 and 11). This sample contained no recognisable volcanic glass shards and could not be analysed for the purposes of tephra correlation. However, sand unit 4B did contain microlites which are indicative of andesitic tephra (B. Alloway, personal communication, 2013). A separate split of this unit (SS-1) was collected (in a light-free stainless steel tube) for OSL dating. Sample SS-1 was submitted to the Victoria University Luminescence Laboratory for OSL analysis. Unfortunately, the time frame for this type of dating means that the result for this sample will not be available until July 2013 and so will be reported at a later time.

In summary, the geologic age dating appears to support/confirm the stratigraphic model that was developed in the field. That is, the radiocarbon date from unit 1D indicates that the channel and ponded section is of Holocene age and at least c. 7000 yr old. Underlying this are two tephra, the older one being well matched to the Karapiti Tephra from the TVC, and having an age of c. 10,000 yr. This is in keeping with our understanding that the thick gravel package that underlies the channel/ponded section is of latest Pleistocene to early Holocene age (at least 10,000-14,000 yr).

2.1.2 Bedrock geology

The bedrock in the area of the A7 dam site and across the Wakarara Block is comprised of Cretaceous age Torlesse (Pahau terrane – Waioeka Petrofacies; c. 145 Ma) greywacke (Lee et al. 2011) - often referred to as (Mesozoic or Torlesse) greywacke in this report. In New Zealand, Torlesse greywacke comprises interbedded layers of weakly metamorphosed sandstone and mudstone units (e.g. Rattenbury et al., 2006).

About 40 m of greywacke bedrock (unit BR; Figure 2.7 and Figure 2.8) was exposed in the floor of the trench over a floor width of 2-4 m. At the east and west ends of the trench the bedrock types (lithologies) were dominated by sandstone facies, while in the middle of the trench (especially between metres 8-28; Figure 2.11), there were more mixed lithologies of sandstone and interbedded mudstone (argillite) facies (Figure 2.6). We observed that defects such as faults and shear zones were more commonly found in the fine-grained argillite-rich beds than within the greywacke sandstone beds. This is consistent with the description of shear zone SZ1 in the Tonkin and Taylor Dam Feasibility reports.

[1] In Chapter 3 we document that the grey sand/silt found above the yellow tephra in this sequence is probably the Poronui Tephra (9840 ± 60 cal yr BP).

This page is intentionally left blank.

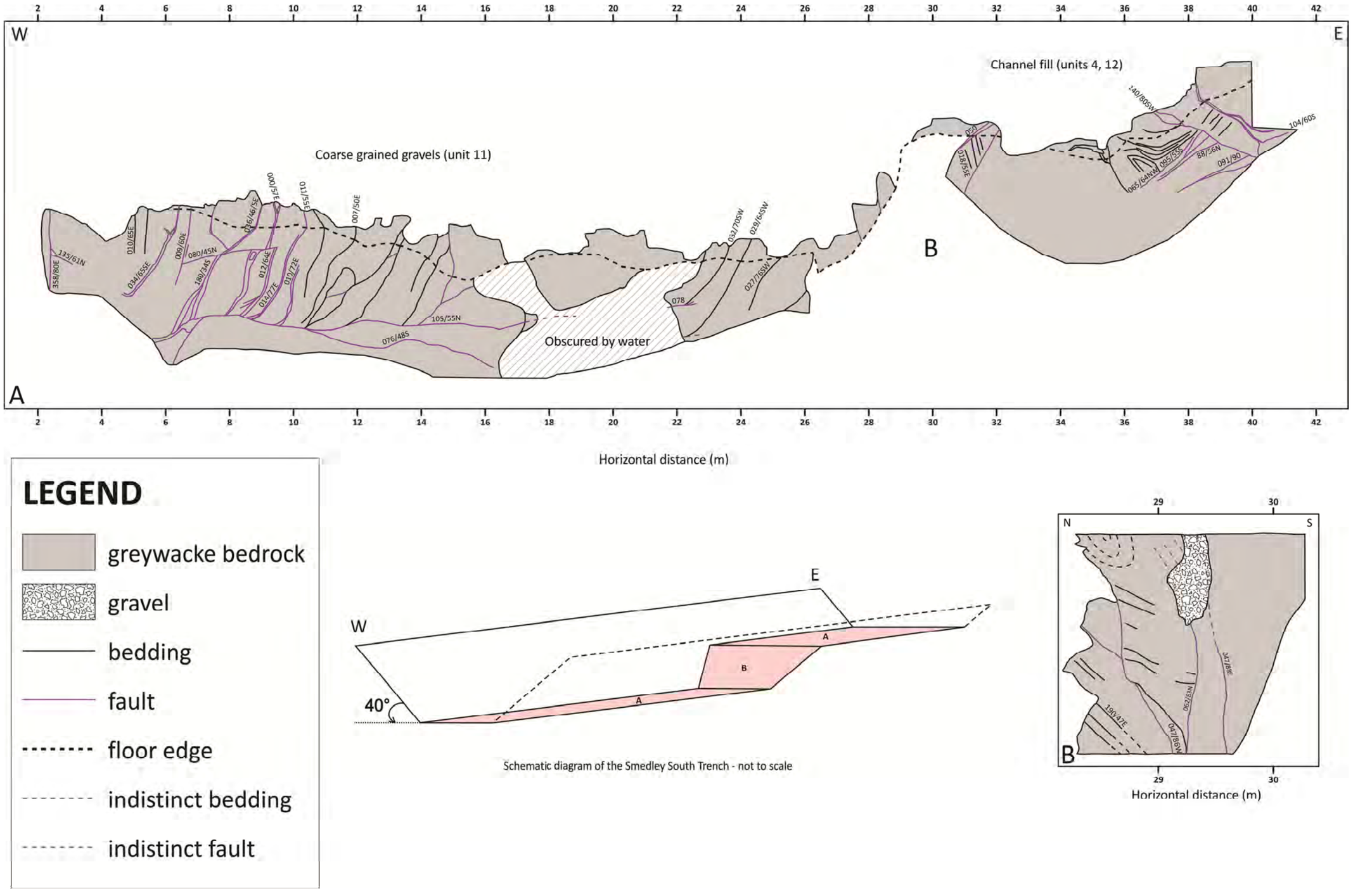

Figure 2.11 Smedley South trench floor. **A).** Geologic log of the bedrock floor of the trench, showing the continuity of beds (black) and faults (purple). **B).** Geologic log of a part of the North Wall between metres-27 to -30. Legend and trench 3-D geometry are also shown.

This page is intentionally left blank.

Argillite beds were commonly 10-30 cm in thickness, while sandstone beds could reach thicknesses of up to 50-100 cm. Common bedrock attitudes (bedding strike and dips) were 000° to 036° (average 017° = NNE) and dips were typically moderate and to the southeast (3 of 17 beds measured dipped to the NW). The average dip to the southeast was c. 59°; thus, the average strike and dip of bedding measured in the trench equates to c. 017/59° SE (Figure 2.12 and Figure 2.13) (Appendix 4). There were a few folds expressed by bed trends that are c. east-west. This is also consistent with bedrock attitude data in the Tonkin and Taylor feasibility reports.

2.1.2.1 Bedrock deformation in the trench

In this section we present the results of mapping bedrock defects in detail for the purposes of understanding fault deformation. Our goals were: (i) to look at the relationship between the bedrock strath surface and overlying deposits to see whether there is any recent (late Quaternary) displacement on these shears and into the cover beds; and (ii) to analyse the shears/fault rocks to assess whether the soft clays are a product of recent faulting or older faulting processes.

2.1.2.2 General definitions of bedrock defects

Defects express the structure and potentially the timing of tectonic (fault) movements within bedrock, which is of high importance to the focus of this study. Bedrock defects refer to fractures (cracks with no displacement or opening), or fissures (fractures with opening between the blocks only) and faults or shear zones (where there is relative horizontal and/or vertical displacement between the blocks) within the rockmass (Appendix 4).

A shear zone is a zone of strong deformation (with a high strain rate) surrounded by rocks with a lower state of finite strain. Shear zones form a continuum of geological structures, ranging from brittle shear zones (or faults) through brittle–ductile shear zones (or semi-brittle shear zones), and ductile–brittle to ductile shear zones. Brittle shear happens at shallow levels of the crust. In brittle shear zones, the deformation is concentrated in a narrow fracture surface separating the wall rocks. Ductile deformation occurs at deeper crustal levels (high temperature and pressure) and the deformation is spread out through a wider zone, the deformation state varying continuously from fault wall to wall. Between these end-members, there are intermediate types of brittle–ductile shear zones (Ramsay and Huber 1983).

In general terms, at the depths exposed in the trench brittle shear would be expected to occur as a consequence of recent rupture. As deformation occurs, the grinding and milling that results when the two sides of the fault zone move along each other results in a material that is made of loose fragments. First a fault breccia will form, but if the grinding continues the rock becomes fault gouge and cataclasite (Appendix 4) (Davis and Reynolds, 1996). In brittle fault rocks and/or on the fault walls, striae or slickensides (lines or groves indicating the direction of relative movement of the fault walls) may form when movement occur. These are used as kinematic indicators (i.e., indicators that there has been movement and/or the actual movement sense. i.e., normal, reverse, horizontal motion).

At deeper levels in the crust, fault rupture will produce semi brittle to ductile deformation and create fault rocks, such as mylonites (Appendix 4) (Davis and Reynolds, 1996). These types of fault rocks are found on the surface only when exhumation brings those deeper materials to the surface. Exhumation is usually a process that lasts from hundreds of thousands to millions of years and thus mylonites found at the surface are commonly features of old

faulting. The shape of the minerals and the mineral shadows within the mylonite are used as kinematic indicators (e.g., sense of movement).

2.1.2.3 Bedrock defects exposed in Smedley South trench

Basement defects exposed in the Smedley South trench ranged from fractures with no infill, to hard sheared rock and also sheared rock with clay to soft clay infills. Shear zones show definitive evidence for past displacement in the form of infills and slickensides. Therefore in this study we paid the most attention to mapping shear zones (faults) with sheared or soft infill, while little attention was given to fractures.

The sheared zones commonly cluster into two strike directions; roughly ENE- and roughly NNE strikes (Figure 2.14). The sheared zones were more concentrated in the argillite beds, i.e. parallel to NNE-striking bedding, but also cross-cut the sandstone beds in places. There were 2 or 3 E-W-striking faults exposed along the length of the trench floor, traceable for up to 10 m along the floor. These faults cross-cut or merge with the NNE-striking faults that were concentrated in argillite beds. Cross-cutting and merging relationships show that the ENE-striking faults could have been active after, or contemporaneously with, the formation of the NNE- faults. The NNE-striking faults are generally shorter (at least in the exposure) but they commonly crop out at the bedrock-gravel (strath).

Structurally, the strath has an undulating form with “topographic” highs that correspond with strong sandstone beds and lows that correspond strongly with weaker argillite beds and sheared zones. In the low areas it was critical to investigate the relationship between the sheared zones and the strath (Figure 2.7), and to determine if the strath and overlying cover deposits are displaced by movement on the bedrock shear zones.

In two locations near metre-28 and metre-38 on the log, significant vertical steps in the strath surface coincided with bedrock faults with soft clay infills. These steps in the strath occur from metre-26 to -30 where the strath steps up by c. 4 m, and from metre-32 to -38, where the strath steps up c. 1.7 m vertically. In these cases there was the possibility that the steps may represent locations of recent (i.e. post-strath) fault displacements. Therefore, in these two cases we looked more carefully at the geologic relationships to better understand whether they were related to deformation. At the first of these near metre 28 (Figure 2.8), at least two steps in the bedrock occurred in the area where the rock climbed sharply to the bedrock high near the east end of the trench. In this area we water-blasted the gravel above a prominent step in the strath above a bedrock shear and mapped layering within the gravel (unit 11). The gravel facies (lines) were not displaced across the top of the step and shear, implying that there was no recent vertical fault deformation related to the 4 m step in the bedrock/gravel contact.

For the other prominent step in the bedrock/gravel strath near metre-38, we looked at the opposite wall of the trench to verify whether there was a similar step in the strath at that point. The log of that part of the south wall (Figure 2.8) indicates that there was no such step across the strath. From this we were able to confirm that the step observed on the north wall was an erosional feature rather than a tectonic displacement. Therefore, in both cases, the steps or topography seen in the strath could be explained as an erosional step in the strath related to the preferential erosion of weaker rock. Further to this, we found no evidence for vertical movement or faulting within any of the cover deposits (gravels, sediments, tephra etc.)

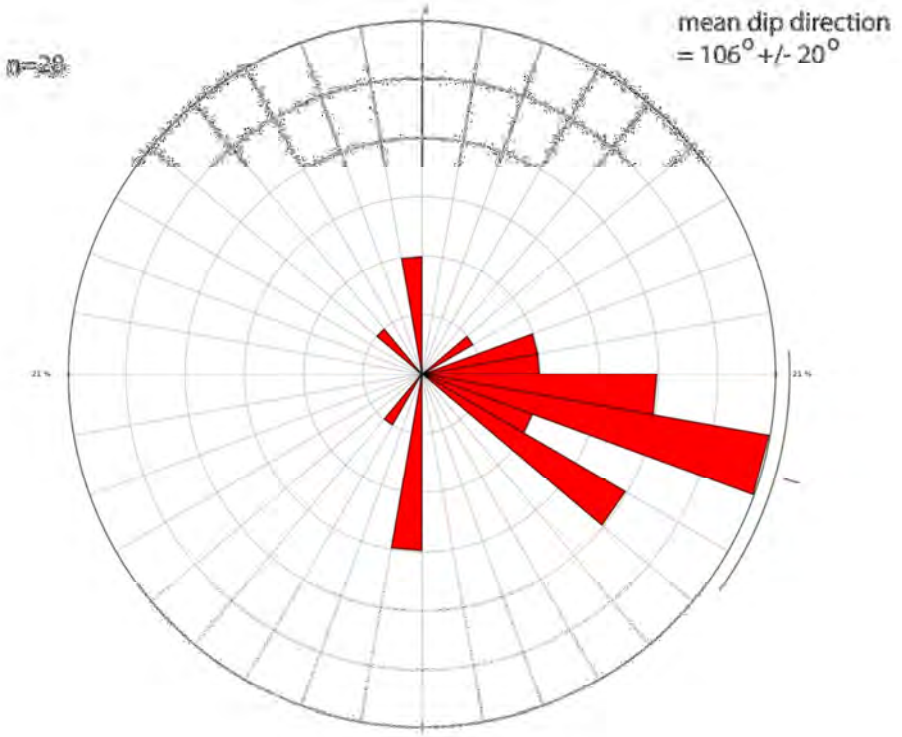

Figure 2.12 Rose diagram displaying the dip directions of all beds measured from the three Smedley Station trenches. The predominant dip direction is ESE, which translates to a predominant NNE strike.

In addition to the analysis of potential deformation, or lack thereof, of the bedrock/gravel strath and/or the overlying late Quaternary gravels described above, we have analysed the nature of the shear zones themselves to assess whether they have experienced recent movements, or not. While a detailed microscopic study of the fault rock is beyond the scope of this study, observation of hand specimens agreed with the results above, that faulting has not occurred recently along the shear zones mentioned. In particular, we paid attention to the nature of the shear zone infill (i.e. does it correspond to materials that could have formed recently such as breccia and fault gouge?) and kinematic indicators (i.e. do they have slickensides?).

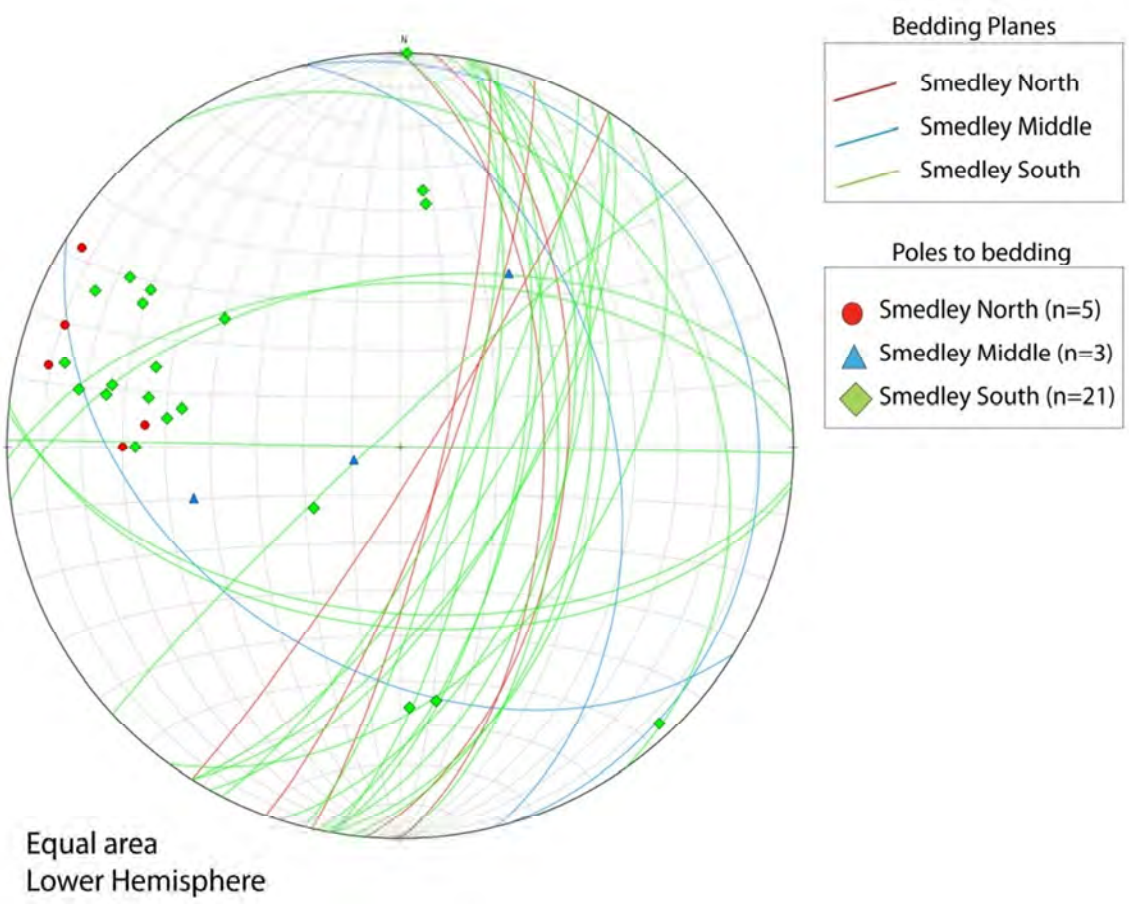

Figure 2.13 Stereonet diagram displaying the poles and great circles of all beds (n=28) measured from the three Smedley Station trenches. E-W striking planes are typically related to folded beds.

Clay infill was found in the two shear zones in Smedley South trench described above (Figure 2.8; at metres-28 and -38 in the trench floor and walls). These two faults have attitudes of 047/86° W and 104/60° S, respectively. In both cases, the clay infill occurred in the upper <0.5 m of the shear plane and fault rock (structured in bands of light coloured minerals, in a dark matrix, likely to represent a cataclasite to mylonite, with left lateral sense of movement) was found below the clay at deeper levels of the same shear zones. Field examination of the transition from fault rock to clay showed that the clay was a product of superficial weathering of the fault rock. The intense weathering of fault rock into clays occurred because of the presence of abundant water at the contact between the Quaternary gravels and the basement at these two locations. Therefore, the clay found as infill of shear zones at the Smedley South trench was not fault gouge produced by 'recent' rupture but instead the product of weathering of an old fault rock. The clay and the fault rock do not show any evidence of current brittle shearing such as slickensides.

Our results indicate that for the Smedley South trench, none of the shears/faults that we observed within the bedrock and up to the level of the bedrock/gravel strath displayed recent fault movement. In addition, no faulting was observed within the cover deposits. This implies a lack of fault movement during at least the last 10,000 years (based on the ages described in section 2.1.1.2). Shear zone SZ1 corresponds to a zone of argillite rich greywacke within the rockmass. This zone must be displaced along E-W striking faults and is therefore semi-continuous in terms of its strike continuity. Finally, clay infill and fault rocks observed within the shear zones are probably not related to recent fault movements.

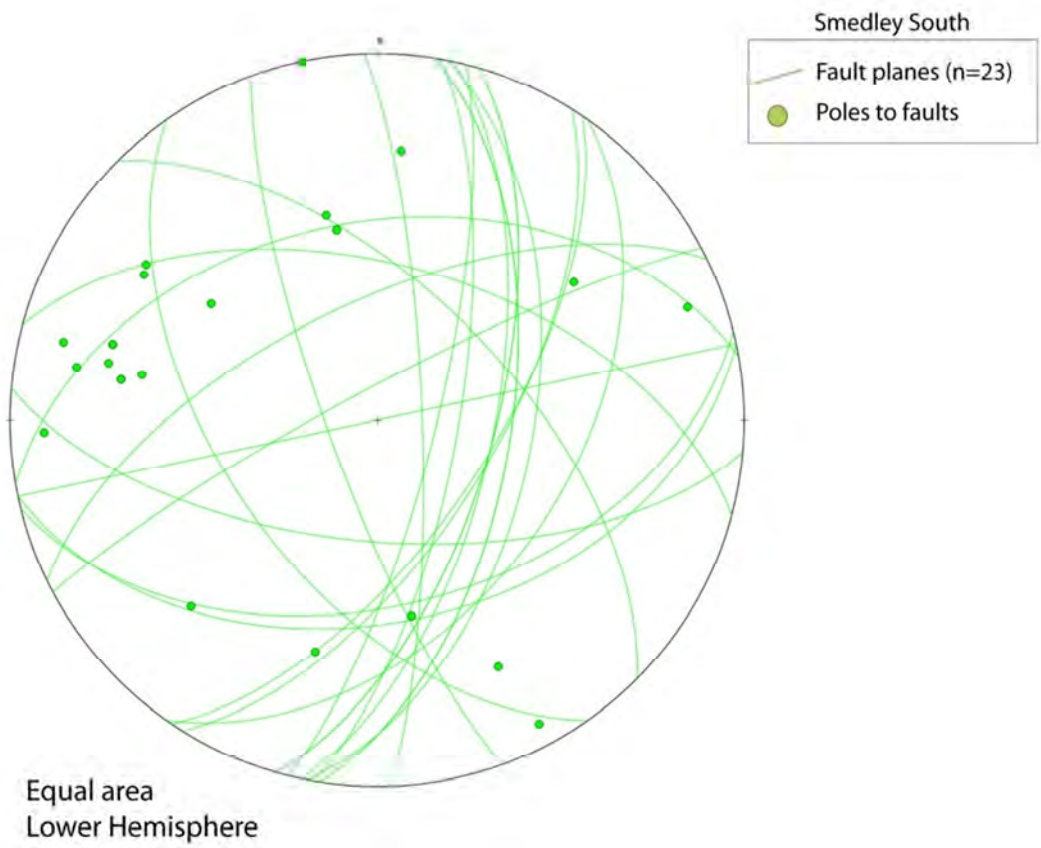

Figure 2.14 Stereonet diagram displaying the poles and great circles of faults (n=21) measured from the Smedley South trench. There is a tendency toward NNE-striking and ESE-dipping faults and E-W striking faults, which are similar to bedding in the Smedley South trench (Figure 2.13).

2.2 SMEDLEY MIDDLE TRENCH

The Smedley Middle trench was excavated c. 270 m NNE of the Smedley South trench across an alluvial terrace at c. 6 m higher elevation than the terrace trenched at Smedley South (Figure 2.1). Two exploratory pits were excavated at the Middle site to test the depth to greywacke bedrock. Because of the excessive depth to bedrock in the upper pit and the need to therefore excavate very large volumes of material, the trench was limited to the lower terrace at the Smedley Middle site (Figure 2.15 to Figure 2.17).

Smedley Middle trench was more than 30 m long and up to 6 m deep. The trench batters were inclined at an angle of c. 45° for safety. As with the Smedley South trench, bedrock was exposed in the floor of the trench and at the base of the batter in order to view both the structure within the bedrock and the nature of the contact between the greywacke bedrock and the overlying gravel cover deposits. The trench was excavated at an orientation of 065° with the hope that we might intercept shear zone SZ1 at the eastern end of the trench (see Figure 2.16).

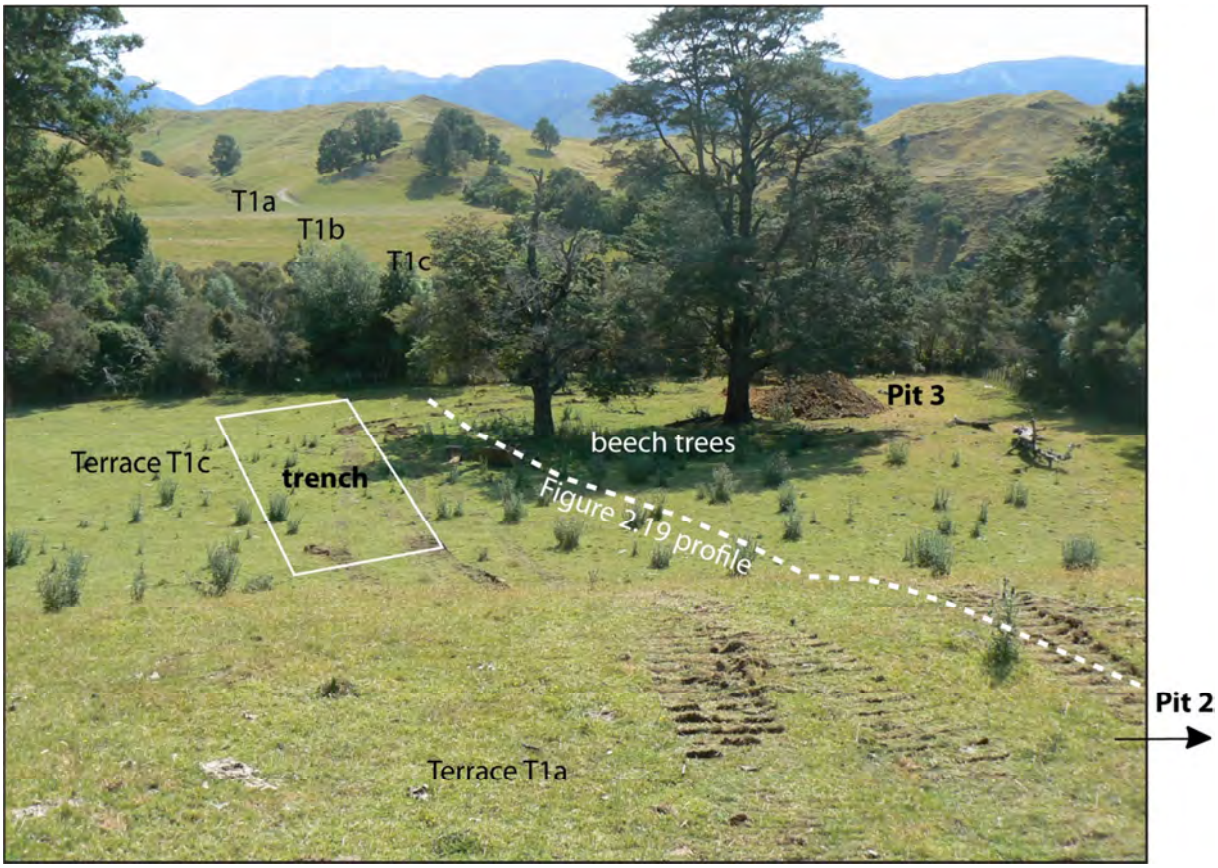

Figure 2.15 The Smedley Middle site, view to the west. At this location alluvial terraces of the Makaroro River (T1a, T1b, T1c) occur on both sides of the gorge (vegetated at centre), just upstream of the proposed footprint of the A7 dam. The photo is taken next to the site of the upper exploratory pit looking toward Pit 2 (spoils at right) and future site of the trench (to the left of the smaller beech tree) – see Figure 2.19b for profile.

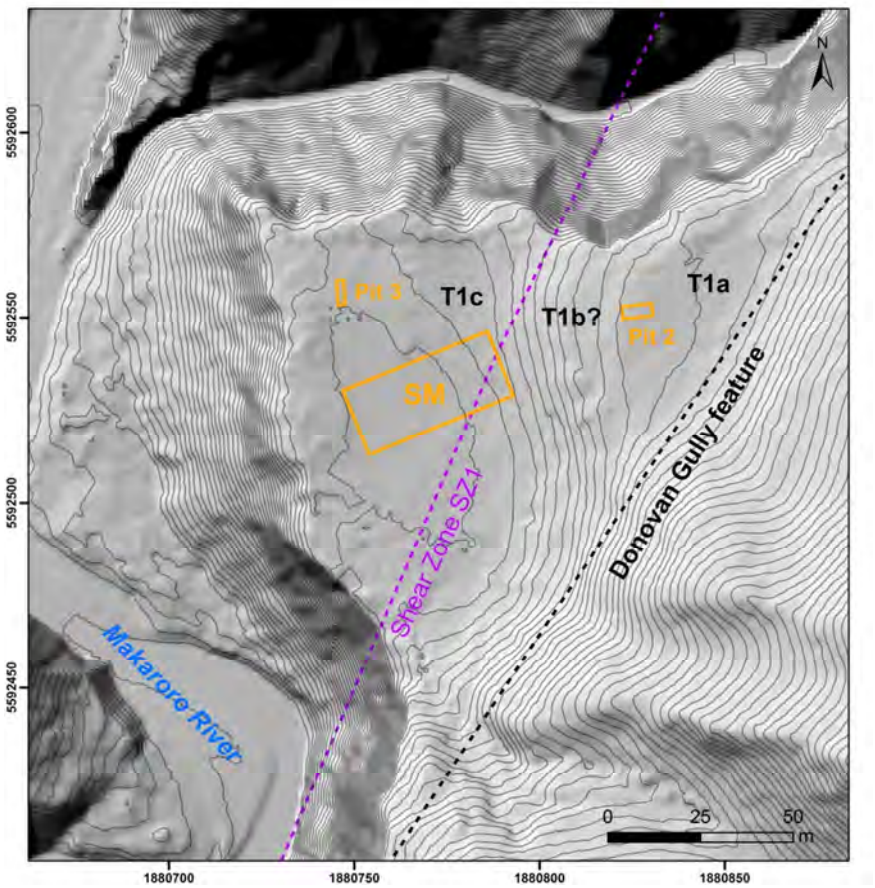

Figure 2.16 Location map of the Smedley Middle site upstream of the proposed foundation area of the A7 dam. The trench was excavated to bedrock on alluvial terrace T1c. Pits 2 and 3 were excavated on T1a and T1c.

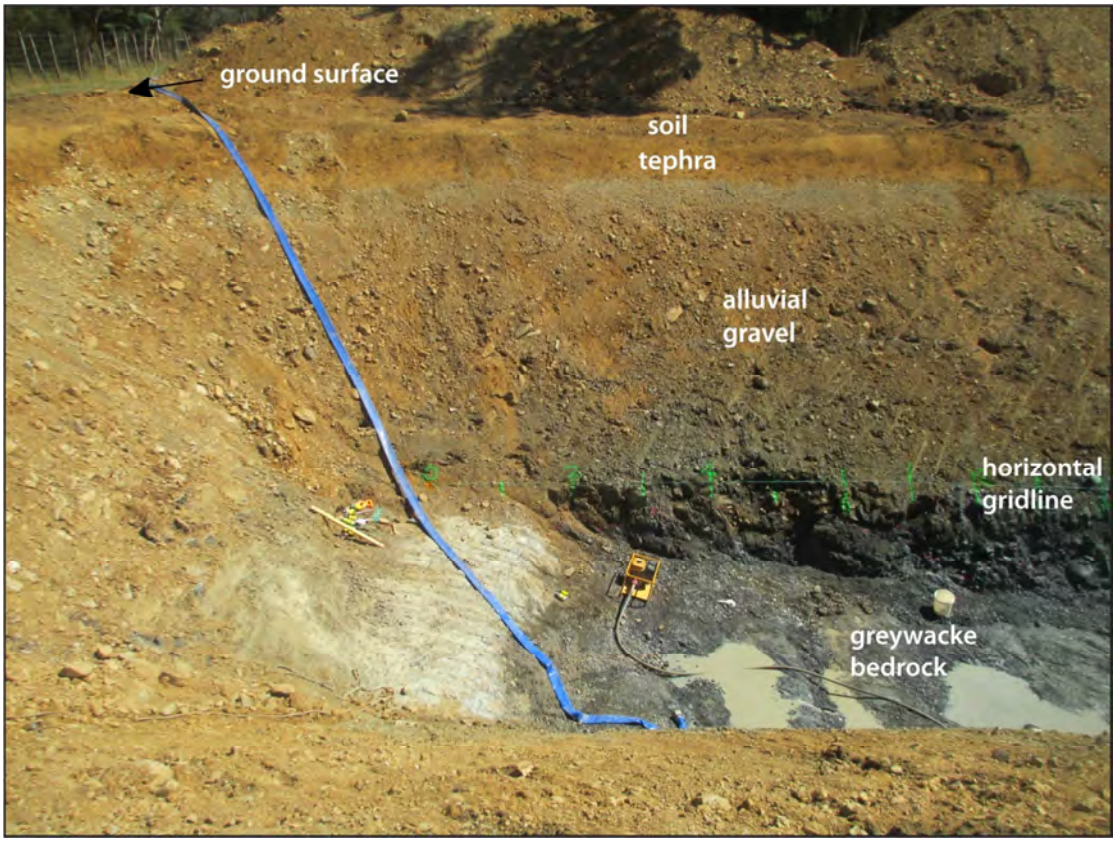

Figure 2.17 Layout of the Smedley Middle trench. Greywacke bedrock makes up the floor of the trench, and is covered by coarse, alluvial gravel and mixed Holocene tephra near the ground surface.

Figure 2.18 The upper exploratory pit at the Smedley Middle trench. The pit was excavated to a depth of 6.2 m but did not reach down to bedrock beneath gravelly deposits.

2.2.1 Stratigraphy at the Smedley Middle site

2.2.1.1 Terrace, pit and cover bed stratigraphy

Exploratory pit #3, adjacent to the Middle trench, exposed bedrock at c. 3.4 m depth. The stratigraphy of this pit is similar to both the Smedley South pit and trench. A fine to coarse cobble gravel deposit, with a thickness of c. 1.8 m, overlies greywacke bedrock. This is overlain by a c. 60 cm thick, moderately well sorted pebble gravel. These two gravel packages that overlie the bedrock/gravel strath surface probably correspond to the aggradation and subsequent degradation gravels described for the Smedley South site. Overlying these units is 15 cm of mixed tephra and gravel and c. 85 cm of light-orange brown sandy tephric cover material. A soil has developed into the uppermost 20 cm of this material. The stratigraphic column for Pit 3 should be used as representative of the coverbed stratigraphy of the lower terrace at this site, i.e. including the trench (Figure 2.19).

The second pit was located on a higher terrace surface, 11 m in elevation higher than the other pit (Figure 2.18). This pit (#2) was excavated to a depth of 6.2 m but did not reach greywacke bedrock. The stratigraphy of Pit #2 and its terrace is shown on Figure 2.19 and summarised in Figure 2.21.

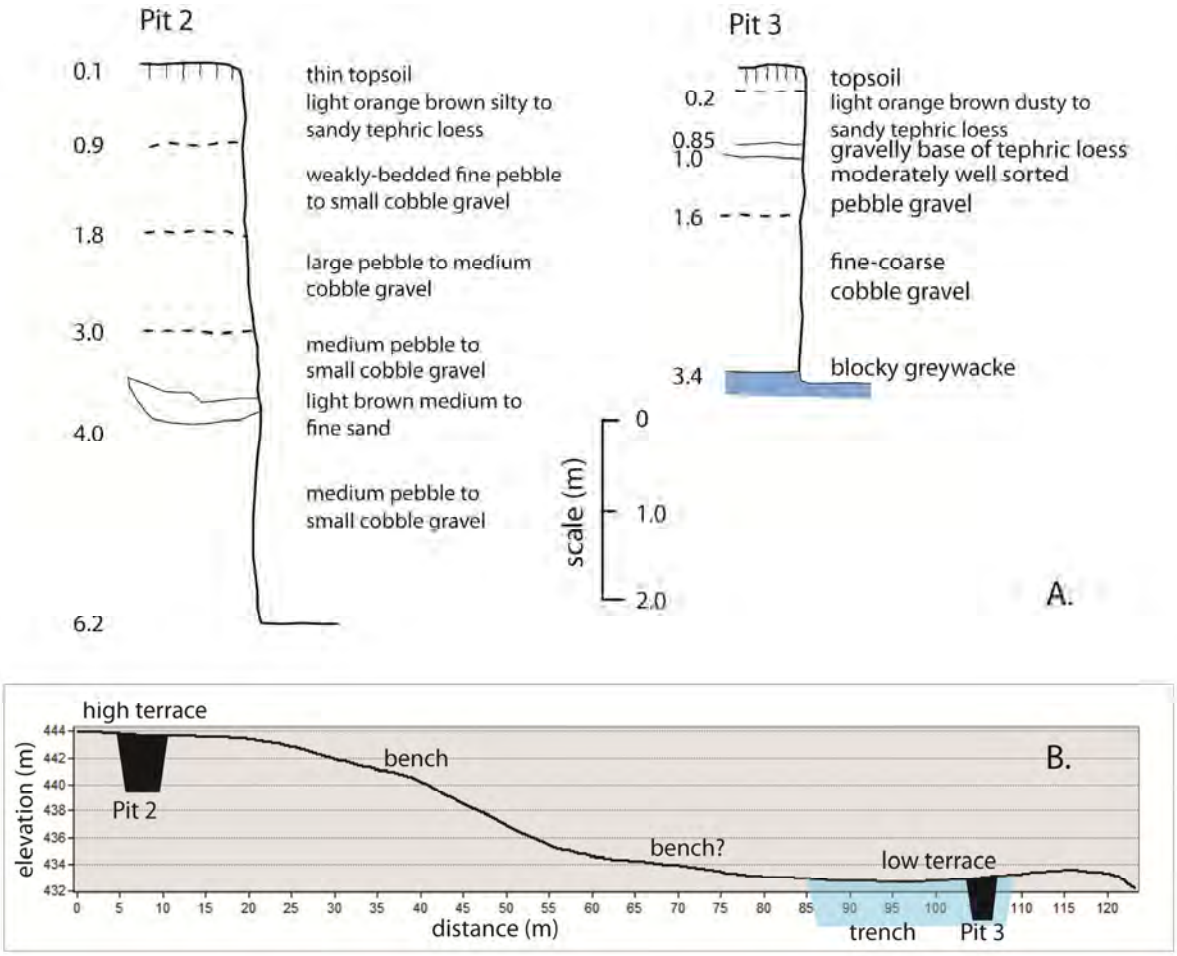

Figure 2.19 Geomorphic and stratigraphic relations at the Smedley Middle site. A. Stratigraphy exposed in the two exploratory pits excavated. B. Topographic profile including the two pits and Smedley Middle trench. Pit 2 was excavated into a terrace surface that is 11 m higher than Pit 3 and the trench. Profile location on Figure 2.15.

2.2.1.2 Bedrock

The bedrock lithologies in the Middle trench were dominated by greywacke sandstone, with less common mixed lithologies of sandstone and interbedded mudstone (argillite). The bedrock/gravel strath was c. 1 m lower at the eastern end of the trench. At the topographically-lowest areas of the strath near metre-11, the contact was overlain by very large rounded boulders of greywacke of up to 70 cm diameter (Figure 2.20). We mapped lithologies within the greywacke and structural features (bedding, faults etc.) in in a similar fashion to the Smedley South trench. Measured bedrock attitudes (strike and dips) were typically ESE- to SSE-striking, e.g. 122/43° S and 166/45° NE (Figure 2.13).

2.2.2 Bedrock defects

In this trench, the bedrock/gravel strath was mapped in detail and bedrock attitudes, faults, shears and joints (defects) were measured (Appendix 3). We also carefully investigated the relationship between bedrock defects, the strath contact and overlying gravel deposits. The bedrock/gravel strath contact was undulatory over the length of the trench exposure. Two of the main topographic lows in the undulations were associated with erosional channel cuts corresponding with soft clay shear zones in the bedrock. They were not related to any visible evidence of recent fault displacement.

Figure 2.20 The bedrock/gravel strath within the Smedley Middle trench near metre-12 (marked by pink dots). Coarse gravels overlie the strath. These have been slightly altered by groundwater. Sub-vertical dark clay shears can be seen within the greywacke bedrock to the right of the scraper.

One of these shear zones was associated with a 10-20 cm wide zone of soft grey clay and black argillite, having an attitude of 145/55° NE in the trench wall. This sheared zone projected up to a low point in the strath which was filled by a channelised gravel. No displacement of the strath or overlying gravel was observed at this location. The soft grey clay and black argillite appeared to be more like weathered fault rock than recent fault gouge.

At the east end of the trench, a second sheared zone occurred directly beneath a step in the bedrock/gravel strath. In this area, two shears, a black argillite shear and a soft grey clay shear, had attitudes of 017/75° E and 039/60° E, respectively. Importantly, these shears did not appear to offset the bedrock/gravel strath, nor the overlying gravel deposits.

Based on the location of the Smedley Middle trench from mapping and surveying (Figure 2.16) we probably did not encounter “shear zone SZ1” in that trench. Smedley Middle trench was dominated by greywacke sandstone facies within which we mapped two pervasive fault zones with sheared clays; at metre-6 and metre-12 on the log (Figure 2.21). Our experience from both the Smedley South and Middle trenches is that though there is focused deformation within beds in the argillite facies of the greywacke (corresponding to shear zone SZ1), there are other individual faults/shear zones within and cross-cutting the rockmass in these trenches. It is an important point with respect to the localisation of faulting and deformation that in this study we have found fault zones both within and outside of the argillite-rich zones within the greywacke rock, i.e. it is likely that there are fault zones/shear zones throughout the rockmass rather than confined to individual shear zones such as SZ1.

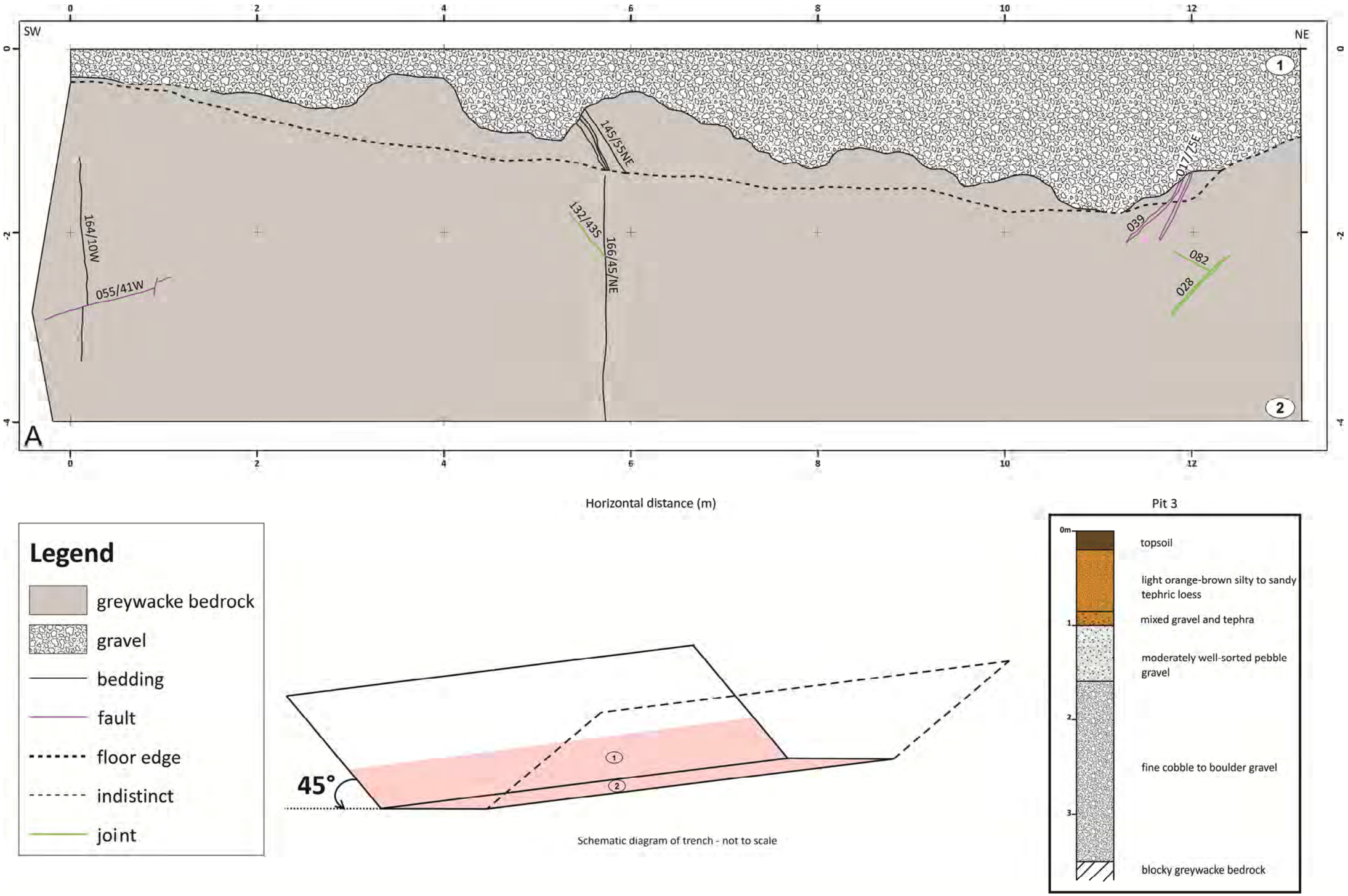

Figure 2.21 Log of the lower wall and floor of the Smedley Middle trench. Bedrock in the floor and batter of the trench is shown as a grey fill pattern.

This page is intentionally left blank.

2.3 SMEDLEY NORTH TRENCH

The Smedley North trench was excavated to the north of the Makaroro River in the area of Donovan Gully (Figure 2.1 and Figure 2.22). As outlined in the project brief, the Smedley North trench was excavated to test whether linear hillslope geomorphology could be related to recent tectonic deformation (faulting). NNE-aligned linear ridges on the NW side of Donovan Gully were previously recognised by Langridge and Villamor (2011) as being an important set of geomorphic features to target in terms of secondary deformation. In addition, this area was farther to the west than the other two Smedley trenches, with respect to the dam site. That is, the Smedley North trench was probably sited to the northwest of both shear zone SZ1 and the Donovan Gully feature. If our hypothesis of some fault activity along the NW side of Donovan Gully is correct then it may be true that a NNE-striking active feature would project along-strike into the proposed footprint of the A7 dam.

The Smedley North trench was excavated across two subparallel linear ridges and two intervening low swales (Figure 2.22 and Figure 2.23). The trench was c. 46 m long and 1-3 m deep. The trench was benched for safety but excavated with vertical walls (Figure 2.24). Bedrock was exposed in the floor and in the walls of the trench in order to view both the structure (bedding, faults, folds) within the bedrock and the nature (geometry, deformation) of the contact between the greywacke bedrock and the overlying cover deposits (Figure 2.25). The trench was excavated at an orientation of 133° or roughly perpendicular to the orientation of the ridges above Donovan Gully and to the contemporary regional structure.

Figure 2.22 View to the north toward the Smedley North trench above Donovan Gully, a side-valley of the Makaroro River. The trench was excavated perpendicular to linear geomorphic ridges on the west side of the valley (marked by black arrows). White spot next to the trench spoil is a 4-wheel drive truck.

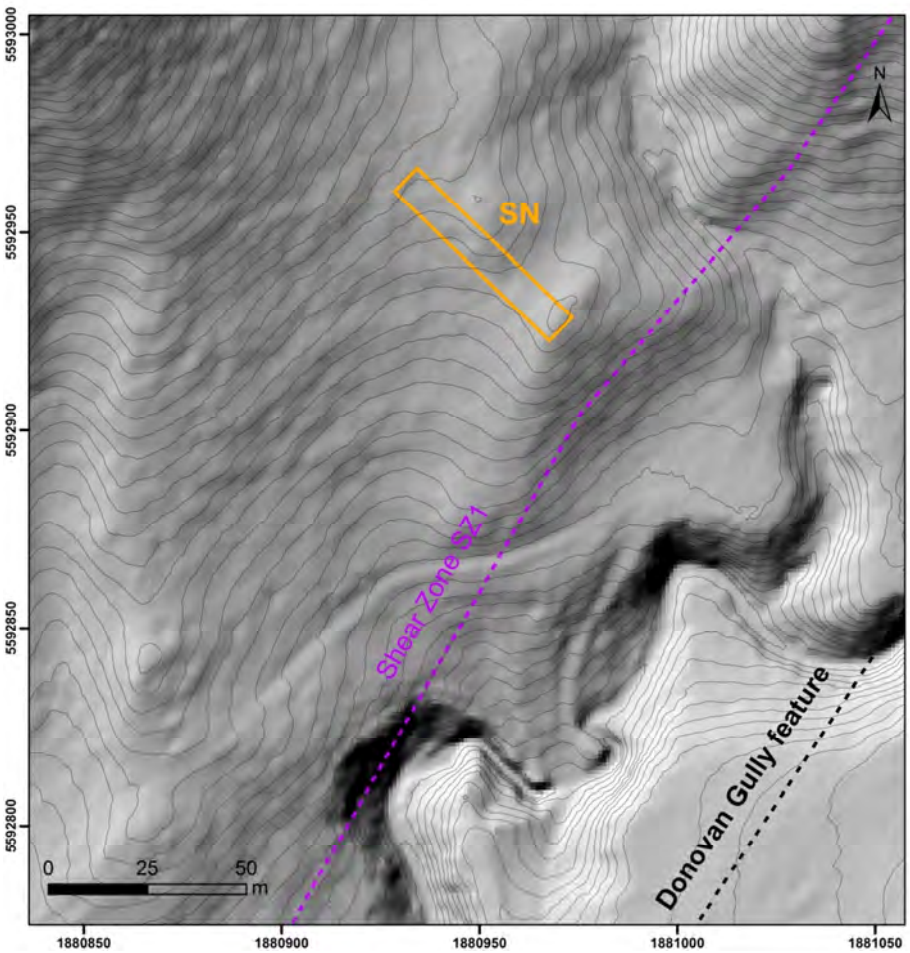

Figure 2.23 Location map of the Smedley North site north of the proposed foundation area of the A7 dam. The trench (orange box) was excavated to bedrock across NNE-striking topography subparallel to Donovan Gully.

Figure 2.24 View to the northwest along the Smedley North trench. The trench traversed two geomorphic highs (ridges) and lows (swales) to investigate the possibility of active faulting at this location.

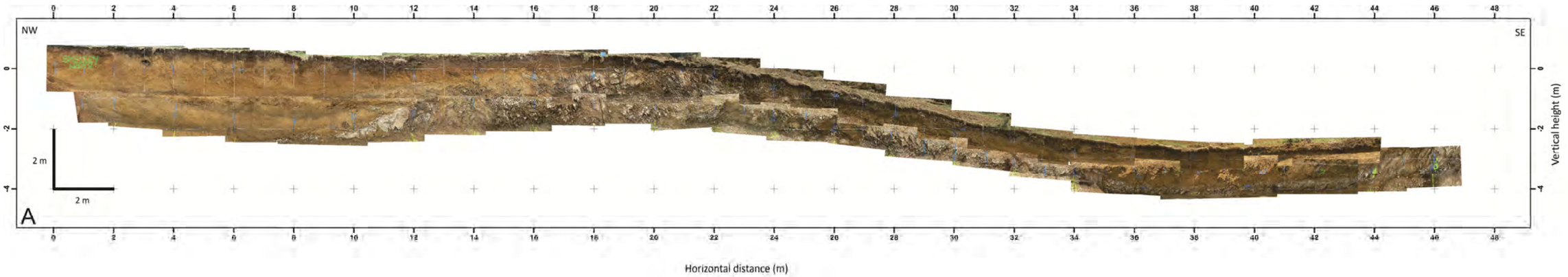

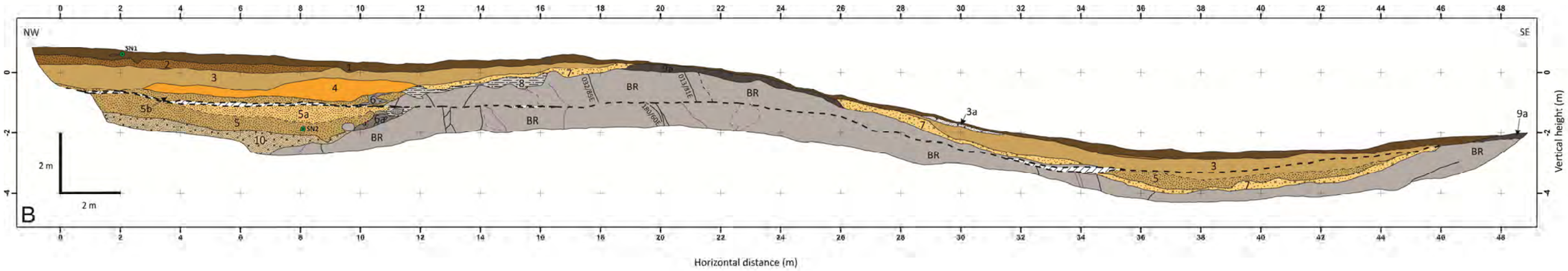

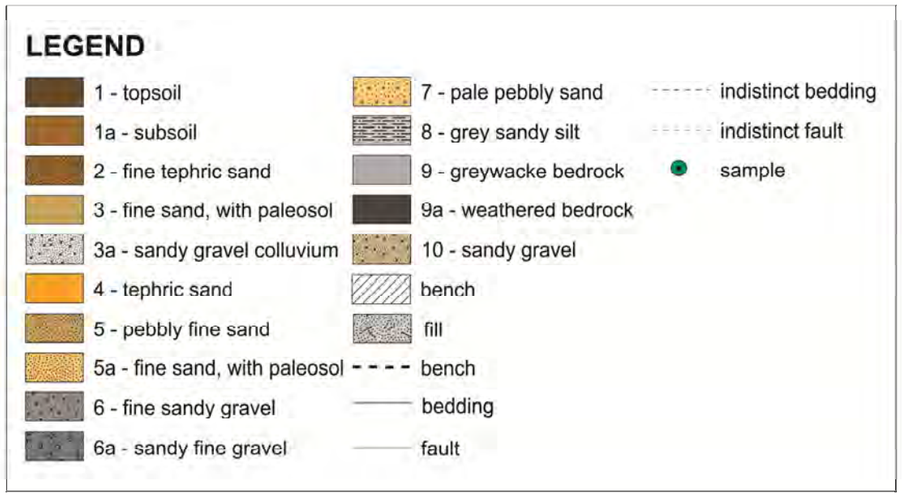

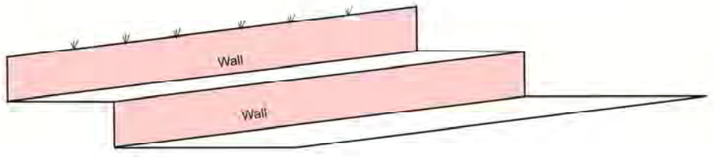

Schematic diagram of Smedley North Trench - not to scale

TEPHRA CORRELATIONS			
Sample name	Sample Type	Correlation	Age C-14 yr BP
SN 1	Tephric	Taupo Tephra	c. 1,720

Figure 2.25 Logs of the vertical walls of the Smedley North trench. **A.** Photo-log of the geometry of the trench wall. **B.** Annotated log of the trench highlighting units, bedding attitudes, faults and samples collected. Log legend, trench 3-D geometry and geologic age constraints are also shown. Sample SN-2 was not analysed. Detailed unit descriptions are presented for each unit in Appendix 1.2.

This page is intentionally left blank.

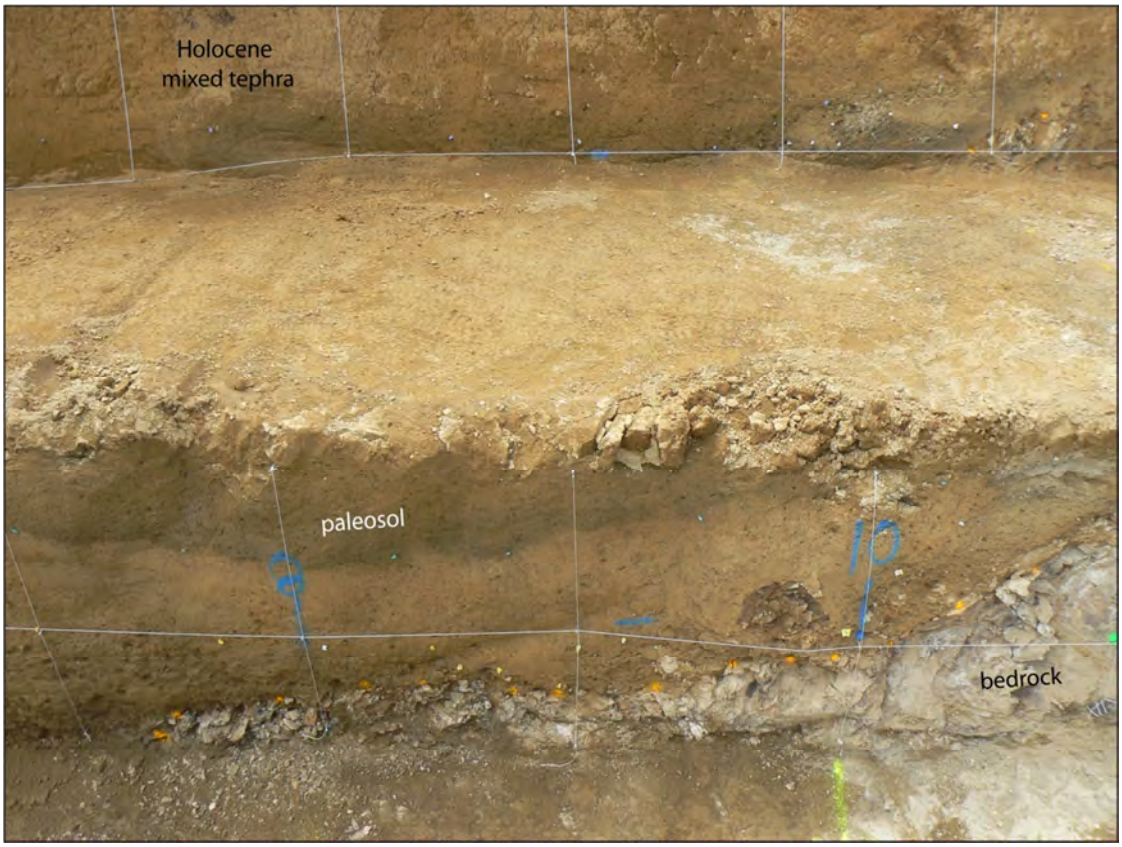

Figure 2.26 Fine-grained cover deposits over bedrock at the NW end of the benched Smedley North trench. A dark paleosol (unit 5a; above number 8) is formed on buff to orange coloured units.

2.3.1 Cover deposits in the trench

Within the Smedley North trench, bedrock was very shallow (0.2-0.4 m) beneath the two linear ridges we excavated across, but rather deeper (c. 1.2 m and >3 m) beneath the swales. Consequently, the cover deposits vary from being a thin soil and mixed tephra over fractured bedrock, to a thick sequence of layered fine-grained fill deposits (Figure 2.25). A prominent paleosol in this thick cover sequence is underlain by more clay- and clast-rich deposits. Their lighter colour, increased clast content and weathering is suggestive of materials deposited in a colder climate period than the Holocene, e.g. they are possibly of last glacial age (Figure 2.26).

Based on this sequence of units we provisionally interpret these basal cover deposits as being of late last-glacial age (30,000-20,000 yr BP), though this model is not supported by independent geologic age data at this time. Above this paleosol the cover deposits have a more orange-brown colour, which is a characteristic of tephra weathered in a warmer climate (i.e. the Holocene; <11,700 yr BP).

Near the top of this sequence a discrete sandy orange tephra is exposed near metre-0. Analyses of volcanic glass from this tephra (sample SN-1) suggest that this tephra is from the Taupo Volcanic Centre and is most strongly correlated to the Taupo Tephra or possibly the Waimihia Tephra (Appendix 2).

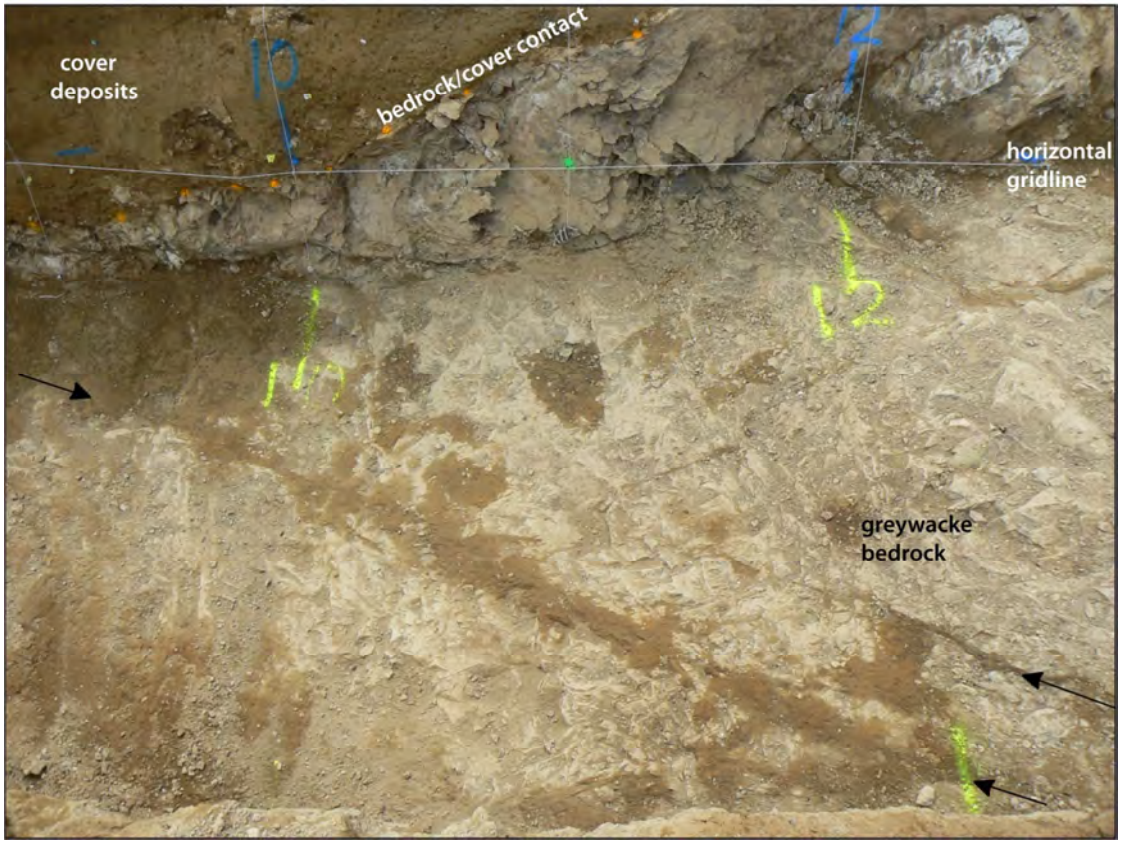

Figure 2.27 Floor of the Smedley North trench between metres-10 to -12. At upper left the contact between greywacke bedrock and cover deposits can be seen (also in Figure 2.26 above). A North-South striking fault can be seen cutting the floor diagonally (marked by black arrows).

2.3.2 Bedrock exposed in the trench

A length of roughly 40 m of greywacke bedrock was exposed in the floor of the trench over a width of 3-4 m (Figure 2.27 and Figure 2.28). Sandstone beds were the predominant facies within the greywacke bedrock exposed in this trench. Measured bedrock attitudes typically had NNE- to NE-strikes with either steep dips to the east (average 72°) or shallow dips to the west (average 15°) (Figure 2.13). The latter set of attitudes may correspond to joints in the rock, rather than to bedding.

2.3.3 Bedrock defects

Two main orientations of faults/shears were observed in the Smedley North trench. The first set of faults ran roughly across the width of the trench floor with N- to NNW-strikes (e.g., 352° to 006°) (Figure 2.28). The second set of faults had strikes sub-parallel to the trench (c. 146°). These faults typically bent or splayed to the north near their mapped ends. In one case, one of these SE-striking faults offset a N-striking (006°) shear. These observations suggest that the SE-striking faults have moved more recently than, or contemporaneously with, the N-striking faults.

Toward the NW end of the trench (at meter-12 on the trench log; Figure 2.28), two ~North-striking faults converge at a point where the buried hillslope angle of the linear ridge is high. In this area the cover deposits have a broken or disturbed appearance, which was investigated to elucidate any possible tectonic genesis to this disturbance. On close inspection we did not observe any evidence that this fault extends into the cover deposits.

We therefore conclude that the disturbance of the unit is due to a slope-related (topographically-driven) movement, rather than a tectonic displacement.

In the field, we analysed the infill and kinematic indicators found in some shears/fissures to further assess if bedrock defects in Smedley North trench could present evidence of recent fault movement. The nature of the fault infill found in the Smedley North trench was diverse and consisted of both tephric silt and mylonite. The tephric silt fill occurred in a few faults exposed at metres-12 to -16 in the upper floor and metre-10 in the lower floor (Figure 2.28), which have trends of 180/76° W, 150/55° SW and 170/90. The tephric infill was constrained to the upper 0.5 m of the shear plane and to locations where the late Pleistocene to Holocene tephra directly overlaid the basement. The infill is interpreted to be part of the tephric loess that infiltrated into open joints in the rock at the ground surface and not related to fault movement. The infill also did not show any evidence of recent brittle deformation such as slickensides.

At metre-34 along the trench floor and wall (Figure 2.28), a 020/80° E striking shear zone with cataclasite/mylonite[2] was observed. These fault rock textures belong to an old episode of shearing. While these fault rocks did not weather into clay at the top part of the shear due to an absence of a permanent wet zone (different to the fault rocks described for Smedley South), it still showed progressive mechanical weathering towards the top (Figure 2.25). Also the fault rocks do not show any evidence of current brittle shearing such as slickensides. In addition, the fault rocks indicate a left lateral sense of movement (based on the shape of the quartz shadows surrounding feldspars clasts), which is inconsistent with the current sense of movement for similar trending active faults in the region. This supports the interpretation that deformation producing the fault rock textures is not associated with the current tectonic regime.

We located two examples of slip direction indicators in the Smedley North trench. In one case (at meter-16; Figure 2.28), we measured sub-vertical slickenlines on the face of a shear with an attitude of 030/85° W (lineation 080/70), which are indicative of vertical to oblique vertical movement on that fault. In the second case (at metre-12; Figure 2.28) we measured sub-horizontal mullions (slickenlines; lineation 140/40) on a fault with an attitude of 180/76° W). These lineations would be indicative of horizontal movement in the rock. In neither case did the material (rock surfaces, infill) appear to have been recently faulted. All of these movement indicators show left-lateral movement. Such movement is not consistent with the current tectonic regime, i.e. left-lateral movement is not observed on N-S striking faults.

A significant result of this work is that while the bedrock attitudes in this trench appear to be sub-parallel to the local (geomorphic) grain and regional structural grain, the faults and sheared zones were aligned at a slightly different trend to the regional fabric (about 20° to the north or counter-clockwise). These sheared zones were not parallel to the hillside ridges above Donovan Gully (or perpendicular to the trench). Our original hypothesis for this topography was that it could have been formed by active faulting. However, based on these results it is more likely that the geomorphology is developed parallel to the strike of greywacke beds, i.e. NNE-strikes. This leads us to conclude that there is no active faulting in relation to the topography observed with this trench.

[2]There is some uncertainty whether we observed mylonite or cataclasite fault rocks in the trenches. Fault rock textures were defined as mylonite in the field, though these are less likely to be found in association with greywacke, a low grade metamorphic rock. Cataclasite defines a shallower, lower grade level of fault rock than mylonite (see Appendix 3).

This page is intentionally left blank.

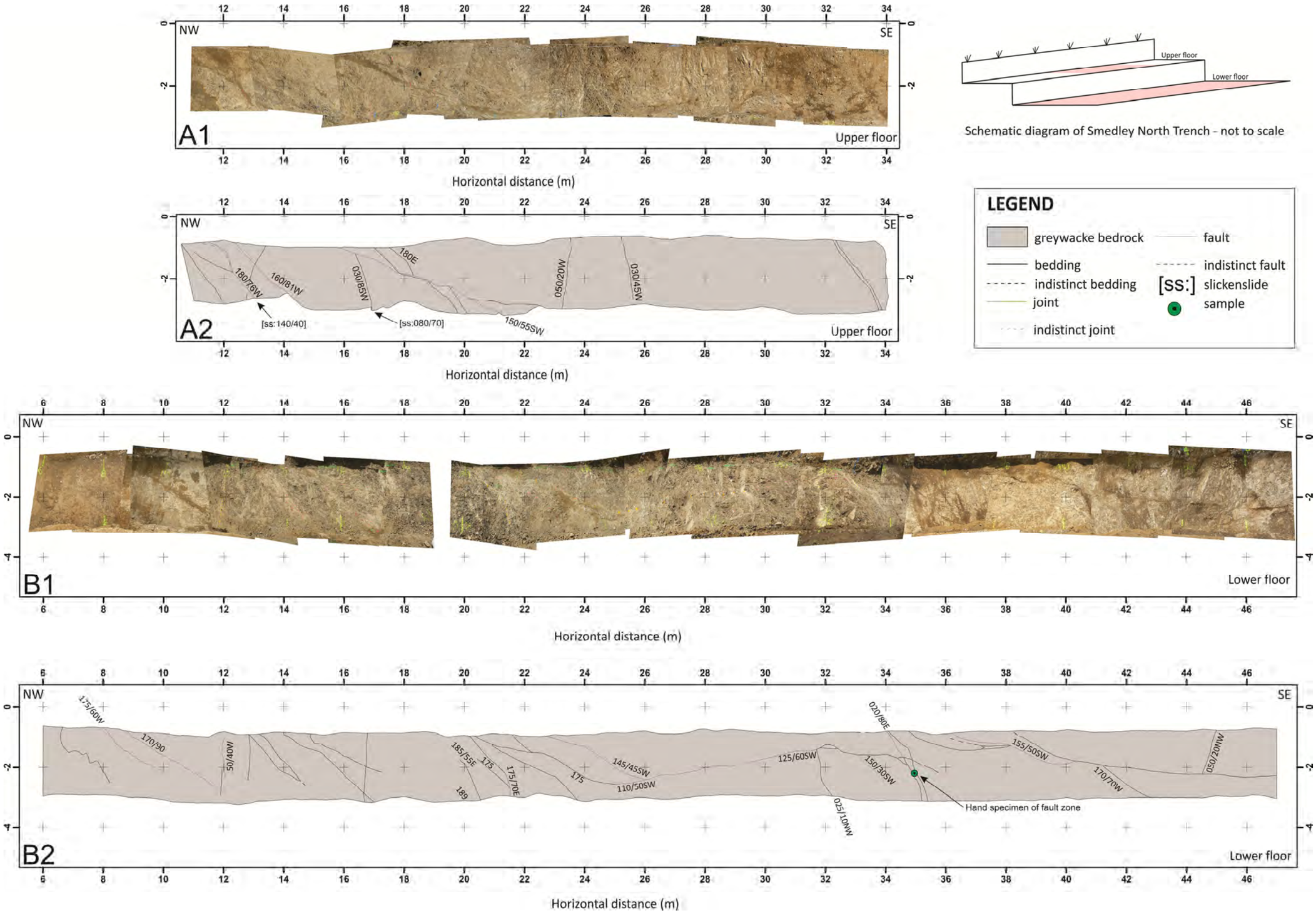

Figure 2.28 The upper and lower bedrock floors of the Smedley North trench. **A1 and B1:** photo-logs of the upper and lower floors. **A2 and B2:** Logs of bedrock and fault attitudes in the upper and lower floors. Unit legend and trench 3D geometry are also shown.

This page is intentionally left blank.

Figure 2.29 Hand specimen of cataclastic/mylonitic rock from within a fault zone at metre-34 in the Smedley North trench. See Figure 2.28 for location.

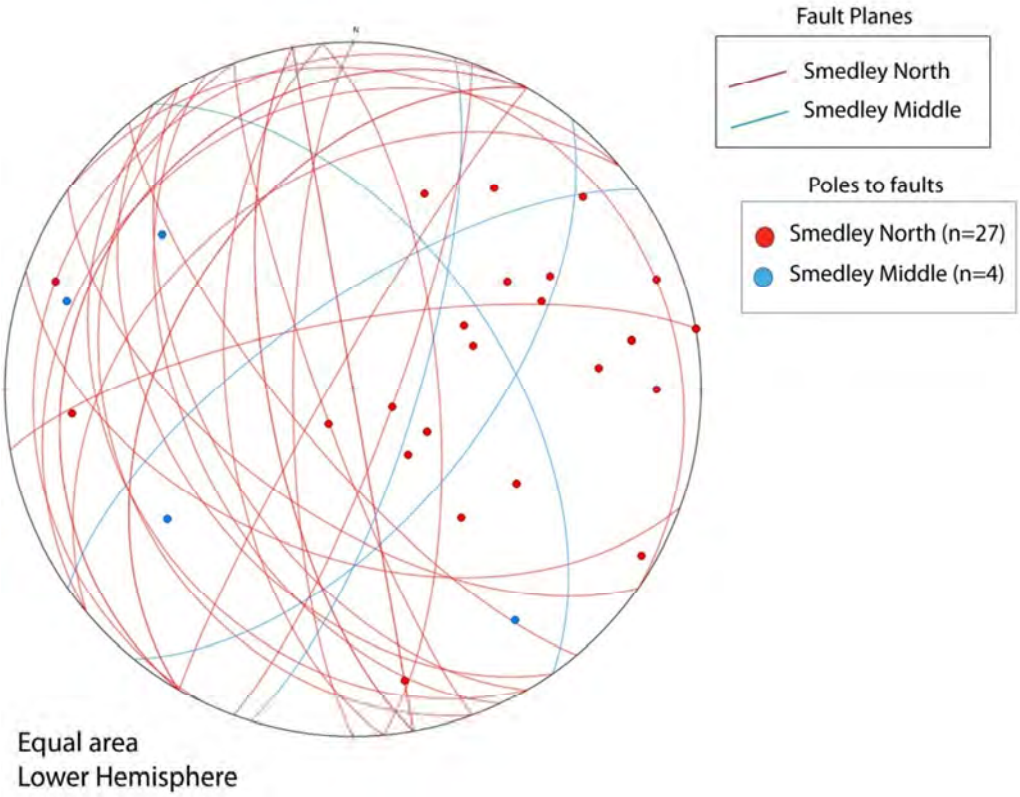

Figure 2.30 Stereonet diagram displaying the poles and great circles of all faults (n=31) measured in the Smedley Middle and North trenches. Fault attitudes from these trenches appear to be more random in nature, though there is a tendency toward N- to NNE-strikes and W- to NNW–dip directions in the Smedley North trench.

This page is intentionally left blank.

3.0 ACTIVE DEFORMATION IN THE GWAVAS FOREST AREA

North of Smedley Station and the Makaroro River, the Mohaka Fault continues to the NNE into a large block of land managed as the PanPac Gwavas pine forest. Recent reports by Tonkin and Taylor (T&T, 2012a, b) and GNS Science (Langridge et al., 2011) have highlighted a linear fault trace on lidar-derived DEMs, striking subparallel to the Mohaka Fault (Figure 3.1). This fault trace is also shown as an active fault on the QMap Hawke's Bay geologic sheet (Lee et al. 2011). It occurs in the Gwavas Forest, c. 6 km north of the proposed A7 dam site.

The fault trace has scarp heights of c. 1-2 m height cutting across hillslopes and alluvial terrace surfaces, seen on the lidar DEM. Therefore, this fault is clearly an active fault, and in this report we name it the 'Gwavas Fault'. Based on the presence of uphill-facing scarps, the dominant style of faulting is normal. It is not clear whether there is a significant component of strike-slip movement across this fault; however, ridge lines and spurs do not appear to be displaced horizontally by the Gwavas Fault, at least to any extent visible in the lidar.

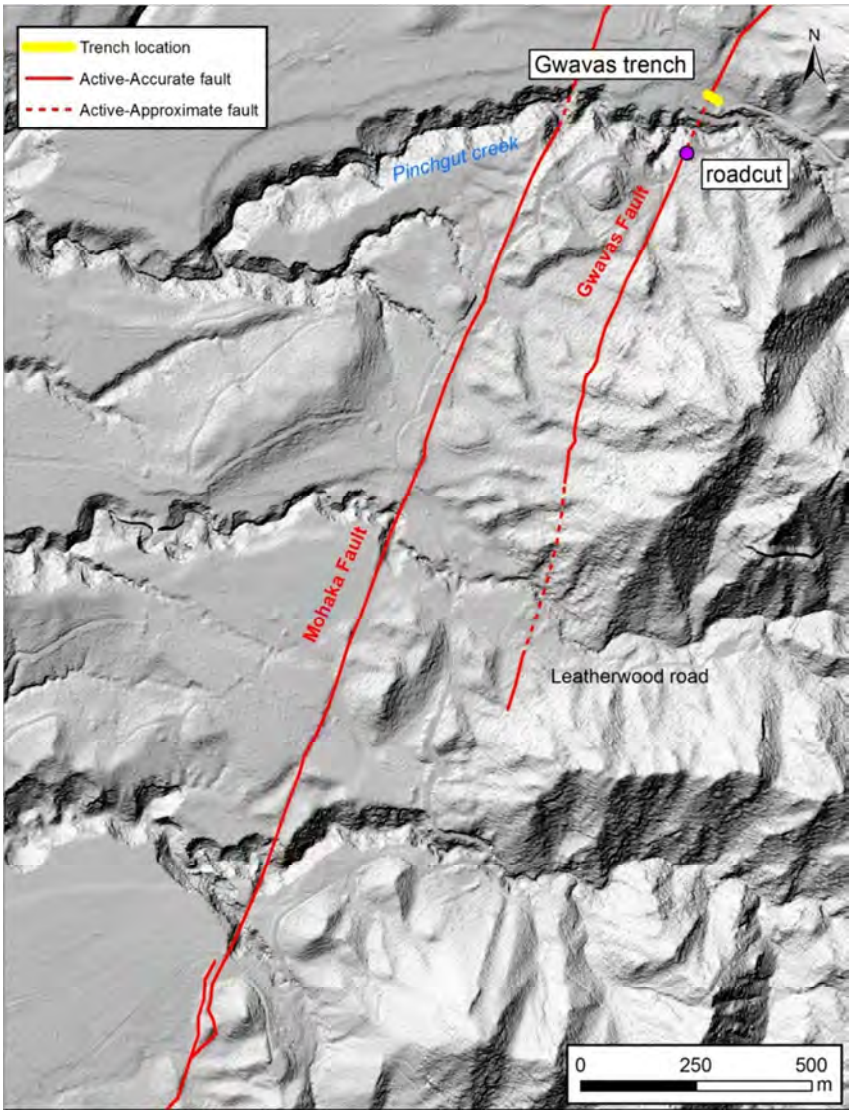

Figure 3.1 Location map of investigations within the PanPac Gwavas Forest. The Gwavas trench was excavated into a forest road adjacent to Pinchgut Creek, across the Gwavas Fault. A roadcut south of the creek provided an exposure of the bedrock fault zone. Mapped fault lines represent the current interpretation of accurate and approximate locations of active faults, including the southern termination of the Gwavas Fault.

3.1 GWAVAS TRENCH

The Gwavas trench was excavated within the PanPac Gwavas Forest adjacent to Pinchgut Creek and c. 6 km NNE of the Smedley trenches (Figure 1.1 and Figure 3.1). The trench was excavated across a c. 2-m high east-facing scarp through a forest road where the scarp was well located and where damage to the pine forest could be minimised. The trench was benched for safety and was up to 3 m deep (Figure 3.2). The trench was oriented at 115° or perpendicular to the strike of the Gwavas Fault. The trench did not expose bedrock but was limited to late Quaternary cover deposits. However, the structure of the bedrock adjacent to the fault could be observed in a nearby roadcut (located in Figure 3.1).

Figure 3.2 Photo of the Gwavas trench excavation looking north at a cross-section through the scarp of the active Gwavas Fault. The zone of dip-slip faulting (marked by red arrows) is expressed by the contrast from grey gravels (left) faulted against orange tephric deposits (centre and right). String grid is 1 m x 1 m.

3.1.1 Stratigraphy of deposits

The stratigraphy of the Gwavas trench comprised gravels, discrete and mixed tephra layers, soils, 'peat' and colluvial deposits (Figure 3.3). The lowermost deposits in the trench are coarse angular gravels. These gravels are inferred to be related to the construction of terraces by Pinchgut Creek. We infer that these gravels were deposited during the Ohakean aggradation episode (30,000-18,000 yr BP). These are overlain by finer, better sorted sub-angular gravels (units 12 and 13).

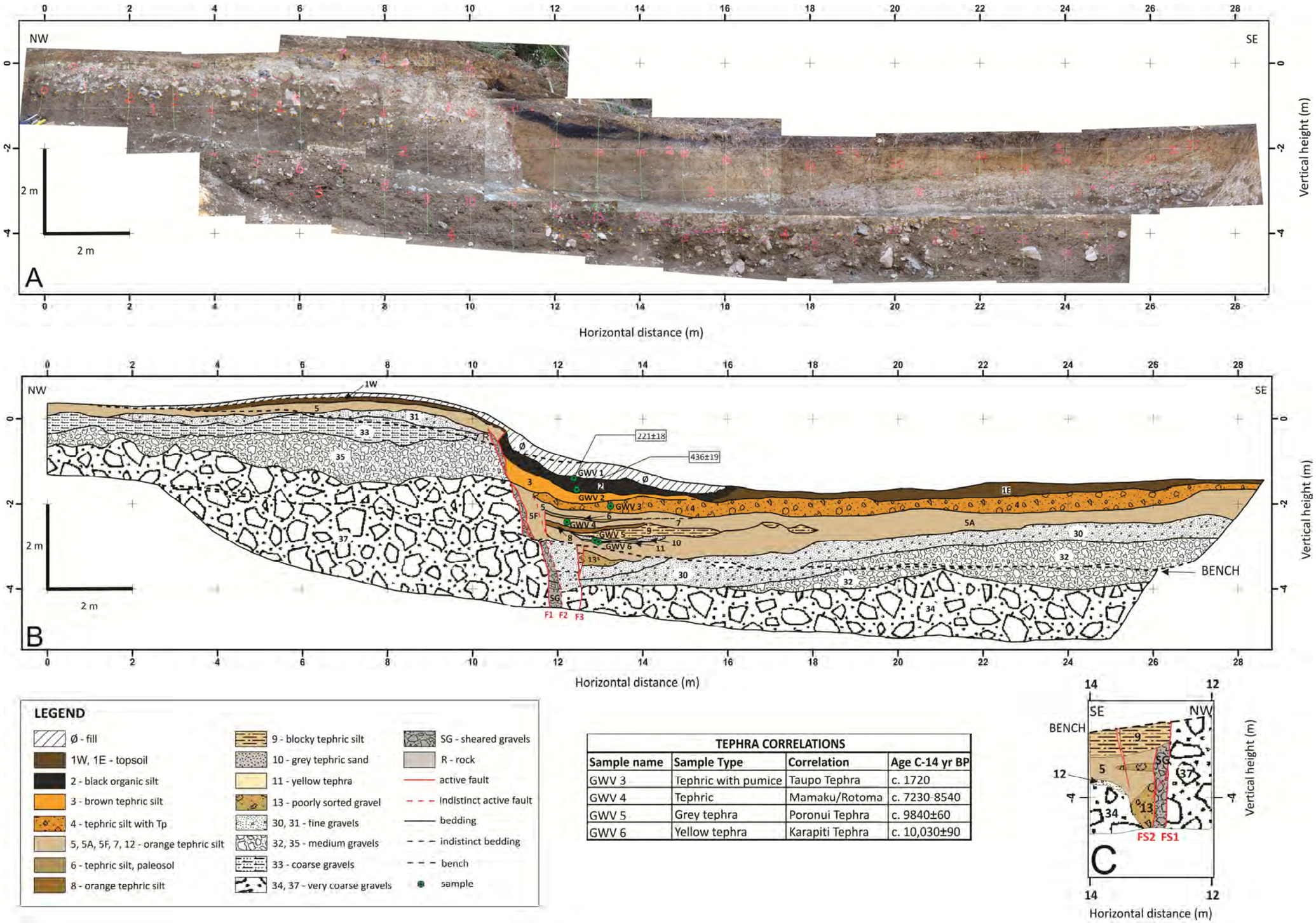

TEPHRA CORRELATIONS

Sample name	Sample Type	Correlation	Age C-14 yr BP
GWV 3	Tephric with pumice	Taupo Tephra	c. 1720
GWV 4	Tephric	Mamaku/Rotoma	c. 7230-8540
GWV 5	Grey tephra	Poronui Tephra	c. 9840±60
GWV 6	Yellow tephra	Karapiti Tephra	c. 10,030±90

Figure 3.3 Geologic logs of the Gwavas trench. **A.** Photo-log. **B.** Log of the northeast wall of the trench. **C.** Log of part of the southwest wall of the trench. Log legend and geologic age constraints are also shown. Radiocarbon dates for unit 2 are shown on the log.

This page is intentionally left blank.

These finer gravels may be related to the waning phases of aggradation in the valley, or indeed degradation as the valley began to undergo incision. These fine gravels are considered to have been deposited toward the end of the last glacial period (18,000-14,000 yr BP). At the southeast end of the trench the cover deposits over the gravels are comprised of up to c. 1 m of orange brown tephra. At this end of the trench there are no discrete tephra layers. A soil is formed into the top of this section.

In the middle of the trench, where a fault zone is exposed, the section of tephric deposits is locally expanded to c. 3 m on the downthrown side of the fault (Figure 3.3 and Figure 3.4). In this area, the section ranges from stony tephric sand at the base through tephric sand. Near the base of the tephric section there is a discrete yellow coloured tephra (unit 11), which is overlain by a firm grey sand (unit 10). This distinctive couplet of units is similar in form and stratigraphic position to those described from the Smedley South trench (units 3A and 3B there) and therefore may be the same couplet of units (and time correlatives). At the Smedley South site, the yellow tephra was found to be a Taupo Volcanic Centre (TVC) eruptive. Based on its glass chemistry, stratigraphic position and nearby radiocarbon dates, this tephra was best correlated with the Karapiti Tephra. The glass chemistry of sample GWV-6 (unit 11) was indistinguishable from sample SS-3 (Appendix 2). Therefore on the basis of its field properties, stratigraphic position and glass chemistry we infer that unit 11 is also the Karapiti Tephra (10,030 ± 90 cal yr BP; Lowe et al., 2012).

In the Gwavas trench the grey sand (sample GWV-5) was also identified as a tephra, with a TVC source (Appendix 2). The glass chemistry of GWV-5 is similar to the Karapiti, Poronui, Opepe and Motutere tephras. Considering both the major element comparisons between CaO vs. FeO and K_2O vs. FeO, the most likely correlatives to sample GWV-5 are the Karapiti and Poronui tephras (Appendix 2). Due to its stratigraphic position and to its proximity to the yellow tephra (probably Karapiti Tephra), unit 10 is likely to be the Poronui Tephra (9840 ± 60 cal yr BP; Lowe et al., 2012). This relationship also fits well with the results from the Smedley South trench and provides some confidence that this couplet was deposited at both sites.

Above this couplet, subtle changes in colour and texture within the tephric material help identify paleosols within the sequence. These are old buried soils that represent periods of time when the landscape is relatively stable such that soils can form. Paleosols cap (have formed into) tephra and tephric material that accumulated at times through the Holocene. A tephra sample from unit 7 was analysed in an attempt to identify an individual eruptive unit of known age. Analyses from unit 7 were dominated by glass shards from Okataina Volcanic Centre (OVC). Based on the stratigraphic position of this sample we suspect that this is a mid-Holocene eruptive from OVC. Major element analysis of glass shards from sample GWV-4 correlate well with the Whakatane, Mamaku and Rotoma tephras. Considering both the major element comparisons between CaO vs. FeO and K_2O vs. FeO, the most likely correlatives to sample GWV-4 are the Rotoma (8530 ± 10 cal yr BP) and Mamaku (7250 ± 20 cal yr BP) tephras (Appendix 2). Major element chemistry cannot distinguish between these two tephra and in practice due to their proximity it is possible that either or both volcanic glasses exist in sample GWV-4. Therefore, unit 7 has been ascribed a nominal age of c. 7230-8540 cal yr BP. The appearance of discrete white pumice grains of c. 2 mm size near the top of this section (within units 4 and 3) suggests that the tephric material includes pumice from the Taupo eruption (c. 1720 cal yr BP; Lowe et al., 2012).

The section of tephric deposits near the fault is overlain by a distinctly black trough-shaped unit that is rich in organic matter. This unit (unit 2) has been described as a ‘pig fern’ or

‘bracken’ peat due to its texture and composition. An organic sample from the top of unit 2 (sample GWV-1) returned a radiocarbon age of 221 ± 18 yr (148-295 cal yr BP) (see Figure 3.3; Table 3.1). A sample from the base of unit 2 returned a radiocarbon age of 436 ± 19 yr (338-501 cal yr BP). These dates are consistent with the position of unit 2 near the ground surface and with its position above the white pumice grains (likely Taupo Tephra). Black bracken soils are considered to form as a result of forest burning and are often linked to the arrival of Polynesians to New Zealand. A common practice amongst Maori was land clearance through burning, which led to the re-colonisation of areas by bracken (B. Alloway, personal communication, 2013). The unit 2 black peat is overlain by mixed soil, clay, gravel and black peat, which we infer to be man-made fill, consistent with foresting activity. Another feature of the section near the fault is the presence of colluvium (mixed, wedge-shaped units). These are described in more detail below in relation to faulting events.

While the downthrown side of the fault is characterised by a thickened section comprising discrete tephra, paleosols and colluvial deposits, the upthrown side of the fault is characterised by a thinned section overlying the gravel units (33, 35 & 37). This is particularly true right at the fault scarp were the units are folded downward toward the fault zone and are typically thinned due to erosion.

Table 3.1 Radiocarbon dates from the Smedley South and Gwavas trench sites.

Trench	Sample I.D.	NZA Lab No.	Δ13 C (‰)	Radiocarbon age (yr BP)	Calibrated age (2σ cal yr BP)	Calibrated age (2σ cal yr)	Material & significance
Smedley South	SS-4	53024	-25.2	6327 ± 24	7028-7270	-	Brown, wedge-shaped paleosol unit, with high tephric component. Probably a slumped soil because it overlies a section of ponded deposits at the hillslope end of trench
Gwavas	GWV-1	53025	-25.4	221 ± 18	148-219 & 270-295	AD 1665-1680 & AD 1731-1802	Fine charcoal (organics) from the top of unit 2. Sample probably pre-dates the most recent faulting event.
	GWV-2	53020	-25.8	436 ± 19	338-354 & 449-501	AD 1449-1501 & AD 1596-1612	Fine charcoal (organics) from the base of unit 2. Sample post-dates the penultimate faulting event in the Gwavas trench.

Notes: Conventional radiocarbon age before present (AD 1950) calculated as defined in Stuiver and Polach (1977) using Libby half-life of 5568 years, and normalized to δ13C of –25 ‰. Quoted error is ± 1σ. Calibrated age: Calendar years before present (AD 1950) using calibration program Winscal5.0 (© Inst. Geological & Nuclear Sciences) and Southern Hemisphere Atmospheric data from McCormac et al. (2004). A lab error multiplier of 1 has been applied to NZA samples. Age ranges listed are minimum and maximum values of the calibrated age range based on a radiocarbon age error of ±2σ.

3.2 RECORD OF RECENT FAULTING

A zone of steep faulting is exposed in the middle of the Gwavas trench, immediately beneath the fault scarp striking at c. 017° and dipping c. 70° east (Figure 3.3 and Figure 3.4). The faulting is normal in style/sense, with older gravels faulted against the younger tephric section across the upper part of the main fault zone. A zone of secondary faulting c. 0.5 m to the east strikes at 014° and probably merges with the main zone of faulting beneath the floor of the trench.

Individual earthquake displacement events can be recognised on the basis of colluvial units shed from the fault scarp and up-ward fault terminations. Colluvium is a mixed deposit often related to a slope where materials are eroded from up-slope and mixed together. Near the base of fault scarps along dip-slip faults, scarp-derived colluvium is a common product of surface fault rupture. That is, when a fault has ruptured the ground surface, a 'free face' forms at the fault scarp. Subsequently, this free face, which will expose units from the upthrown side of the fault, erodes or collapses to form a colluvial unit. This colluvium will be composed of units that were in the scarp at the time of the earthquake rupture. Thus, this process of deposition on the downthrown side of the fault as colluvial wedges is matched/synchronous with erosion of units from the upthrown side of the fault.

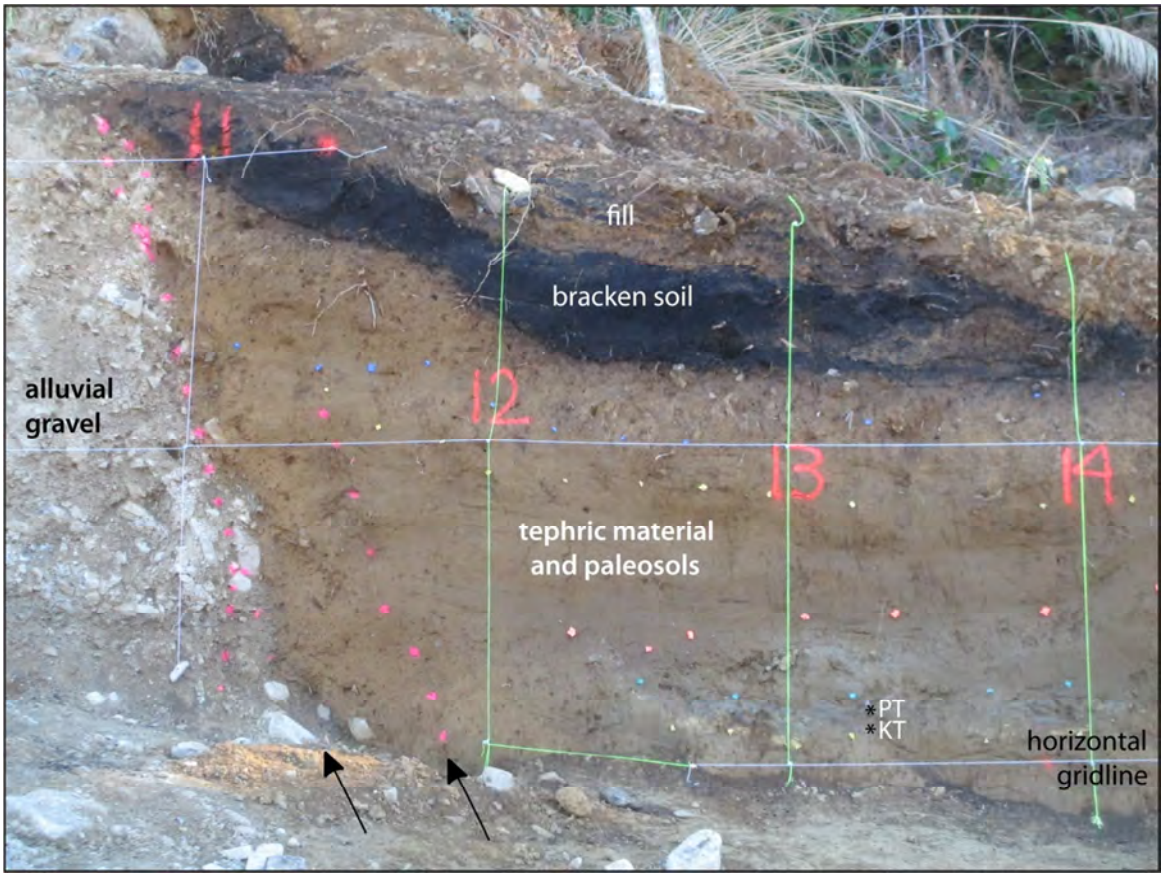

Figure 3.4 Close-up view to the north showing the North wall of the Gwavas trench (faults marked by pink dots and black arrows). Black 'bracken' peat caps the intact section on the downthrown side of the fault. Yellow and green pins mark the position of the yellow tephra (KT, unit 11) and grey tephra (PT, unit 10), respectively.

3.2.1 Evidence and timing of paleo-earthquake ruptures

On the basis of upward-terminating faults, the presence of several scarp-derived colluvial deposits and unconformities we present evidence for up to seven past surface-rupturing events on the Gwavas Fault as revealed in the Gwavas trench (Figure 3.3 and Figure 3.4).

Most recent faulting event - Based on the faulting and dragging of the western edge of unit 2 we infer that the most recent faulting event probably occurred after the deposition of unit 2, and therefore post-295 cal yr BP (i.e. post-AD 1655; Table 3.1). By definition, this is a very young and conceivably historic surface-faulting event. Both the Wellington Fault in the south, and the Mohaka Fault in this region have evidence for a young surface faulting event that has occurred during the last 300 years or so (Langridge et al., 2012; Hanson, 1998; Zachariasen et al., unpublished data).

Penultimate faulting event - The penultimate faulting event occurred before the formation of unit 2 and is related to the generation of a mixed unit (unit 3) that contains Taupo (pumice) Tephra. Unit 3 is wedge-shaped and limited in its geometry to within 3 m of the fault scarp. Unit 3 is therefore interpreted as a scarp-derived colluvium. The base of unit 3 defines the ground surface immediately prior to the surface-rupturing event that generated the scarp free-face from which unit 3 was derived. A fault tip or upward-termination can be mapped up to the base of the Taupo pumice unit (unit 4) and may be related to this penultimate event. The age of this rupture event must therefore post-date the Taupo eruption and predate the base of unit 2 (i.e. c. 340-1720 yr BP; Table 3.1).

Faulting event III - The third distinct faulting event is defined from the upward-termination of fault F2. The eastern branch of F2 cuts all units up to the level of paleosol unit 6 but cannot be traced through unit 5 or the Taupo Pumice-rich unit 4. Therefore, we consider that this could represent a distinct faulting event. Unit 5, which overlies the unit 6 paleosol could be considered as wedge-shaped fill, as it is limited to within 3 m of the fault zone. On the south wall, a distinct fissure of up to 6 cm width was mapped to as high as the bench (Figure 3.3C). The fissure cuts all units up to and including the reworked colluvium containing the grey sand (unit 8; described below). This fissure could therefore be related to the third faulting event. This event must precede the deposition of Taupo Pumice, i.e. >c. 1720 yr BP, but post-date the deposition of the Mamaku or Rotoma tephras, i.e. <c. 8540 yr BP (Lowe et al., 2012).

Event IV - The fourth distinct faulting event is defined by the form and composition of unit 9, which is interpreted as a scarp-derived colluvium. Unit 9 occurs as a wedge- or trough-shaped unit (on opposing walls) that thins from the fault zone to a distance of c. 3 m. Unit 9 contains clasts of the unit 10 and 11 tephras that have been ripped up and re-deposited, probably from the upthrown side of the fault. The upper and lower contacts of this unit appear to be unconformable with the stratigraphy below and above them. These relationships support the indications that unit 9 is colluvial. This event must post-date the yellow tephra and grey sand (units 10 and 11), which have been correlated with the Poronui and Karapiti tephras from the TVC. In addition, Event IV must have occurred before the deposition of the Mamaku or Rotoma tephras, i.e. >c. 7230 yr BP (Lowe et al., 2012). The range for the timing of Event IV is therefore 7230-9900 cal yr BP.

Event V - Some evidence exists for another faulting event that pre-dates the deposition of the yellow tephra (unit 11) and the grey sand (unit 10). Firstly, the trough-shaped form of these two units is suggestive of deformation prior to their deposition. Second, fault zone F3 appears to terminate immediately beneath these units and within unit 12. This implies that unit 12 is faulted and that it was near the ground surface during these events. Units 10 and

11 do not appear as discrete beds on the south wall of the trench, so it is difficult to place an event horizon in this position in the stratigraphy. However, fault FS2 clearly terminates at the base of unit 9 on that wall. This therefore provides further evidence for either: (i) faulting related to this event (V) if units 10 and 11 were eroded or not deposited in that view (wall), or, (ii) Event IV where the faulting continues to the base of unit 9. Event V faulting must precede the deposition of the yellow tephra Unit 11; Karapiti Tephra), that is >9920 cal yr BP, though not by a considerable amount of time.

Event VI – On the south wall a prominent stoneline occurs within unit 12 (Figure 3.3). A stoneline is considered to be a type of colluvium; in this case the stoneline has clasts of up to 6-10 cm, is faulted by fault FS2, but thins away from the fault scarp. At this level in the stratigraphy and during latest Pleistocene times the first fine-grained tephric materials were accumulating on the landscape at this location. If a fault rupture had occurred during this time a gravelly tephric colluvium (stoneline) such as this would have formed on the downthrown side of the fault.

Event VII – Both walls display evidence for an event which must have occurred at or immediately following the cessation of aggradation at the site, i.e., when gravel deposition ceased because Pinchgut Creek started incising into its valley fill. On the north wall, the top of the gravel sequence is capped by a wedge-shaped, fine, poorly sorted gravel (unit 11) which is truncated by fault F3. We interpret this to be a colluvial wedge deposit comprising only gravel. The top of this unit marks the first influx of the fine, weathered tephric material. On the south wall, within the fault zone, this contact between orange, weathered tephra and gravel is angular, whereas the next contact higher in the section (the stoneline) is rather flat or conformable (Figure 3.3). This provides further evidence for an event that we call Event VII. The timing of this event must be pre-Karapiti Tephra and post-abandonment of degradation gravels. We consider that Event VII is close in age to the latter, and the onset of tephra preservation at the site (c. 13,000-14,000 yr BP).

3.2.2 Recurrence interval and single-event displacement

In summary, there is clear evidence from the trench that the Gwavas Fault is an active normal fault and that it has had up to 7 large earthquake displacements during the last c. 14,000-18,000 yr, i.e. since the end of gravel aggradation in the valley. In addition, based on the identification of the Karapiti and Poronui tephras within the trench, there have been 4-5 faulting events during the last 10,000-14,000 yr. Therefore, we derive a preliminary recurrence interval for faulting on the Gwavas Fault of 2000-2800 yr.

Based on the scarp height (c. 1.9 ± 0.2 m), and assuming up to 5 faulting events, the likely single-event vertical displacement at the site is c. 35-53 cm per event since the deposition of the yellow and grey tephra pair at the site. Alternatively, if we consider the total displacement since the end of gravel aggradation at the site (c. 2.6 ± 0.3 m), and assuming up to 7 faulting events, the likely single-event vertical displacement at the site is c. 33-48 cm per event. Based on displacement of c. 2.6 ± 0.3 m during the last c. 14,000 years, or c. 2 m during the last 10,000 years, the vertical slip rate of the Gwavas Fault from this trench is c. 0.2 mm/yr.

As an independent check of the average single-event displacement we can look at the amount of deformation that has occurred in individual faulting events. The unit 2 black peat has been dragged by up to c. 1 m across the fault scarp. Unit 4, the Taupo pumice-rich tephric deposit is c. 2.6 m lower on the downthrown side than where it would have been deposited on the upthrown side of the fault, suggesting at least 1.6 m of vertical difference in this event. This value does not reflect the fact that there was probably a pre-existing scarp at

this location and that a tephra would have draped the scarp. Therefore, while c. 1 m could be considered the maximum displacement for this fault, it is noted that in such a case the scarp height and total displacement would be much greater.

Alternatively, near the base of the Holocene section, there are two colluvial deposits that could be used to assess the amount of single-event displacement. The thickness of colluvial wedges near the fault can be considered to be approximately half the vertical displacement, for a normal fault. The colluvium related to Event VII has a projected thickness of 50 cm at the main fault, while the stoneline related to Event VI has a projected thickness of 14 cm. The two values imply a displacement of c. 28-100 cm in two distinct faulting events. These values are consistent with the estimates of average displacement (c. 33-50 cm) but highlight the possible ranges for individual single-event displacement.

In summary, the calculated range for vertical single-event displacement at this site on the Gwavas Fault is c. 33-50 cm. The wider range for the displacement could be as large as c. 28 cm and as much as c. 100 cm.

3.3 BEDROCK EXPOSED CLOSE TO THE ACTIVE FAULT

South of the Gwavas trench, along Wakarara Road (located in Figure 3.1), greywacke bedrock is exposed in a roadcut (Figure 3.5). At this location we could not observe the active trace of the fault but could instead observe the bedrock within a few metres of the active trace of the Gwavas Fault. The bedrock in the roadcut exposure had prominent closely spaced brittle fractures with the same orientations of the active fault trace. The rock away from this exposure was also highly fractured. This type of fracturing was not observed in any of the Smedley trenches described in Chapter 2. The appearance of the rock was of highly fractured and sheared rock with many slickenside textures. The fault attitude at this location was 034/76° E. These results are consistent with other observations of bedrock adjacent to currently active faults, e.g. exposures of the Wellington Fault in the Wellington area (see Begg et al., 2010). These show a core of highly damaged rock surrounding a gouge or pug zone. Again, this type of deformation was not observed in any of the Smedley trenches described in Chapter 2.

Figure 3.5 Roadcut south of Pinchgut Creek showing highly deformed argillite and sandstone beds in the vicinity of the Gwavas Fault shear zone. Beds with near-vertical dip have both east and west dip directions.

3.4 SOUTHERN EXTENT OF THE GWAVAS FAULT

An important aspect of this investigation along the Gwavas Fault was to consider whether active deformation on the Gwavas Fault could continue south toward the proposed A7 dam site, as can possibly be implied from the QMap Hawke's Bay geologic map (Lee et al., 2011). The interpretation of these faults differs between this map and from those presented by Langridge et al. (2011).To address this we re-mapped the fault from the lidar DEM (Figure 3.1).

Lee et al. (2011) show the active trace of the Gwavas Fault both splaying toward the Mohaka Fault and also continuing for several hundred metres to the south of Leatherwood Road along an un-named, approximately located fault. This fault bends to the south and is shown connecting onto the SSW-striking Donovan Gully feature. Alternatively, Langridge et al. (2011) show the Gwavas Fault (in their Figure 4.3) as splaying from, or linking into, the Mohaka Fault near Leatherwood Road. Re-mapping of this area at a scale of c. 1:5000 using the lidar DEM shows that neither of these interpretations best reflects the accuracy at which we can map the Gwavas Fault in this area.

Our new mapping (Figure 3.1) shows that the fault can be clearly mapped from the northern limit of the lidar DEM, to as far south as Leatherwood Road. After this point the fault cannot be positively mapped either continuing, or bending to the SSE or SSW, as earlier reports suggested/implied. Therefore, Figure 3.1 shows the most up-to-date and least interpretive view of the fault.

The implications for this study are that we cannot find any evidence in the landscape, in terms of clear evidence of active fault traces, to continue the deformation related to the Gwavas Fault to the south beyond Leatherwood Road.

4.0 SUMMARY AND DISCUSSION

In this chapter we address the list of questions that were posed in Chapter 1 by summarising the conclusions from the data collected at the four trenches and relevant mapping. The conclusions stated here supersede those made in the GNS Interim Report (CR 2013/31LR).

4.1 IS SECONDARY FAULT DISPLACEMENT POSSIBLE AT THE A7 DAM SITE?

The question posed in Chapter 1 was: "could fault displacement occur on secondary/subsidiary faults within the bedrock of the dam foundation area as a consequence of movements on the major active faults?"

To answer this we excavated three trenches to bedrock at Smedley Station. In this study we have chosen the best candidate targets for excavation to bedrock, i.e. those we expected would help define whether structurally-oriented zones and geomorphically-oriented features could be related to recent faulting within and near the dam site foundation. The results from these trenches are summarised below.

4.1.1 Smedley South trench

Our results indicate that none of the many shears/faults that we observed in the greywacke bedrock exposed in the 38 m length of floor and sidewalls, up to the level of the bedrock/gravel strath, displayed any evidence for recent fault movement. In addition, we found no evidence for shearing of the cover deposits overlying the bedrock. Based on geologic dates and geomorphic inferences from the terrace and deposits overlying the bedrock strath, our data indicates that none of the faults exposed in the bedrock show evidence for displacement during at least the last 10,000 years (based on the ages described in section 2.1.1.2).

Our analysis of the bedrock shear and fault materials (gouge, mylonite) provided further support of the lack of activity on these sheared zones. The soft clays have cataclasite to mylonite fabrics that have been weathered in place by groundwater that occurred near the strath contact. There was no evidence for fabric in the shears/faults related to recent movement; rather, we observed a weathered shear fabric that probably formed during older movements.

In the trench, the NNE-striking fault sets were offset by (or contemporaneous with) the east-west fault sets, which provides further evidence that those faults sub-parallel to the regional fault fabric have not moved in recent times.

We found that many of the bedrock attitudes and shear zones in the trench, had a sub-parallel strike compared to the assumed regional structure, i.e. of a NNE-striking grain sub-parallel to the Mohaka Fault or Wakarara Range. However, the longest faults in the trench were more E-W striking and cross-cut the bedding. These results suggest it would be possible to re-activate the exposed bedrock shears during this regime of contemporary tectonic deformation.

4.1.2 Smedley Middle trench

We did not observe any evidence for recent fault displacement in 13 m of exposed bedrock within the Smedley Middle trench. The gravel cover deposits observed at this trench are correlated with those in the Smedley South trench, implying there has been no movement on the faults exposed in the bedrock within the last 10,000 years or more. As with the Smedley South trench, steps and elevation low points in the bedrock/gravel strath are better explained by erosional processes rather than tectonic displacements.

Detailed mapping and surveying indicate that we probably did not expose shear zone SZ1 within the Smedley Middle trench. As with the Smedley South trench, discrete faults and shear zones were recognised cross-cutting sandstone units in the trench.

4.1.3 Smedley North trench

We found no positive evidence of recent faulting, within the 40 m length of exposed bedrock. The shears that we observed in bedrock did not displace presumed late-last glacial or Holocene deposits. In addition, the NNE-aligned ridge and swale topography was shown to not be related to recent faulting, and was instead probably controlled by the strike and lithological variations of bedding within the host greywacke.

4.1.4 Concluding statement

From the exposures we investigated within (c. 40 m of bedrock) and outside of (c. 53 m) the dam site foundation on Smedley Station, we did not find any compelling evidence for recent faulting in the bedrock. That is, there was no evidence for displacement of the bedrock/gravel strath in the Smedley South and Middle trenches, and the bedrock erosion surface in Smedley North trenches. There is also no evidence for displacement of the cover deposits overlying this strath. Fault materials such as cataclasite/mylonite are identified as having formed at significant depths in the crust, and have weathered to soft clays in a near-surface setting. This provides further evidence that the faults observed in these trenches are not currently active.

4.2 WHAT IS THE RELEVANCE OF THE GWAVAS FAULT?

In Chapter 1 we posed dual questions regarding the Gwavas Fault: “are there active splays of the Mohaka Fault in the Gwavas Forest?”; and if so, “what is the role of these active splays with respect to the approximate, inactive faults within the Wakarara Block and in the vicinity of the proposed A7 dam site”?

In Chapter 3 we documented that the Gwavas Fault is an active normal fault with an average recurrence interval of 2000-2800 yr, a slip rate of c. 0.2 mm/yr, and with an average single-event vertical displacement of c. 0.33-0.5 m. Bedrock surrounding the active trace of the Gwavas Fault is highly fractured with shears that trend parallel to the active trace.

The Gwavas Fault is best explained as a splay of, or a secondary fault related to, the Mohaka Fault, which strikes sub-parallel to the Gwavas Fault. Preliminary results suggest that both the timing of faulting events are conceivably consistent with the Mohaka Fault (Hanson, 1998; J. Zachariasen, unpublished data) and that displacements are in the range expected for secondary deformation on such a fault. Therefore, the Gwavas Fault is probably a good example of a secondary fault, i.e. one which slips in relation to a nearby primary fault movement. The recurrence interval for the Gwavas Fault is c. 2-3 times longer than that of

the Mohaka Fault (average c. 1125 yr), implying that secondary displacement on the Gwavas Fault does not occur during every Mohaka Fault rupture.

4.3 WHAT IS THE POSSIBLE SIZE, STYLE AND RECURRENCE OF SECONDARY FAULTING?

This question was posed in Chapter 1 as: "if secondary displacement could occur at the dam site, what are the possible size, style and recurrence of the observed secondary fault displacements?"

The sites we chose to excavate to bedrock on the true left side of the Makaroro River were considered to be good candidate sites to look for characterising the potential for secondary fault displacement because they either provided an opportunity to investigate/excavate: the bedrock within the A7 dam foundation area; the nature of the Donovan Gully feature/shear zone SZ1; or, to intercept evident geomorphic features that may indicate recent fault movements. The purpose of candidate selection for excavation to bedrock was therefore, to target those areas in which secondary faulting in recent geologic time would be most likely, such that some confidence could be expressed about the potential size of secondary displacements within the dam foundations.

Size of possible secondary faulting

We did not observe, and thus could not measure, secondary displacements near the A7 dam site at the best candidate trench sites. However, in the absence of evidence for recent secondary displacement in the Smedley trenches, we consider it valid to rely on the international literature review of historic secondary fault movements as presented in Langridge et al. (2011) and evidence from the probable secondary fault movements along the Gwavas Fault, to estimate the size of possible secondary faulting at the A7 site.

That literature review indicates that the range of displacement values anticipated are c. 0.1-0.5 m (at 1 standard deviation uncertainty at c. 750 m from the Mohaka Fault) up to 2 km or more from the primary fault rupture (Langridge et al., 2011). These values are consistent with actual displacements observed on the Gwavas Fault. The observed displacements at Gwavas along with the close proximity of the Gwavas Fault to the Mohaka Fault (c. 200 m) compared to the distance between the A7 site and the Mohaka Fault (c. 750 m), provides a reasonable basis to state that the size of potential secondary displacement at the dam site, would be in the range derived from literature review (0.1-0.5 m at 1 sigma uncertainty).

Style of possible secondary faulting

The style, or sense of displacement, of secondary faulting, on rock defects in association with rupture along the Mohaka Fault is dictated by the orientation and dip of the defect planes, and the orientation of the main tectonic stresses in the area. Townend et al. (2012) assess the maximum horizontal compression stress (Sh_{max}) to be oriented at 045-070° and the tectonic regime to be strike-slip in the region. This is clearly manifested by the presence of large strike-slip faults such as the Mohaka Fault. If we look at the typical diagram that shows the type of deformation associated with strike-slip faulting (Figure 4.1; the diagram has been oriented to match the trend of the Mohaka fault), and the corresponding orientation of the maximum compression axis (S_1), we observed that the orientation of the compression axis is approximately the same as that estimated by Townend et al. (2012). We can use the diagram on Figure 4.1 to predict the style of displacement on secondary features associated to the Mohaka Fault. The secondary displacement along the rock defects that were measured in the trenches Smedley South and Middle, excavated within or close to the future

foundations of the dam, will also follow the same styles. We also need to take into account that the dip of the fault plane will determine whether the movement is likely to be strike-slip (lateral or horizontal) if dips are vertical (~90º) or subvertical, or dip-slip (that is with a vertical component) if dips are inclined (that is <90º).

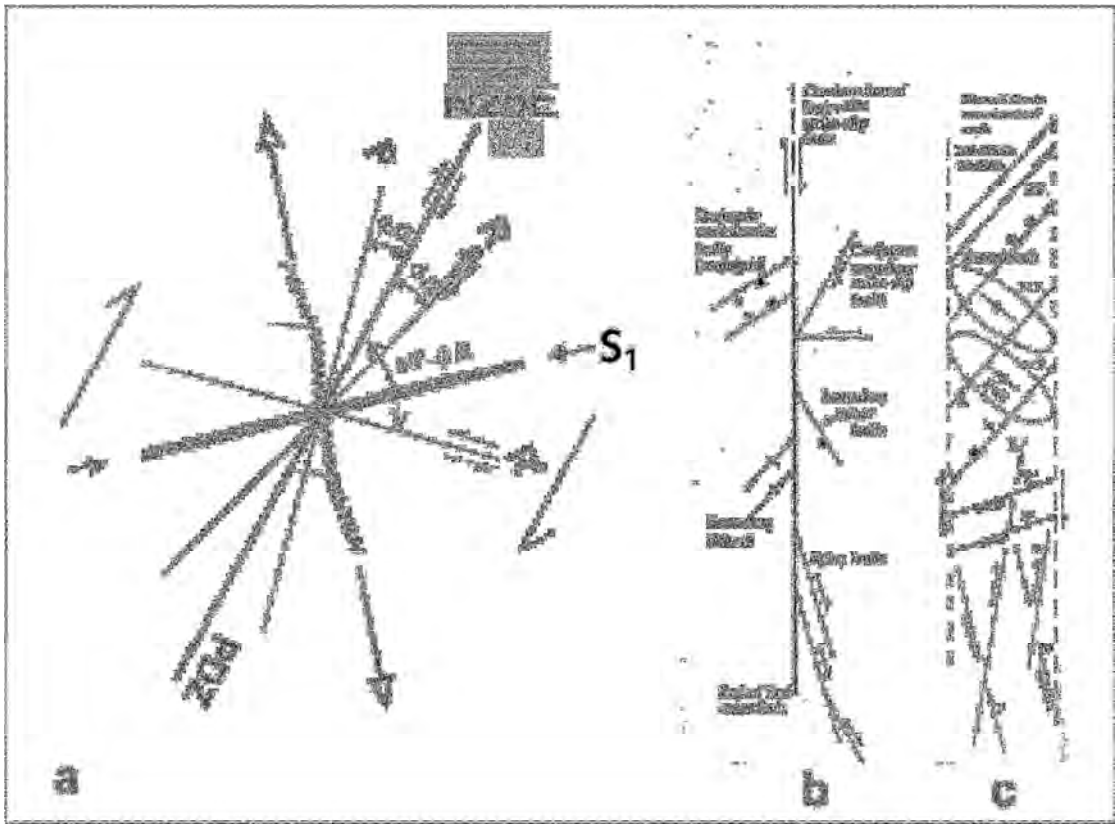

Figure 4.1 Simplified plan view models of strike-slip faulting (modified from Villamor 2001). A). PDZ is the primary fault (principal displacement zone), shown in the orientation of the Mohaka Fault. R refers to Riedel or right-lateral shears; R' to left- lateral shears; and P to thrust shears B) Types of tectonic structures on the main fault plane of strike-slip faults in bedrock. and C) Secondary tectonic features around main fault plane in bedrock, Price and Cosgrove, 1990). Ø is the friction angle.

If we extract the defect orientations from Figure 2.13 and Figure 2.30 and compare those to the features in Figure 4.1, we can predict that measured rock defects (faults and bedding) with NE strikes and vertical or subvertical dips are likely to move in a strike-slip (horizontal) fashion with right lateral displacement. Those defects with NW to E-W strikes and vertical dips are likely to move in a left lateral sense. For defect planes with inclined dips, those with ENE to the E-W strikes are likely to have a normal sense of movement, while those ranging from NW to N-S strikes will have a reverse sense of displacement. For defects with dips smaller than 90°, it is possible that the sense of displacement is a combination between horizontal and vertical displacement depending on the orientation and dip of the plane. In future, if a more precise evaluation of the deformation style for a specific defect tor defects than the one presented here is required than shown in this preliminary analysis, we recommended that local stress orientations are obtained from structural analysis of defects found in the dam foundations when the full area of the dam foundation is exposed.

Recurrence of possible secondary faulting

The minimum recurrence time for secondary displacement must be related to the recurrence interval of the Mohaka Fault, whose average recurrence interval is c. 1125 yr. We note that for the well-expressed and active Gwavas Fault, that the recurrence interval is 2-3 times that

of the Mohaka Fault, at the level that we can recognise faulting events in a trench. This suggests secondary displacement occurs commonly though not in every Mohaka Fault rupture event. In contrast, we cannot easily assess the recurrence time of secondary faulting within the dam foundation due to: the lack of observed faulting in the trenches; and; the limited amount of exposure. Based on the possible age of the alluvial strath and its cover deposits in the trenches, we have not observed any measureable secondary faulting during the last 10,000 yr or more.

4.4 WHAT IS THE RELEVANCE OF THE DONOVAN GULLY FEATURE OR SHEAR ZONE SZ1?

The final question left to answer from Chapter 1 is related to those discussed above, i.e. "what is the relevance of the 'inactive Donovan Gully feature' or 'shear zone SZ1' in the context of the bedrock underlying the dam site and what is the potential for faulting anywhere within the dam foundation of the proposed A7 dam site?"

The faults shown within the Wakarara Block by Lee et al. (2011), including the Donovan Gully feature, are interpretive and are meant to display the geology at a scale of 1:250,000. These faults are approximately located (± 250 m accuracy), and potentially may not exist. In reality, it is unlikely that any geologist has ever been within the inaccessible core of the Wakarara Range, and these faults are merely representations of the strike of the bedrock and geomorphic ridge and valley features. The key point is that this mapping was undertaken at a regional scale that cannot be considered accurate at the scales necessary to investigate structures such as large dams.

Some caution should be associated with assigning the terms "fault" or "accurately located" to features such as the Donovan Gully feature, as there is minimal geologic data constraining the location or certainty of such a feature. There is almost certainly structure that defines Donovan Gully from the competent ridge of greywacke that makes up Long Spur, and equally the weaker gully that the Makaroro River follows parallel to the Mohaka Fault upstream from the dam site. The connection of disparate structural data into a continuous mappable shear zone, e.g. SZ1, certainly has some merit. However this zone does not correlate exactly with the Donovan Gully feature. This philosophy of defining a specific zone of deformation (e.g. SZ1) also focuses attention on one narrow zone and discounts the notion that there could be more widespread, but unseen, deformation through the rockmass.

We note from the Smedley South trench that there is a coherent zone of interbedded argillite and sandstone in the floor of the trench over a width of c. 20 m. This could well correlate with the shear zone SZ1 described by Tonkin and Taylor. An important point to note that has probably not been observed in other locations (riverbanks, boreholes) is that this zone of argillite-rich greywacke is truncated within the trench by east-west striking faults. That means that it is unlikely that there is a through-going zone of active shearing within the argillite (i.e. SZ1).

We cannot exclude the possibility that shears/faults exist at any point within the rock volume that will underlie the dam foundation. As such we believe that these features would not necessarily be limited to the zone described as shear zone SZ1, or along the "Donovan Gully feature" shown on the Lee et al. (2011) geologic map of Hawke's Bay, but could potentially occur within other parts of the rockmass underlying the foundation of the A7 dam site. However, we do wish to again stress that in the trenches excavated as part of the current investigation that exposed the rockmass in 'isolated' patches within or near to the proposed footprint of the A7 dam site, no evidence for active displacement was found. Cross-sections

and borehole data from the Tonkin and Taylor Feasibility reports indicate that there are other argillite-rich zones within the rockmass, such as Pt2 (which was encountered on the true right side of the valley in a drillhole), and a zone of intensely-sheared bedrock within c. 200 m of the Mohaka Fault itself.

5.0 RECOMMENDATIONS

The absence of recent secondary faulting in the bedrock trenches excavated in this study is only applicable to the areas that we excavated, and should not be taken to indicate an absence of recent secondary faulting anywhere in the dam site. For example, the Tonkin and Taylor Feasibility reports indicate an argillite zone (Pt2) beneath terrace T1c on the true right side of the Makaroro River within the dam foundation.

During the construction phase of the A7 dam the bedrock needs to be carefully examined for evidence of secondary faulting. If any active secondary faults are found, the timing and amount of displacement need to be quantified, such that appropriate defensive design measures are incorporated into the dam construction. Full geological mapping of the structural features across the exposed foundation is recommended, to allow thorough structural analysis and verification of the deformation style.

This page is intentionally left blank.

6.0 REFERENCES

Beanland, S. 1995. The North Island Dextral Fault Belt, Hikurangi subduction margin, New Zealand. Unpubl. PhD thesis, Victoria University of Wellington, Wellington, New Zealand.

Beanland, S., Melhuish A., Nicol A., Ravens J. 1998. Structure and deformational history of the inner forearc region, Hikurangi subduction zone, New Zealand. *New Zealand Journal of Geology and Geophysics* 41: 325-342.

Berryman, K., Beanland, S. 1991. Variation in fault behaviour in different tectonic provinces of *New Zealand.* Journal of Structural Geology 13 (2): 177-189.

Davis, G.H., Reynolds, S.J. 1996 (2nd ed.). Structural Geology – Of Rocks and Regions. John Wiley and Sons, Inc.

Downes, G.L, 1995. Atlas of isoseismal maps of New Zealand earthquakes. *Institute of Geological & Nuclear Sciences Monograph 11,* 304 p., Lower Hutt, New Zealand. Institute of Geological & Nuclear Sciences Limited.

Froggatt, P., Lowe, D.J. 1990. A review of late Quaternary silicic and some other tephra formations from New Zealand: their stratigraphy, nomenclature, distribution, volume and age. New Zealand Journal of Geology and Geophysics 33: 89-109.

Gledhill, K., Ristau, J., Reyners, M., Fry, B., Holden, C., and the GeoNet Team 2010. The Darfield (Canterbury) earthquake of September 2010: Preliminary Seismological Report. Bulletin of the New Zealand Society for Earthquake Engineering, 43 (4): 215-221.

Hanson, J.A. 1998. The neotectonics of the Wellington and Ruahine faults between the Manawatu Gorge and Puketitiri, North Island, New Zealand. Unpublished D.Phil. thesis, Massey University, Palmerston North, New Zealand.

Kelsey, H.M., Hull, A.G., Cashman, S.M., Berryman, K.R., Cashman, P.H., Trexler, J.H. Jr, Begg, J.G. 1998. Paleoseismology of an active reverse fault in a forearc setting: The Poukawa Fault Zone, Hikurangi forearc, New Zealand. Tectonics 110: 1123-1148.

Kaiser, A., Holden, C., Beavan, J., Beetham, D., Benites, R., Celentano, A. Collett, D., Cubrinowski, M., Denys, P., Fielding, E., Fry, B., Gerstenberger, M., Langridge, R., Massey, C., Motagh, M., Pondard, N., McVerry, G., Ristau, J., Stirling, M., Thomas, J., Uma, S.R., Zhao, J. 2012. The Mw 6.2 Christchurch earthquake of February 2011: Preliminary Report. New Zealand Journal of Geology and Geophysics 55: 67-90. doi: 10.1080/00288306.2011.641182.

Klos, P.Z. 2009. Neotectonic evaluation of seismic hazard along the Ruataniwha Fault, Dannevirke region, New Zealand. B.S thesis, Dept. of Geological Sciences, Colorado College, Colorado Springs, USA.

Langridge, R.M., Villamor, P. 2013. Ruataniwha Scheme – Phase 1C: Progress Report. GNS Letter Report 2013/31LR.

Langridge, R.M., Van Dissen R, Rhoades D, Villamor P, Little T, Litchfield N, R, Clark K, Clark D 2011. Five thousand years of surface ruptures on the Wellington Fault, New Zealand: Implications for recurrence and fault segmentation. Bull. Seismological Soc. America 101 (5): 2088-2107.

Langridge, R.M., Villamor, P. 2011. The A7 Makaroro River dam site Phase 1: Initial site evaluation for active deformation. GNS Science Client Report 2011/117. 35 p.

Langridge, R.M., Villamor, P., McVerry, G.H., Cabeza, M. 2011. The A7 Makaroro River dam site - Phase 1B: Updated active fault and surface rupture displacement hazard and acceleration response spectra reassessment. GNS Science Client Report 2011/300. 60 p.

Langridge, R.M.; Zhao, J.X., Zajac A., McVerry G.H. 2010. Spectra and compilation of fault data for Central Hawke's Bay Water Augmentation Scheme. GNS Science Client Report 2010/121.

Lee, J., Bland, K., Kamp, P.J.J. (compilers), 2011. Geology of the Hawke's Bay area. Institute of Geological & Nuclear Sciences 1:250,000 geological map 8. 1 sheet + 71 p. Lower Hutt, New Zealand. GNS Science.

Litchfield, N.J., Berryman, K.R. 2005. Correlation of late Quaternary river (fill) terraces in the eastern North Island, New Zealand: Implications for the relative effects of climate and baselevel controls on terrace formation in an actively uplifting tectonic setting. Geomorphol. 68: 291-313.

Lowe, D.J., Blaauw, M., Hogg, A.G. Newnham, R.M. 2013. Ages of 24 widespread tephra erupted since 30,000 years in New Zealand, with re-evaluation of the timing and paleoclimatic implications of the Lateglacial cool episode recorded at Kaipo bog. Quat. Science Reviews.

Petersen, M.D., Dawson, T.E., Chen, R., Cao, T., Wils, C.J., Schwartz, D.P., and Frankel, A.D. 2011. Fault displacement hazard for strike-slip faults. Bull. Seismologic. Soc. America 101: 805-825.

Price, N.J., Cosgrove, J.W. 1990. Analysis of geological structures. Cambridge University Press.

Ramsay, J.G., Huber, M.I. 1993 (5th ed.). The Techniques of Modern Structural Geology. Academic Press Ltd, London.

Rattenbury, M.S., Townsend, D.B., Johnston, M.R. (compilers) 2006. Geology of the Kaikoura area. Institute of Geological & Nuclear Sciences 1:250,000 geological map 13. 1 sheet + 70 p. Lower Hutt, New Zealand: GNS Science.

Stirling, M.W., McVerry, G., Gerstenberger, M., Litchfield, N., Van Dissen, R., Berryman, K., Barnes, P., Wallace, L., Bradley, B., Villamor, P., Langridge, R., Lamarche, G., Nodder, S., Reyners, M., Rhoades, D., Smith, W., Nicol, A., Pettinga, J., Clark, K. and Jacobs., K. 2012. National Seismic Hazard Model for New Zealand: 2010 Update. Bull. Seismol. Soc. Am. 192: 1514-

Tonkin and Taylor, 2012a. Ruataniwha Water Storage Project, Report on Engineering Geological Investigations A7 Site. For: Hawke's Bay Regional Council. T&T Ref:27690.200.Final.

Tonkin and Taylor, 2012b. Ruataniwha Plains Water Storage Project Technical Feasibility Study Feasibility Report. For: Hawke's Bay Regional Council. T&T Ref: 27690.100/3.

Townend, J., Sherburn, S., Arnold, R., Boese, C., Woods, L. 2012. Three-dimensional variations in present-day tectonic stress along the Australia-Pacific plate boundary in New Zealand. Earth and Planetary Science letters 353-354: 47-59.

Twiss, R.J., Moores, E.M., 1992. Structural Geology. W.H. Freeman and Company.

Villamor Perez, M.P. 2002. Cinematica Terceria y cuaternaria de la falla de Alentejo-Plasencia y su influencia en la peligrosidad sismica del interior de la peninsular iberica. Doctoral thesis, Universidad Complutense de Madrid, Madrid, Spain.

APPENDICES

This page is intentionally left blank.

APPENDIX 1: UNIT DESCRIPTIONS

A1.1 SMEDLEY SOUTH TRENCH

Interpretations of deposition or environment in [square brackets].

Unit 1 Light grey brown, friable, silt over terrace sequence, pebble nutty structure. [Topsoil]

Unit 1B Light brown friable silt, slightly moist, occasional angular chips of greywacke. [Topsoil on slope]

Unit 1C Medium grey-brown stony silt. Clasts granule – medium pebbles, friable. [Slope colluvium]

Unit 1D Medium chocolate brown, prismatic, firm, slightly moist, silt, stone free

Unit 2 Light orange-brown, silty, friable, very fine sandy silt. B-horizon of soil. Grades downward to medium orange-brown = C-horizon. [Tephric silt].

Unit 2B Medium chocolate brown silt, slightly stony, friable, nutty-prismatic (similar to 1D).

Unit 2D Stony orange-brown fine sandy silt – clasts subangular – rounded, pebble to cobble size, max 25cm. [Stony tephric silt]

Unit 3A Medium grey very fine sandy silt, firm but friable, slightly deformed, boudined (sp.?) and injected by units above and below. [Tephric silt]

Unit 3B Light orange-yellow laminated (mm-cm) pumiceous silt to clayey silt. [Tephra – Waiohau?]

Unit 4 Light brown-grey mottled tephric sandy silt, common 1-2mm sized pumice clasts. Massive. [Ponded tephra/tephric silt]

Unit 4B Light grey-brown mottled fine to medium sand, friable, dusty (low density). [tephric sand]

Unit 4C Light grey-brown, lightly mottled, moist, well-sorted fine sand. [ponded tephric sand]

Unit 10 Fine gravel, light grey pebble-boulder gravel with sandy matrix, typically medium pebble to large cobble size, pseudo-bedded, loose. [Upper gravel sequence]

Unit 11 Light orange brown, lightly oxidised, pebble to boulder gravels (max 1m). Sub-angular – sub-rounded. Matrix = silty sand. Medium grey alteration halo in lower 1 metre in groundwater zone, above sheared rock. [Lower terrace sequence]

Unit 12 Medium orange-grey-brown, silty sandy poorly sorted gravels (cobble-pebble). Slightly oxidised. [Basal lag gravel of back-edge channel]

Unit 13 Light yellow brown silty gravel, poorly sorted, clasts pebble-boulder size. Sub-angular to sub-rounded. Matrix supported – matrix = silt to fine gravel. [Old terrace/colluvium]

Unit BR Undifferentiated Mesozoic greywacke bedrock. Sandstone and argillite beds; as mapped on trench logs.

A1.2 SMEDLEY NORTH TRENCH

Interpretations of deposition or environment in [square brackets].

Unit 1 Grey sandy silt loam, crumb structure – dry, fine to very fine. Colour: 7.5YR4/1. Occasional fine yellow brownish ash beneath. Loose. [Topsoil/subsoil]

Unit 2 Loose, pale yellow-brown very fine sand. Colour: 10YR5/6. Tephric, dry, massive. [Tephric sand]

Unit 3 Fine sand, yellow-brown 10YR5/6. Slightly more compact than unit 2. Paleosol. Dry with blocky structure (when dry). [Paleosol]

Unit 3a Large 5-10cm angular greywacke clasts in fine grey sandy matrix – beneath topsoil. [Colluvial wedge]

Unit 4 Firm pale yellow-brown sand 10YR6/6. Tephric, dry, massive. [Tephric sand]

Unit 5 Firm, moist, fine sand yellow brown 10YR4/6. Fine clasts, up to 1cm (sparse at top, abundant at bottom). Massive. [Fine sand]

Unit 5a Paler than 5, pale yellow-grey. Fine clasts <2mm. Dry. Sub-angular to angular clasts.

Unit 6 Pale grey fine gravel lenses within unit 5, 2.5Y7/1. Just above bedrock loose sandy matrix. Very dry. [Fine gravel]

Unit 6a Similar to 6 but moist and more matrix

Unit 7 Pale yellow-brown sand with 2-10mm angular greywacke clasts. [Sand]

Unit 8 Grey sandy silt. Loose, fine to very fine with numerous angular greywacke clasts, 5-10mm. Moderately moist. [Silt]

Unit 9 Greywacke bedrock (unit BR; bedrock)

Unit 9a Soil penetrating on broken up bedrock and look colluvial in some places. [Weathered bedrock with topsoil]

Unit 10 As for 5 but larger 2-3cm clasts at the base. Matrix supported – gravels up to 5cm but mainly ~1cm. Angular to sub-angular. [Sandy Gravel]

A1.3 GWAVAS TRENCH

Interpretations of deposition or environment in [square brackets].

Unit Ø Banded orange brown with black bands and stones, in places these are mixed together [Foresting fill]

Unit 1 [Topsoil]

Unit 1W Light orange brown soft, friable sandy tephric silt. [Topsoil of upthrown side], but could be disturbed deforestation layer.

Unit 1E Medium greyish brown friable silt, often stripped by forest activity. crumb structure, loose, ashy to tephric. [topsoil]

Unit 2 Dark purple, black moist organic silt. Contains charcoal and bracken fragments. Samples = GWV-1 and -2. [Black bracken soil].

Unit 3 Light brown stony silt containing grains of Taupo (Tp) pumice (see 4 and 4A), friable upper 5cm is characterised by greywacke clasts of 1-5cm ?* on base of black soil. [Brown silt]

Unit 4 Light or brown tephric silt with clasts of Taupo (Tp) pumice 1-3mm occasionally up to 1cm. Sample GWV-3. [Tephric silt]

Unit 4A Light orange brown fine sandy silt, friable, loose, contains pumice grains of 2-3mm. Dries to nutty texture. [B horizon of soil].

Unit 5 Medium brown, soft friable tephric silt [Tephra]

Unit 5A Medium brown-orange, very fine sandy silt, distinct in that it does not contain pumice c.f. 4A dries to nutty structure. [Holocene tephra]

Unit 6 Medium brown clayey silt, tephric. Slightly browner than 5 or 7. [Paleosol]

Unit 7 Similar to unit 5. Sample: GWV-4 taken from this unit.

Unit 8 Dark orange brown clayey silt, tephric [Mid Holocene admixed tephra]

Unit 9 reworked units 10 and 11. Light orangish brown tephric silt with ripped up clasts of unit 10 (particularly) and 11. [Colluvial wedge]

Unit 10 Light purplish grey ‘scratchy’ silty sand with slightly vesicular texture, sample GWV-5. [Grey tephra]

Unit 11 Light yellow orange moist fine sandy silt, tephric. Sample GWV-6. Slightly pumiceous. [Tephra]

Unit 12 Medium brown orange soft friable tephric silt, occasional stones. [Tephric silt]

Unit 13 Medium brown orange stony clayey silt. Clasts of greywacke 1-3cm typically c. 2cm. [Basal stony Holocene]

Unit 30 Light orange grey brown bedded fine gravels, typically sub-angular shape clasts are typically 1-5cm average 2 cm, max 12cm. Clast supported, matrix = coarse sand. [Top of aggradation sequence]

Unit 31 Split in two as on downthrown side – Unit 30 (well sorted, clast supported pebble gravel) or unit 32 (moderately sorted, pebble to cobble gravel). [Fine gravels]

Unit 32 Pseudo-bedded medium gravels silty matrix, clast supported sub-angular to sub-rounded. [Medium gravels]

Unit 33 Moderately to poorly sorted angular to sub-angular gravel, matrix supported coarse sand to fine pebble matrix with clasts 5-20cm, average clast size 12cm. [Alluvial Gravel]

Unit 34 As 37 – clast up to 0.5m. Sub-angular to sub-rounded.[Alluvial gravel]

Unit 35 Matrix supported – light brown sandy silt matrix. [Alluvial Gravel]

Unit 37 Medium orange grey brown matrix supported gravels, matrix is clayey, gritty silt clasts are pebble to large cobble size max. 26cm = boulder sub-angular clasts. [Alluvial Gravel]

APPENDIX 2: TEPHRA ANALYSIS

Table A 2.1 Summary of glass shard major element compositions of tephra beds and tephric material.

Sample	SiO2	Al2O3	TiO2	FeO	MgO	MnO	CaO	Na2O	K2O	Cl	Total	n
SS-1	76.45 (0.29)	12.94 (0.12)	0.17 (0.03)	1.73 (0.11)	0.16 (0.01)	0.05 (0.02)	1.34 (0.05)	4.07 (0.09)	2.94 (0.09)	0.14 (0.01)	100.66 (0.63)	15
GWV-6	76.49 (0.23)	12.89 (0.18)	0.16 (0.02)	1.70 (0.09)	0.14 (0.02)	0.06 (0.03)	1.34 (0.07)	4.07 (0.10)	3.00 (0.10)	0.14 (0.02)	99.94 (1.35)	16
GWV-4	77.58 (0.86)	12.62 (0.25)	0.14 (0.04)	1.22 (0.44)	0.13 (0.04)	0.06 (0.02)	0.90 (0.24)	4.11 (0.13)	3.10 (0.19)	0.15 (0.01)	100.03 (1.31)	13
GWV-5	76.24 (0.46)	12.99 (0.17)	0.18 (0.03)	1.84 (0.22)	0.15 (0.02)	0.06 (0.01)	1.39 (0.10)	4.01 (0.14)	2.99 (0.04)	0.15 (0.02)	100.26 (0.67)	5
SN-1	76.15 (0.14)	12.97 (0.09)	0.19 (0.02)	1.93 (0.11)	0.16 (0.01)	0.08 (0.02)	1.24 (0.02)	4.42 (0.09)	2.70 (0.12)	0.16 (0.01)	99.54 (0.95)	15
ATHO-Std	75.60 (0.45)	12.20 (0.10)	0.24 (0.02)	3.29 (0.12)	0.09 (0.01)	0.11 (0.02)	1.70 (0.10)	3.75 (0.17)	2.64 (0.06)	0.04 (0.01)	99.66 (0.55)	84

All major element determinations were made on a JEOL Superprobe (JXA-8230) housed at Victoria University of Wellington, using the ZAF correction method. Analyses were performed using an accelerating voltage of 15 kV under a static electron beam operating at 8 nA. The electron beam was defocused at 10 µm. Oxide values are recalculated to 100% on a volatile-free basis. Total Fe expressed as FeOt. Mean and ± 1 standard deviation (in parentheses), based on n analyses. All samples normalised against glass standards ATHO. Analyst: B.V. Alloway.

A2.1 INTERPRETATION

Two populations are evident. One population (OVC; Okataina Volcanic Centre) represented by GWV-4 and another population (TVC; Taupo Volcanic Centre) dominated by the rest of the unknowns.

GWV-4 is a mixed population with dominantly OVC sourced shards with subordinate TVC shards - hence redeposited. In considering the OVC-sourced shards; they are indistinguishable from Mamaku, Rotoma or even the Whakatane tephras (all known to occur in coverbeds of this region). Based on major element chemistry and graphs (Figure A 2.1) the most likely correlatives are the Rotoma and Mamaku tephras.

SS-1 and GWV-6 are indistinguishable and most likely correlate with the Karapiti Tephra from the TVC. GWV-5 is redeposited on the basis of dispersed glass shard chemistry, but most grains are indistinguishable from SS-1 and GWV-6. Based on its stratigraphy, position above the Karapiti Tephra, it is most likely to be the Poronui Tephra, which has a similar chemistry and age to the Karapiti Tephra. SN-1 is chemically indistinguishable from the Taupo Tephra. This interpretation is preferred over the field interpretation of Waimihia Tephra.

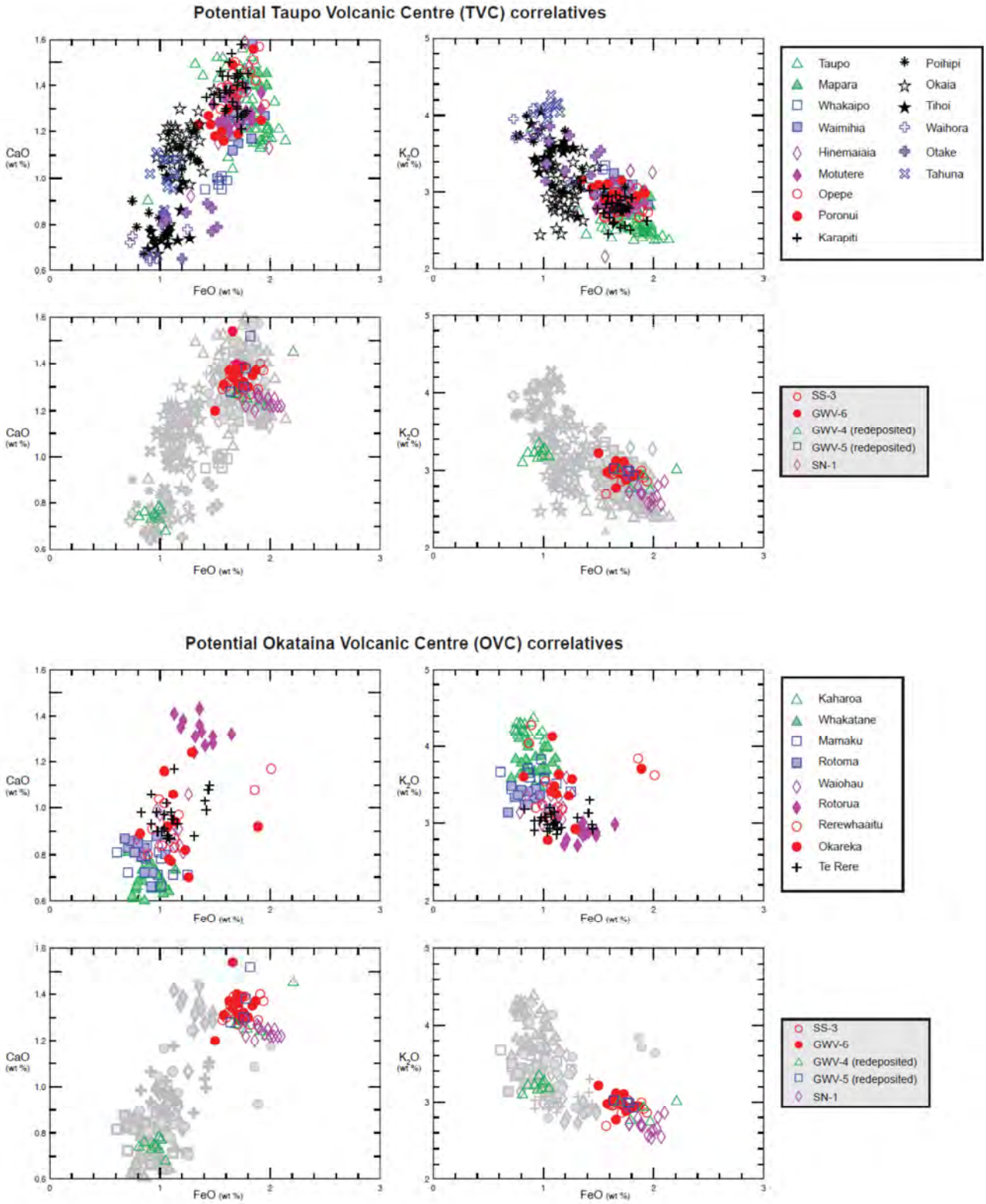

Figure A 2.1 Chemical analyses of volcanic glass shards from tephra samples, submitted to Victoria University. Five of the six samples have a TVC affinity. Analyses undertaken by B.V. Alloway.

APPENDIX 3: TABLE OF FAULT ROCK TEXTURES

Table A 3.1 Definitions of fault rocks from brittle to ductile and from less to more strain. From Davis and Reynolds (1996) and Twiss and Moores (1992).

Breccia (brittle)	Fault rocks composed of angular fragments (clasts) of wall rock set in a finer-grained matrix of crushed wall-rock material. Matrix is subordinate to clasts, comprising less than 30% of the breccia.
Fault gouge	Fault gouge is an unconsolidated rock with a very small grain size. Fault gouge has no cohesion; it is normally an unconsolidated rock type, unless cementation took place at a later stage. Fault gouge forms in the same way as fault breccia, the former having smaller clasts.
Cataclasite (brittle)	A fault rock whose grain size is similar to gouge, typically less than 0.1 mm, although it can contain up to 50% visible though still fine-grained clasts. Typically it is ultra-fine-grained and nearly glassy in appearance. It is usually cohesive.
Ultracataclasite (brittle)	A cataclasite that is the very finest, hardest, glassiest of the cataclasites.
Mylonite (ductile)	Rocks formed as a result of ductile deformation, which occurs in crustal rocks at temperatures usually exceeding 250-350 degrees C. This usually takes place in a ductile shear zone. The mylonite usually consists of more than one mineral, and the minerals behave differently to the shearing. Commonly a quartz will "flow" or be have plastically and feldspar crystals will behave brittlely and break into chips. The fabric thus created will contain feldspar crystals wrapped in quartz ribbons.
Ultramylonite (ductile)	A more thoroughly deformed and fine-grained rock containing more than 90% matrix and less than 10% relict grains.

APPENDIX 4: ATTITUDES MEASURED IN TRENCHES

SMEDLEY SOUTH

Position on log (m)	Feature	Attitude (strike/dip)
4.8	bedding	010/65E
8.6	"	036/46SE
9.1	"	000/57E
9.4	"	032/64E
9	"	012/64E
9.8	"	010/72E
9	"	014/77E
10.2	"	011/55E
11.7	"	007/50E
23.3	"	032/70SE
23.9	"	029/64SE
24.8	"	027/76SE
31.1	"	018/55E
36.5	"	145/22NE
37.6	"	082/55N
38.2	"	095/55S
38.5	"	088/56N
39.3	"	096/52S
39.3	"	091/90
29.2	"	047/86W
28.8	"	190/47E
28.5	fold axis	30
2.2	fault	358/80E
5.3	"	034/65SE
2.7	"	135/61N
6.7	"	080/45N
7.2	"	130/15NW

8.6	"	035/46SE
9.3	"	032/64E
8.6	"	095/63S
9.8	"	010/72E
9	"	014/77E
9	"	012/64E
6.4	"	009/60E
6.5	"	016/64E
40.5	"	104/60 S

SMEDLEY MIDDLE

Position on log (m)	Feature	Attitude (strike/dip)
0.1	joint	164/10E
5.5	"	122/43S
5.7	"	166/45NE
0.1	fault	055/70W
5.8	"	145/55NE
11.9	"	017/75E
11.5	"	039/60E
12.1	bedding	028/steep
12	joint	082/?

SMEDLEY NORTH

Position on log (m)	Feature	Attitude		
		Strike/Dip	Slickenside	Rake
22.6	fault	140/75S		
21	"	150/55SW		
25.5	"	030/45W		
21	bedding	013/81E		
20	"	180/60E		
17.8	"	032/85E		
12.7	fault	180/76W		
13.7	"	160/82W	110	140/40

13	"	080/74N		
16.8	"	030/85W		
17.8	bedding	180/?	70	80/70
23.4	joint	050/20 W		
35.2	bedding	030/80SE		
20	bedding	185/55E		
	joints	030/45W		
	"	025/10NW		
44.8	"	030/20NW		
21.5	fault	175/70E		
23	"	160/30W		
23.7	"	175/80		
22	"	170/90		
25.7	"	145/45SW		
25.6	"	110/50SW		
31.5	"	125/60SW		
31.8	"	025/10NW		
34.5	"	020/80E		
33.4	joint	150/30 SW		
19.5	bedding	189/?		
38.4	fault	155/50SW		
41.1	"	170/70SW		
8.4	"	175/60W		
9.2	"	170/90		
12	"	050/40W		

GWAVAS TRENCH

Position on log (m)	**Feature**	**Attitude (strike/dip)**
11.5	fault	071/70E
12.5	"	014/88W